Improving treatment
of Renal Cell Carcinoma with
monoclonal antibody cG250

Jeannette Oosterwijk-Wakka
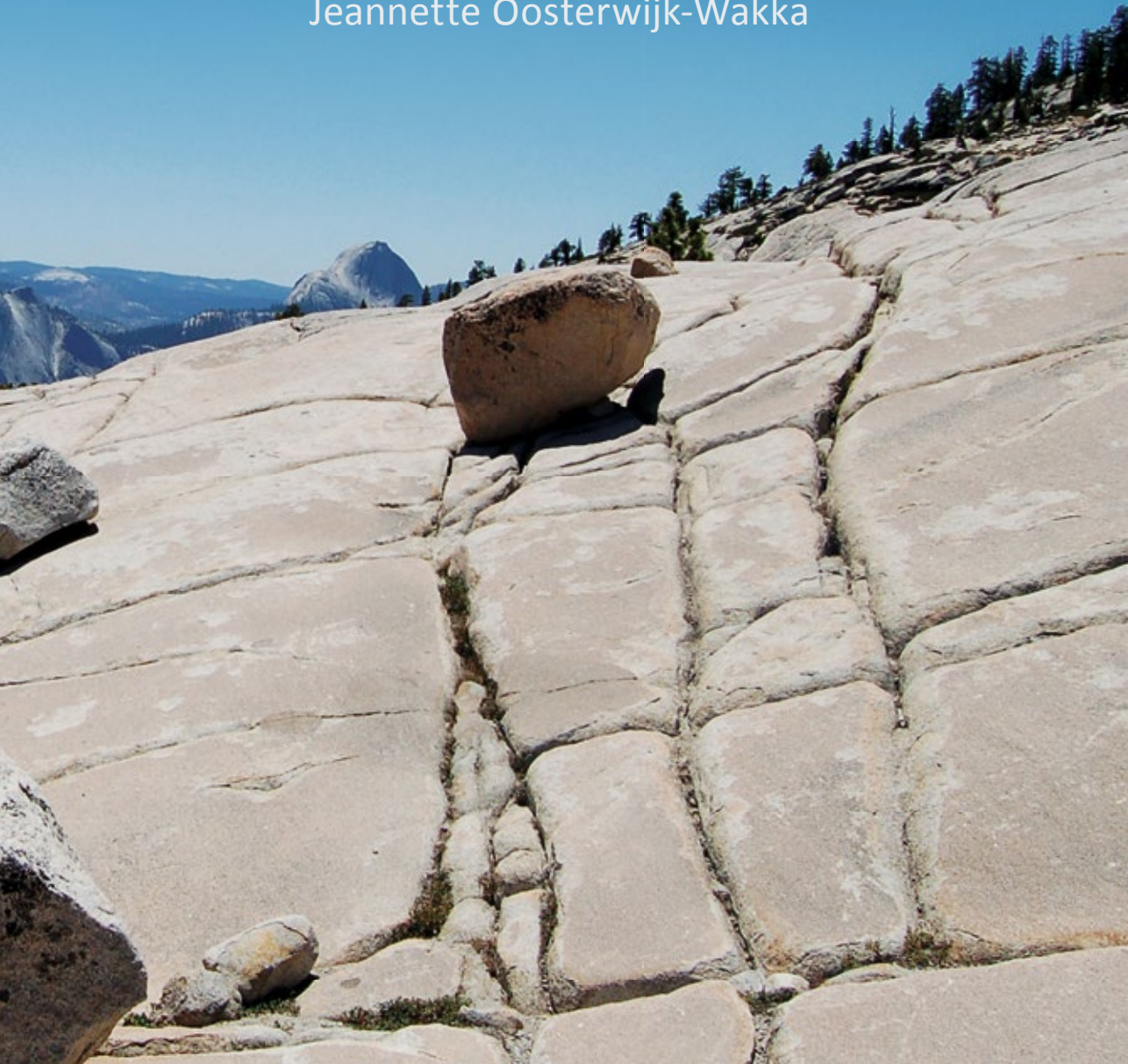
Improving treatment of Renal Cell Carcinoma with monoclonal antibody cG250

Jeannette Catharine Oosterwijk-Wakka

Cover design:	In Zicht Grafisch Ontwerp, Arnhem, The Netherlands
Lay-out:	Jeannette Oosterwijk-Wakka & In Zicht Grafisch Ontwerp
Printed by:	Ipskamp Printing, Nijmegen, The Netherlands

ISBN:	**978-90-824794-2-3**

Improving treatment of Renal Cell Carcinoma with monoclonal antibody cG250

Een wetenschappelijke proeve
op het gebied van de Medische Wetenschappen

Proefschrift

Ter verkrijging van de graad van doctor
aan de Radboud Universiteit Nijmegen
op gezag van de rector magnificus J.H.J.M. van Krieken,
volgens besluit van het college van decanen
in het openbaar te verdedigen op vrijdag 9 december 2016
om 12.30 uur precies

door
Jeannette Catharine Oosterwijk-Wakka
geboren op 16 augustus 1961
te Leiden

Voor mama

Table of Content

Chapter 1

General introduction
and thesis outline

Renal Cancer

Renal cell carcinoma (RCC) is the most common type of kidney cancer, accounting for 80-90% of all kidney cancers. In 2012 approximately 338.000 new cases were diagnosed with RCC worldwide and 143.000 patients died from metastasized RCC (mRCC) [1,2]. The incidence of RCC is increasing by approximately 2% per year, probably due to incidentally discovered renal masses by non-invasive imaging performed for other reasons [3,4]. It is possible that because such imaging is becoming more common, more RCC is being diagnosed, and at an earlier stage. In contrast, mortality is stable. The male: female incidence ratio is approximately 1.7:1.

There are three major histological subtypes of RCC, of which clear cell renal cell carcinoma (ccRCC) is the most prominent subtype (Table 1) [5].

Table 1 Renal cell carcinoma classification

RCC subtype	Incidence (%)
Clear cell	75
Papillary	10
Chromophobe	5
Collecting ducts of Bellini	1
Medullary	Rare
Xp11 translocation	Rare
After Neuroblastoma	Rare
Mucinous tubular and spindle cell	Rare
Unclassified	4-6

(Adapted from Lopez-Beltran et al. European urology 2006;49:798–805)

Despite advances in detection, about 30% of patients present with synchronous metastases and 20-30% of patients will develop metastatic disease after nephrectomy with curative intent [6]. The five year overall survival (OS) of patients with RCC decreases from 85-90% for localized disease to approximately 15% for metastasized disease [7].

In the majority of ccRCC patients, the tumor suppressor gene VHL is inactivated or mutated in the tumor cells (Fig. 1). Consequently the VHL protein is unable to interact, bind and degrade the transcription factors hypoxia-inducible factor α (HIFα), leading to HIFα accumulation and nuclear translocation where it activates a large number of target genes, amongst others Vascular Endothelial Growth Factor (VEGF) and Platelet Derived Growth Factor (PDGF). This increased production of VEGF and PDGF in ccRCC results in very well vascularized tumors [8].
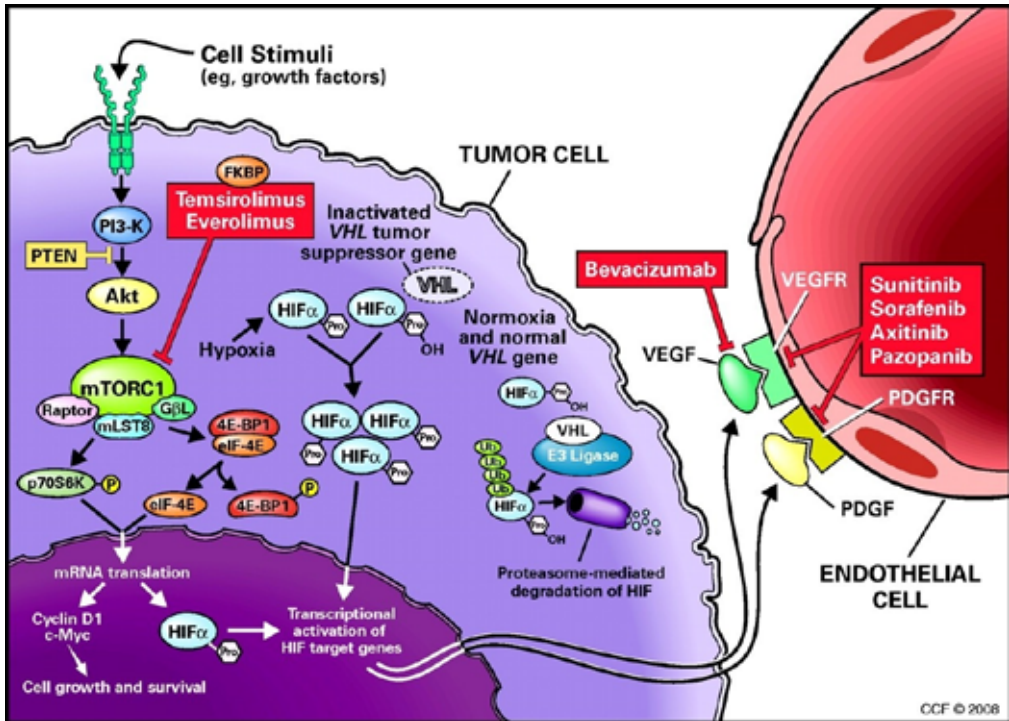
Figure 1. Biological pathway in Renal Cell Carcinoma
In conditions of normoxia and normal von Hippel Lindau (VHL) gene function, VHL protein is the substrate for hypoxia-inducible factor alpha (HIFα) leading to ubiquitination and degradation. In hypoxia or when the VHL gene is mutated (in RCC), the VHL protein is unable to bind to HIFα, leading to accumulation of HIF transcription factors. HIF accumulation can also result from activation of mammalian target of rapamycin (mTOR) downstream of the PI3-K/Akt pathway. Activated mTOR also promotes an increase in the translation of mRNAs that encode cell cycle regulators such as c-Myc and cyclin D1 leading to cell growth and survival. Activated HIF translocates into the nucleus and leads to transcription of a large number of target genes including vascular endothelial growth factor (VEGF) and platelet derived growth factor (PDGF). These ligands bind to their related receptors present on the surface of endothelial cells, leading to cell migration and proliferation. Sites of action of targeted therapies are illustrated. Temsirolimus and everolimus inhibit the kinase activity of the mTOR complex 1 (mTORC1). Bevacizumab is a VEGF ligand-binding antibody. Sunitinib, sorafenib, axitinib and pazopanib are small molecule inhibitors of multiple tyrosine kinase receptors including VEGFR and PDGFR.
Reprinted from The Lancet, Vol.10 number 10, Brian I. Rini, Michael B. Atkins, Resistance to targeted therapy in renal-cell carcinoma, Pages 992-1000, Copyright (2009), with permission from Elsevier.

Treatment of patients with advanced RCC

Targeted therapy

Up to 2006, IFNα monotherapy was the standard of treatment for patients with advanced RCC. Since the unraveling of genetic events in ccRCC, therapies targeting pathways involved in tumor angiogenesis have been developed.

Sunitinib, an oral tyrosine kinase inhibitor (TKI) of VEGFR2, PDGFR-α,β, Fms-like tyrosine kinase 3 (FLT-3) and stem cell factor receptor (SCFR/c-KIT), was the first TKI that was approved by the FDA in 2006 as first-line treatment for patients with advanced ccRCC. In the first pivotal trials, sunitinib demonstrated activity in patients with cytokine-refractory

mRCC [9,10]. In a large multicenter, randomized phase 3 trial sunitinib was superior compared to Interferon-α (IFNα) [11] with improved progression free survival (PFS, 11 vs. 5 months) and OS (26 vs. 21 months). Since then numerous agents targeting the VEGF pathway have been clinically implemented: TKIs such as sorafenib, pazopanib and axitinib, monoclonal antibody (mAb) bevacizumab in combination with IFNα and mTOR inhibitors everolimus and temsirolimus. Clinical benefit was proven for all of these agents either as first- or second-line treatment (Table 2) [12]. The median PFS with first-line sunitinib, pazopanib or bevacizumab plus IFNα is 8 to 11 months, while second-line axitinib or everolimus yields a median PFS of 4-5 months [13-16]. However, not all patients benefit from this treatment as responses are usually transient with tumor resistance occurring in patients when treated for an extended period. Moreover, patients may experience significant toxicities leading to dose reduction or cessation of treatment. Finally, complete responses are rare and improvement of survival is measured in months. To further improve therapeutic outcome TKI combinations and combinations of TKI with cytokines [17-19], bevacizumab [20,21] or mTOR inhibitors [22,23] were attempted but these efforts were unsuccessful due to enhanced toxicity, the need to reduce drug doses, and the lack of evidence of clinical benefit.

Because TKI combination treatments were intolerable, sequential treatments were investigated. Sequential treatment of sunitinib followed by sorafenib (So-Su) or vice versa (Su-So) did not significantly improve mean PFS (12.5 months for So-Su vs. 14.9 months for Su-So) and OS (31.5 months for So-Su vs. 30.2 months for Su-So) [24]. Moreover, the results demonstrated that sorafenib followed by sunitinib and vice versa have similar clinical benefit in mRCC.

Standard treatment now often involves treatment with an mTOR inhibitor after disease progression on a TKI, supported by studies addressing the sequence in which anti-VEGF therapies and mTOR agents were administered. In the RECORD-3 study, 471 patients with untreated mRCC were randomized to receive either 1st-line sunitinib or everolimus until disease progression, at which point they crossed over to the alternate drug [25]. The median combined PFS was 21.1 months for sequential everolimus-sunitinib and 25.8 months for sequential sunitinib-everolimus; the median OS was 22.4 months for sequential everolimus-sunitinib and 32.0 months for sequential sunitinib-everolimus trending towards worse OS in the everolimus group.

Fortunately, additional targeted agents and novel approaches are emerging. In April 2016 the FDA approved Cabozantinib for the treatment of patients with mRCC who have received previous antiangiogenic therapy. Cabozantinib is distinct from other approved targeted agents, as it targets multiple tyrosine kinases involved in the development of RCC, including VEGFR2, MET proto-oncogene receptor tyrosine kinase and AXL receptor tyrosine kinase. The approval was granted on the basis of results from the phase III METEOR trial, which compared cabozantinib with everolimus for second-line RCC [26] . Median PFS, the trial's primary outcome, was significantly better with cabozantinib than with everolimus (7.4 vs. 3.8 months; P < .0001). Notably, median OS was also better with cabozantinib than with

everolimus (21.4 vs. 16.5 months; P = .0003). However as with other TKI, substantial toxicity was observed. Dose reduction rates were 60% for cabozantinib and 24% for everolimus and treatment was discontinued in 10% of patients of both treatment arms because of adverse reactions.

In conclusion, although there has been substantial progress in the treatment of mRCC, targeted therapy has been primarily palliative in nature and further improvement is necessary.

Table 2. Systemic therapy for patients with clear cell mRCC

MSKCC risk group	First-line	Second-line
Favorable	Sunitinib Pazopanib Bevacizumab & IFN	Axitinib Sorafenib Everolimus Cabozantinib
Intermediate	Sunitinib Pazopanib Bevacizumab & IFN	Axitinib Sorafenib Everolimus Cabozantinib
Poor	Temsirolimus	Any targeted agent

MSKCC: Memorial Sloan-Kettering Cancer Center; mRCC: metastatic renal cell carcinoma
Adapted from evidence-based recommendations for systemic therapy of patients with clear cell mRCC [12]

Immuno-oncology: Checkpoint inhibitors

The last 30 years of immuno-oncology research have provided solid evidence that tumors are recognized by the immune system and that their development can be stopped or controlled long term through a process known as immune surveillance. Nevertheless, if the immune response fails to completely eliminate the tumor, cancer cells that can resist, avoid, or suppress the antitumor immune response are selected, leading to tumor escape and a progressively growing tumor. With a tumor microenvironment that prevents the expansion of helper and cytotoxic T cells and instead promotes the production of proinflammatory cytokines and other factors, suppressive cell populations that inhibit instead of promote immunity, accumulate.

The understanding of the molecular mechanisms of T cell activation and inhibition have led to the rapid development of therapeutic mAbs targeting inhibitory immune checkpoints

such as cytotoxic T-lymphocyte-associated antigen-4 (CTLA-4) and programmed death 1 or its ligand programmed death ligand 1 (PD-1/PD-L1). By blocking the inhibitory checkpoints, T cell responses will be sustained and tumor immunity enhanced (Fig. 2). CTLA-4 is upregulated on activated T-cells and outcompetes costimulatory molecule CD28 for binding to B7 on antigen presenting cells (APC) to dampen T-cell activation in response to tumor cells (early inhibitory signal). PD-1 is expressed on the surface of activated T cells, B cells, and macrophages. T-cell activation is inhibited by PD-1 binding to its ligand PD-L1 present on tumor cells thereby contributing to the tumor's ability to evade the immune system (late inhibitory signal) (Fig. 2).

Clinical trials with mAbs blocking CTLA4, PD-1 and PD-L1 have resulted in clinical benefits in several so called immunogenic tumortypes, i.e. melanoma, Non-small-cell lung carcinoma and RCC [28]. In contrast to the mostly transient clinical responses with targeted therapies, durable responses were induced with checkpoint inhibitors in subsets of patients. Nivolumab, a fully human IgG4 mAb targeting PD-1 and blocking interactions with PD-L1 and PD-L2 is now approved for the treatment of advanced RCC based on the checkmate 025 study that demonstrated superiority of nivolumab in safety profile and OS (25 mo vs. 9.6 mo) over everolimus after 1 or 2 antiangiogenic therapies [29].

Small studies with the anti-CTLA-4 antibody ipilimumab (human IgG1) in mRCC as monotherapy showed some clinical activity but major toxicities were observed, with 33% of patients experiencing grade 3 or 4 immune-mediated adverse events [30]. Additional investigation of ipilimumab as monotherapy in patients with advanced RCC has not been pursued. Promising results were gathered in a phase 1a study with a humanized PD-L1 antibody, Atezolizumab [31]. Atezolizumab demonstrated a manageable safety profile and promising antitumor activity in 63 patients with mRCC with median OS and PFS of 28.9 months and 5.6 months respectively. Currently, studies combining atezolizumab with bevacizumab are ongoing (NCT02420821, NCT01984242).

Although responses with immune-oncology drugs are durable, they are effective in a subset of patients and these drugs can induce high grade tissue-specific inflammatory side effects which cause injury to non-cancer tissue, particularly with CTLA-4 blockade. Most toxicities are related to immune activation and can be challenging to manage.

To improve response rates, different combinations are being explored including those with other immuno-oncology agents, targeted agents, hormonal therapies, chemotherapies and radiation therapies. The most successful of combinations involve ipilimumab with nivolumab which was tested in a phase II trial, in two different regimen. Acceptable safety and durable antitumor responses were observed with the regimen nivolumab 3 mg/kg + ipilimumab 1 mg/kg (N3I1) in pre-treated patients with mRCC [32]. Confirmed objective response rates of 43% (N3I1) and 48% (N1I3) appeared higher than those reported for nivolumab monotherapy. Because of higher toxicity rates and treatment discontinuation in the N1I3 group, the dosing schedule N3I1 was selected for further studies. A phase III trial comparing first-line sunitinib vs. N3I1 is currently ongoing and should demonstrate superiority.
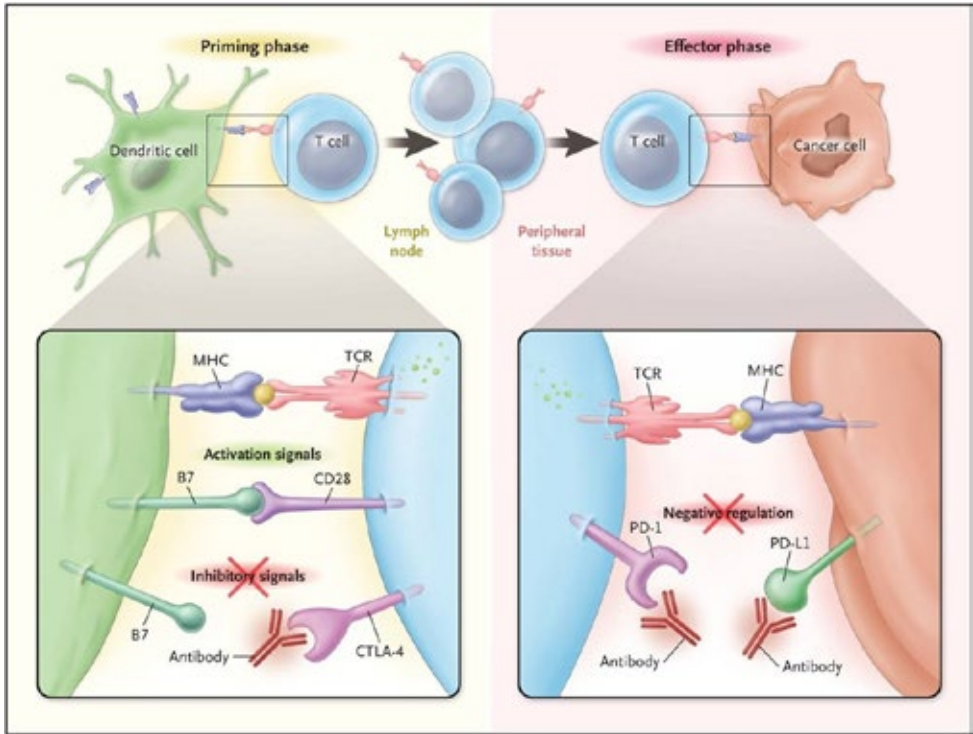
Figure 2. Blockade of PD-1 or CTLA-4 signaling in Tumor Immunotherapy
T cells recognize antigens presented by the major histocompatibility complex (MHC) on the surface of cancer cells through their T-cell receptor (TCR). This first signal is not enough to turn on a T-cell response, and a second signal delivered by the B7 costimulatory molecules B7-1 (or CD80) and B7-2 (or CD86) is required. Cytotoxic T-lymphocyte–associated antigen 4 (CTLA-4) is up-regulated shortly after T-cell activation and initiates negative regulation signaling on T cells during ligation with the B7 costimulatory molecules expressed by antigen-presenting cells. When these molecules bind to CD28, they provide activation signals; when they bind to CTLA-4, they provide inhibitory signals. The interaction between CTLA-4 and the costimulatory molecules happens primarily in the priming phase of a T-cell response within lymph nodes. Programmed death 1 (PD-1) inhibitory receptor is expressed by T cells during long-term antigen exposure and results in negative regulation on T cells during ligation with PD-L1 and PD-L2, which are primarily expressed within inflamed tissues and the tumor microenvironment. The PD-1 interaction happens in the effector phase of a T-cell response in peripheral tissues. Its blockade with antibodies to PD-1 or PD-L1 results in the preferential activation of T cells with specificity for the cancer.
Reproduced with permission from N Engl J Med 2012; 366:2517-2519, Antoni Ribas, Tumor Immunotherapy Directed at PD-1, Copyright Massachusetts Medical Society [27]

The combined treatment with sunitinib and the anti-CTLA-4 antibody tremelimumab (human IgG2), was not successful in RCC patients; treated patients experienced dose limiting toxicity, mainly due to renal failure and 1 patient suffered sudden death. Further investigations were not recommended [33]. Multiple clinical studies combining targeted therapies with checkpoint therapies are either planned or ongoing [34].

Despite the promising results with CTLA-4 and PD-1 inhibitors, there is an urgent need for even more agents and combinations to enter clinical use to improve treatment of renal cell cancer. The most challenging issue will be the clinical management of these new class of agents with their adverse events and toxicities when targeted therapies and immunotherapies are combined.

Monoclonal antibody G250 targeting CAIX

Monoclonal antibody G250 (mAbG250) recognizes a conformational determinant on carbonic anhydrase IX (CAIX) [35]. This protein is expressed by almost all ccRCC, but expression in normal tissues is restricted to the (upper) gastrointestinal mucosa (stomach, ileum, proximal and middle colon) and gastrointestinal related structures (intra- and extra-hepatic biliary system, pancreas) [36,37]. The G250-producing hybridoma was isolated after fusion of splenocytes of a mouse immunized with fresh human RCC with a mouse myeloma line [38]. Immunohistochemical analysis of mAbG250 on RCC specimen showed homogeneous expression in most (>85%) primary RCC and 70% of metastatic lesions. Originally, no association with a particular histological RCC subtype was noted, but it is now clear that the antigen recognized by mAbG250 is almost ubiquitously expressed (>95%) in ccRCC [35,39,40]. Molecular studies showed that CAIX gene expression was exclusively HIF1-α dependent, providing a direct link between the presence of an aberrant VHL gene product and CAIX expression [41]. These studies provided a straightforward explanation for the almost ubiquitous CAIX expression in ccRCC. The homogeneous CAIX expression in ccRCC and the excellent targeting capability of mAbG250 in animal models has led to the initiation of multiple clinical trials: both murine G250 (mG250) and chimeric G250 (cG250/Girentuximab), produced after grafting the G250-specificity on a human IgG1 Fc region [42], have been studied in patients with ccRCC, both diagnostically as therapeutically [35].

Diagnostic studies

In several clinical studies the outstanding targeting and imaging ability of mAbG250 has been confirmed [37,42-44] and cG250-based immunoPET imaging holds great promise as diagnostic modality, both in detecting localized and advanced disease [45-48]. However, the current data are inconclusive as to which tracer is superior in the diagnostic performance; the performance of ^{111}In-cG250 and [124]I-cG250 has not been directly compared yet. Moreover [89]Zirconium, another PET-imageable tracer may permit even better delineation of lesions. Recently, a clinical trial with [89]Zr-cG250 has been initiated in our center, which will provide additional information about the use of cG250-based immunoPET in ccRCC.

Therapeutic studies

Clinical trials with unmodified cG250 suggested that treatment with cG250 can influence the disease course of mRCC patients [49-53]. Based on this information an adjuvant trial has been performed (ARISER), aimed at reducing the recurrence of disease in nephrectomized RCC patients who have a high risk of relapse. Although this trial did not meet its primary endpoint (reduced recurrence in treated patients, [54]), preliminary results of a retrospective subanalysis appear to indicate a positive correlation between CAIX expression and treatment response [55]. Therefore, treatment with unmodified cG250 for ccRCC in the adjuvant setting might still be an option in a highly defined subpopulation. However, to validate whether cG250 treatment is of value, large randomized trials are needed.

Girentuximab-based radio immunotherapy (RIT) holds promise for the treatment of advanced RCC patients with small-volume disease. In a phase 1 dose escalating study with ^{177}Lu-cG250, disease stabilization was observed in 17/23 (74%) previously progressive mRCC patients [56]. In the ongoing phase 2 trial 8 patients have been treated until now. After the first RIT cycle, disease stabilization was observed in 5/8 (62.5 %) patients. Three of these responding patients received a second cycle of RIT leading to prolongation of disease stabilization in two patients. Inclusion of more patients will shed light on the therapeutic efficacy of this treatment modality in patients with advanced RCC.

Finally, there are still several hurdles that prevent implementation of cG250-based RIT as a new treatment for patients with mRCC. Besides better patient selection in the future, advances in dosimetric analysis will presumably contribute to the improvement of RIT, as the trade-off between efficacy and toxicity can be better tailored to the individual patient. Lastly, an important deficit in our current knowledge is how to optimally combine cG250-based RIT with the current standard of care of metastatic ccRCC patients.

Thesis outline

The aim of this thesis was to investigate new treatment strategies for patients with advanced RCC using monoclonal antibody G250 in preclinical models.

Chapter 2 reviews the diagnostic and therapeutic preclinical and clinical studies of murine and chimeric monoclonal antibody G250. Also, the development and characterization of the antibody is described.

In **Chapter 3**, a genetically engineered G250-TNF fusion protein was studied. In-vitro characterization of cG250-TNF comprised biochemical analysis and bioactivity assays, alone and in combination with Interferon-γ (IFNγ). Results of biodistribution studies on radiolabeled ^{125}I-G250-TNF and antitumor activity of cG250-TNF, alone and in combination with IFNγ, performed in mice with human RCC xenografts, are discussed.

Chapter 4 describes the effect of several TKI (sunitinib, sorafenib and vandetanib) on the biodistribution of monoclonal antibody cG250. Mice with human RCC xenografts were treated with sunitinib, vandetanib or sorafenib and injected with ^{125}I-labeled cG250. Results of antibody distribution and immunohistochemical analysis for the presence of endothelial cells, laminin, smooth muscle actin, CAIX expression and uptake of mAb cG250 performed to investigate whether TKI can be combined with mAb G250, are described**.**

In **Chapter 5**, we explored the importance of timing as well as sequence of administration of sunitinib and [111]In- cG250 in mice with human RCC xenografts. In two different tumors (SK-

RC-52 and NU12) biodistribution of cG250 was studied. Immunohistochemical analyses were performed to study the tumor vasculature and CAIX expression and to confirm cG250 uptake.

In **Chapter 6**, the therapeutic efficacy of sunitinib in combination with low dose ^{177}Lu-cG250 RIT was evaluated in mice with human RCC xenografts (SK-RC-52 and NU12) and compared to single treatments. Tumor growth was monitored for 21 to 23 weeks in mice treated with 1 or 2 cycles of sunitinib and ^{177}Lu-cG250 RIT.

References

1. Torre, L.A.; Bray, F.; Siegel, R.L.; Ferlay, J.; Lortet-Tieulent, J.; Jemal, A. Global cancer statistics, 2012. *Ca-Cancer J Clin* **2015**, *65*, 87-108.
2. Znaor, A.; Lortet-Tieulent, J.; Laversanne, M.; Jemal, A.; Bray, F. International variations and trends in renal cell carcinoma incidence and mortality. *Eur Urol* **2015**, *67*, 519-530.
3. Capitanio, U.; Montorsi, F. Renal cancer. *Lancet* **2015**, *387*, 894–906
4. Ferlay, J.; Soerjomataram, I.; Dikshit, R.; Eser, S.; Mathers, C.; Rebelo, M.; Parkin, D.M.; Forman, D.; Bray, F. Cancer incidence and mortality worldwide: Sources, methods and major patterns in globocan 2012. *Int J Cancer* **2015**, *136*, E359-E386.
5. Lopez-Beltran, A.; Scarpelli, M.; Rodolfo, M.; Kirkali, Z. 2004 who classification of the renal tumors of the adults. *Eur Urol* **2006**, *49*, 798-805.
6. Molina, A.M.; Motzer, R.J. Current algorithms and prognostic factors in the treatment of metastatic renal cell carcinoma. *Clin Genitourin Canc* **2008**, *6*, S7-S13.
7. Karakiewicz, P.I.; Trinh, Q.D.; Bhojani, N.; Bensalah, K.; Salomon, L.; de la Taille, A.; Tostain, J.; Cindolo, L.; Altieri, V.; Ficarra, V.*, et al.* Renal cell carcinoma with nodal metastases in the absence of distant metastatic disease: Prognostic indicators of disease-specific survival. *Eur Urol* **2007**, *51*, 1616-1624.
8. Rini, B.I.; Atkins, M.B. Resistance to targeted therapy in renal-cell carcinoma. *Lancet Oncol* **2009**, *10*, 992-1000.
9. Motzer, R.J.; Rini, B.I.; Bukowski, R.M.; Curti, B.D.; George, D.J.; Hudes, G.R.; Redman, B.G.; Margolin, K.A.; Merchan, J.R.; Wilding, G.*, et al.* Sunitinib in patients with metastatic renal cell carcinoma. *Jama* **2006**, *295*, 2516-2524.
10. Motzer, R.J.; Michaelson, M.D.; Redman, B.G.; Hudes, G.R.; Wilding, G.; Figlin, R.A.; Ginsberg, M.S.; Kim, S.T.; Baum, C.M.; DePrimo, S.E.*, et al.* Activity of su11248, a multitargeted inhibitor of vascular endothelial growth factor receptor and platelet-derived growth factor receptor, in patients with metastatic renal cell carcinoma. *Journal of clinical oncology : official journal of the American Society of Clinical Oncology* **2006**, *24*, 16-24.
11. Motzer, R.J.; Hutson, T.E.; Tomczak, P.; Michaelson, M.D.; Bukowski, R.M.; Rixe, O.; Oudard, S.; Negrier, S.; Szczylik, C.; Kim, S.T.*, et al.* Sunitinib versus interferon alfa in metastatic renal-cell carcinoma. *The New England journal of medicine* **2007**, *356*, 115-124.
12. Ljungberg, B.; Bensalah, K.; Canfield, S.; Dabestani, S.; Hofmann, F.; Hora, M.; Kuczyk, M.A.; Lam, T.; Marconi, L.; Merseburger, A.S.*, et al.* Eau guidelines on renal cell carcinoma: 2014 update. *Eur Urol* **2015**, *67*, 913-924.
13. Motzer, R.J.; Hutson, T.E.; Cella, D.; Reeves, J.; Hawkins, R.; Guo, J.; Nathan, P.; Staehler, M.; de Souza, P.; Merchan, J.R.*, et al.* Pazopanib versus sunitinib in metastatic renal-cell carcinoma. *New Engl J Med* **2013**, *369*, 722-731.
14. Escudier, B.; Bellmunt, J.; Negrier, S.; Bajetta, E.; Melichar, B.; Bracarda, S.; Ravaud, A.; Golding, S.; Jethwa, S.; Sneller, V. Phase iii trial of bevacizumab plus interferon alfa-2a in patients with metastatic renal cell carcinoma (avoren): Final analysis of overall survival. *J Clin Oncol* **2010**, *28*, 2144-2150.
15. Rini, B.I.; Escudier, B.; Tomczak, P.; Kaprin, A.; Szczylik, C.; Hutson, T.E.; Michaelson, M.D.; Gorbunova, V.A.; Gore, M.E.; Rusakov, I.G.*, et al.* Comparative effectiveness of axitinib versus sorafenib in advanced renal cell carcinoma (axis): A randomised phase 3 trial. *Lancet* **2011**, *378*, 1931-1939.
16. Motzer, R.J.; Escudier, B.; Oudard, S.; Hutson, T.E.; Porta, C.; Bracarda, S.; Grunwald, V.; Thompson, J.A.; Figlin, R.A.; Hollaender, N.*, et al.* Efficacy of everolimus in advanced renal cell carcinoma: A double-blind, randomised, placebo-controlled phase iii trial. *Lancet* **2008**, *372*, 449-456.
17. Motzer, R.J.; Hudes, G.; Wilding, G.; Schwartz, L.H.; Hariharan, S.; Kempin, S.; Fayyad, R.; Figlin, R.A. Phase i trial of sunitinib malate plus interferon-alpha for patients with metastatic renal cell carcinoma. *Clin Genitourin Canc* **2009**, *7*, 28-33.
18. Grunwald, V.; Desar, I.M.E.; Haanen, J.; Fiedler, W.; Mouritzen, U.; Olsen, M.W.B.; van Herpen, C.M.L. A phase i study of recombinant human interleukin-21 (ril-21) in combination with sunitinib in patients with metastatic renal cell carcinoma (rcc). *Acta Oncol* **2011**, *50*, 121-126.
19. Ryan, C.W.; Goldman, B.H.; Lara, P.N.; Mack, P.C.; Beer, T.M.; Tangen, C.M.; Lemmon, D.; Pan, C.X.; Drabkin, H.A.; Crawford, E.D. Sorafenib with interferon alfa-2b as first-line treatment of advanced renal carcinoma: A phase ii study of the southwest oncology group. *J Clin Oncol* **2007**, *25*, 3296-3301.

20. Feldman, D.R.; Baum, M.S.; Ginsberg, M.S.; Hassoun, H.; Flombaum, C.D.; Velasco, S.; Fischer, P.; Ronnen, E.; Ishill, N.; Patil, S.*, et al.* Phase i trial of bevacizumab plus escalated doses of sunitinib in patients with metastatic renal cell carcinoma. *J Clin Oncol* **2009**, *27*, 1432-1439.

21. Bruce, J.Y.; Kolesar, J.M.; Hammers, H.; Stein, M.N.; Carmichael, L.; Eickhoff, J.; Johnston, S.A.; Binger, K.A.; Heideman, J.L.; Perlman, S.B.*, et al.* A phase i pharmacodynamic trial of sequential sunitinib with bevacizumab in patients with renal cell carcinoma and other advanced solid malignancies. *Cancer Chemoth Pharm* **2014**, *73*, 485-493.

22. Patel, P.H.; Senico, P.L.; Curiel, R.E.; Motzer, R.J. Phase i study combining treatment with temsirolimus and sunitinib malate in patients with advanced renal cell carcinoma. *Clin Genitourin Canc* **2009**, *7*, 24-27.

23. Molina, A.M.; Feldman, D.R.; Voss, M.H.; Ginsberg, M.S.; Baum, M.S.; Brocks, D.R.; Fischer, P.M.; Trinos, M.J.; Patil, S.; Motzer, R.J. Phase 1 trial of everolimus plus sunitinib in patients with metastatic renal cell carcinoma. *Cancer-Am Cancer Soc* **2012**, *118*, 1868-1876.

24. Michel, M.S.; Vervenne, W.; Goebell, P.J.; Von Weikersthal, L.F.; Freier, W.; De Santis, M.; Zimmermann, U.; Bos, M.M.E.M.; Trojan, L.; Lerchenmuller, C.A.*, et al.* Phase iii randomized sequential open-label study to evaluate efficacy and safety of sorafenib (so) followed by sunitinib (su) versus sunitinib followed by sorafenib in patients with advanced/metastatic renal cell carcinoma without prior systemic therapy (switch study): Safety interim analysis results. *J Clin Oncol* **2012**, *30*.

25. Motzer, R.J.; Barrios, C.H.; Kim, T.M.; Falcon, S.; Cosgriff, T.; Harker, W.G.; Srimuninnimit, V.; Pittman, K.; Sabbatini, R.; Rha, S.Y.*, et al.* Phase ii randomized trial comparing sequential first-line everolimus and second-line sunitinib versus first-line sunitinib and second-line everolimus in patients with metastatic renal cell carcinoma. *J Clin Oncol* **2014**, *32*, 2766-+.

26. Choueiri, T.K.; Escudier, B.; Powles, T.; Mainwaring, P.N.; Rini, B.I.; Donskov, F.; Hammers, H.; Hutson, T.E.; Lee, J.L.; Peltola, K.*, et al.* Cabozantinib versus everolimus in advanced renal-cell carcinoma. *New Engl J Med* **2015**, *373*, 1814-1823.

27. Ribas, A. Tumor immunotherapy directed at pd-1. *New Engl J Med* **2012**, *366*, 2517-2519.

28. Callahan, M.K.; Postow, M.A.; Wolchok, J.D. Targeting t cell co-receptors for cancer therapy. *Immunity* **2016**, *44*, 1069-1078.

29. Motzer, R.J.; Escudier, B.; McDermott, D.F.; George, S.; Hammers, H.J.; Srinivas, S.; Tykodi, S.S.; Sosman, J.A.; Procopio, G.; Plimack, E.R.*, et al.* Nivolumab versus everolimus in advanced renal-cell carcinoma. *New Engl J Med* **2015**, *373*, 1803-1813.

30. Yang, J.C.; Hughes, H.; Kammula, U.; Royal, R.; Sherry, R.M.; Topalian, S.L.; Suri, K.B.; Levy, C.; Allen, T.; Mavroukakis, S.*, et al.* Ipilimumab (anti-ctla4 antibody) causes regression of metastatic renal cell cancer associated with enteritis and hypophysitis. *J Immunother* **2007**, *30*, 825-830.

31. McDermott, D.F.; Sosman, J.A.; Sznol, M.; Massard, C.; Gordon, M.S.; Hamid, O.; Powderly, J.D.; Infante, J.R.; Fasso, M.; Wang, Y.V.*, et al.* Atezolizumab, an anti-programmed death-ligand 1 antibody, in metastatic renal cell carcinoma: Long-term safety, clinical activity, and immune correlates from a phase ia study. *J Clin Oncol* **2016**, *34*, 833-841.

32. Hammers, H.; Plimack, E.R.; Infante, J.R.; Ernstoff, M.; Rini, B.I.; McDermott, D.F.; Razak, A.; Pal, S.K.; Voss, M.; Sharma, P.*, et al.* Phase i study of nivolumab in combination with ipilimumab in metastatic renal cell carcinoma (mrcc). *Ann Oncol* **2014**, *25*.

33. Rini, B.I.; Stein, M.; Shannon, P.; Eddy, S.; Tyler, A.; Stephenson, J.J., Jr.; Catlett, L.; Huang, B.; Healey, D.; Gordon, M. Phase 1 dose-escalation trial of tremelimumab plus sunitinib in patients with metastatic renal cell carcinoma. *Cancer-Am Cancer Soc* **2011**, *117*, 758-767.

34. Hughes, P.E.; Caenepeel, S.; Wu, L.C. Targeted therapy and checkpoint immunotherapy combinations for the treatment of cancer. *Trends in immunology* **2016**, *37*, 462-476.

35. Stillebroer, A.B.; Mulders, P.F.; Boerman, O.C.; Oyen, W.J.; Oosterwijk, E. Carbonic anhydrase ix in renal cell carcinoma: Implications for prognosis, diagnosis, and therapy. *Eur Urol* **2010**, *58*, 75-83.

36. Pastorekova, S.; Parkkila, S.; Parkkila, A.K.; Opavsky, R.; Zelnik, V.; Saarnio, J.; Pastorek, J. Carbonic anhydrase ix, mn/ca ix: Analysis of stomach complementary DNA sequence and expression in human and rat alimentary tracts. *Gastroenterology* **1997**, *112*, 398-408.

37. Brouwers, A.H.; Buijs, W.C.; Oosterwijk, E.; Boerman, O.C.; Mala, C.; De Mulder, P.H.; Corstens, F.H.; Mulders, P.F.; Oyen, W.J. Targeting of metastatic renal cell carcinoma with the chimeric monoclonal antibody g250 labeled with (131)i or (111)in: An intrapatient comparison. *Clin Cancer Res* **2003**, *9*, 3953S-3960S.

38. Oosterwijk, E.; Ruiter, D.J.; Hoedemaeker, P.J.; Pauwels, E.K.J.; Jonas, U.; Zwartendijk, J.; Warnaar, S.O. Monoclonal-antibody g-250 recognizes a determinant present in renal-cell carcinoma and absent from normal kidney. *Int J Cancer* **1986**, *38*, 489-494.

39. Bismar, T.A.; Bianco, F.J.; Zhang, H.; Li, X.; Sarkar, F.H.; Sakr, W.A.; Grignon, D.J.; Che, M. Quantification of g250 mrna expression in renal epithelial neoplasms by real-time reverse transcription-pcr of dissected tissue from paraffin sections. *Pathology* **2003**, *35*, 513-517.

40. Zhang, B.Y.; Thompson, R.H.; Lohse, C.M.; Dronca, R.S.; Cheville, J.C.; Kwon, E.D.; Leibovich, B.C. Carbonic anhydrase ix (caix) is not an independent predictor of outcome in patients with clear cell renal cell carcinoma (ccrcc) after long-term follow-up. *Bju Int* **2013**, *111*, 1046-1053.

41. Grabmaier, K.; de Weijert, M.C.A.; Verhaegh, G.W.; Schalken, J.A.; Oosterwijk, E. Strict regulation of caix(g250/mn) by hif-1 alpha in clear cell renal cell carcinoma. *Oncogene* **2004**, *23*, 5624-5631.

42. Steffens, M.G.; Boerman, O.C.; Oosterwijk-Wakka, J.C.; Oosterhof, G.O.; Witjes, J.A.; Koenders, E.B.; Oyen, W.J.; Buijs, W.C.; Debruyne, F.M.; Corstens, F.H.*, et al.* Targeting of renal cell carcinoma with iodine-131-labeled chimeric monoclonal antibody g250. *J Clin Oncol* **1997**, *15*, 1529-1537.

43. Oosterwijk, E.; Bander, N.H.; Divgi, C.R.; Welt, S.; Wakka, J.C.; Finn, R.D.; Carswell, E.A.; Larson, S.M.; Warnaar, S.O.; Fleuren, G.J.*, et al.* Antibody localization in human renal-cell carcinoma - a phase-i study of monoclonal antibody-g250. *J Clin Oncol* **1993**, *11*, 738-750.

44. Steffens, M.G.; Boerman, O.C.; Oyen, W.J.; Kniest, P.H.; Witjes, J.A.; Oosterhof, G.O.; van Leenders, G.J.; Debruyne, F.M.; Corstens, F.H.; Oosterwijk, E. Intratumoral distribution of two consecutive injections of chimeric antibody g250 in primary renal cell carcinoma: Implications for fractionated dose radioimmunotherapy. *Cancer research* **1999**, *59*, 1615-1619.

45. Divgi, C.R.; Pandit-Taskar, N.; Jungbluth, A.A.; Reuter, V.E.; Gonen, M.; Ruan, S.; Pierre, C.; Nagel, A.; Pryma, D.A.; Humm, J.*, et al.* Preoperative characterisation of clear-cell renal carcinoma using iodine-124-labelled antibody chimeric g250 (i-124-cg250) and pet in patients with renal masses: A phase i trial. *Lancet Oncol* **2007**, *8*, 304-310.

46. Pryma, D.A.; O'Donoghue, J.A.; Humm, J.L.; Jungbluth, A.A.; Old, L.J.; Larson, S.M.; Divgi, C.R. Correlation of in vivo and in vitro measures of carbonic anhydrase ix antigen expression in renal masses using antibody i-124-cg250. *J Nucl Med* **2011**, *52*, 535-540.

47. Divgi, C.R.; Uzzo, R.G.; Gatsonis, C.; Bartz, R.; Treutner, S.; Yu, J.Q.; Chen, D.; Carrasquillo, J.A.; Larson, S.; Bevan, P.*, et al.* Positron emission tomography/computed tomography identification of clear cell renal cell carcinoma: Results from the redect trial. *J Clin Oncol* **2013**, *31*, 187-194.

48. Muselaers, C.H.J.; Boerman, O.C.; Oosterwijk, E.; Langenhuijsen, J.F.; Oyen, W.J.G.; Mulders, P.F.A. Indium-111-labeled girentuximab immunospect as a diagnostic tool in clear cell renal cell carcinoma. *Eur Urol* **2013**, *63*, 1101-1106.

49. Varga, Z.; de Mulder, P.; Kruit, W.; Hegele, A.; Hofmann, R.; Lamers, C.; Warnaar, S.; Mala, C.; Ullrich, S.; Mulders, P. A prospective open-label single-arm phase ii study of chimeric monoclonal antibody cg250 in advanced renal cell carcinoma patients. *Folia Biol-Prague* **2003**, *49*, 74-77.

50. Bleumer, I.; Knuth, A.; Oosterwijk, E.; Hofmann, R.; Varga, Z.; Lamers, C.; Kruit, W.; Melchior, S.; Mala, C.; Ullrich, S.*, et al.* A phase ii trial of chimeric monoclonal antibody g250 for advanced renal cell carcinoma patients. *Br J Cancer* **2004**, *90*, 985-990.

51. Bleumer, I.; Oosterwijk, E.; Oosterwijk-Wakka, J.C.; Voller, M.C.; Melchior, S.; Warnaar, S.O.; Mala, C.; Beck, J.; Mulders, P.F. A clinical trial with chimeric monoclonal antibody wx-g250 and low dose interleukin-2 pulsing scheme for advanced renal cell carcinoma. *The Journal of urology* **2006**, *175*, 57-62.

52. Davis, I.D.; Wiseman, G.A.; Lee, F.T.; Gansen, D.N.; Hopkins, W.; Papenfuss, A.T.; Liu, Z.; Moynihan, T.J.; Croghan, G.A.; Adjei, A.A.*, et al.* A phase i multiple dose, dose escalation study of cg250 monoclonal antibody in patients with advanced renal cell carcinoma. *Cancer immunity* **2007**, *7*, 13.

53. Siebels, M.; Rohrmann, K.; Oberneder, R.; Stahler, M.; Haseke, N.; Beck, J.; Hofmann, R.; Kindler, M.; Kloepfer, P.; Stief, C. A clinical phase i/ii trial with the monoclonal antibody cg250 (rencarex(a (r))) and interferon-alpha-2a in metastatic renal cell carcinoma patients. *World J Urol* **2011**, *29*, 121-126.

54. Belldegrun, A.S.; Chamie, K.; Kloepfer, P.; Fall, B.; Bevan, P.; Storkel, S.; Wilhelm, O.; Pantuck, A.J. Ariser: A randomized double blind phase iii study to evaluate adjuvant cg250 treatment versus placebo in patients with high-risk ccrcc-results and implications for adjuvant clinical trials. *J Clin Oncol* **2013**, *31 (suppl)* abstr 4507.

55. Chamie, K.; Klopfer, P.; Bevan, P.; Storkel, S.; Said, J.; Fall, B.; Belldegrun, A.S.; Pantuck, A.J. Carbonic anhydrase-ix score is a novel biomarker that predicts recurrence and survival for high-risk, nonmetastatic renal cell carcinoma: Data from the phase iii ariser clinical trial. *Urologic oncology* **2015**, *33*, 204 e225-233.

56. Stillebroer, A.B.; Boerman, O.C.; Desar, I.M.E.; Boers-Sonderen, M.J.; van Herpen, C.M.L.; Langenhuijsen, J.F.; Smith-Jones, P.M.; Oosterwijk, E.; Oyen, W.J.G.; Mulders, P.F.A. Phase 1 radioimmunotherapy study with lutetium 177-labeled anti-carbonic anhydrase ix monoclonal antibody girentuximab in patients with advanced renal cell carcinoma. *Eur Urol* **2013**, *64*, 478-485.

Chapter 2

Application of Monoclonal Antibody G250 recognizing Carbonic Anhydrase IX in Renal Cell Carcinoma

Jeannette C. Oosterwijk-Wakka[1], Otto C. Boerman[2], Peter F.A. Mulders[1] and Egbert Oosterwijk[1]

[1]Department of Urology, [2]Department of Radiology and Nuclear Medicine, Radboud university medical center, Nijmegen, The Netherlands

Abstract

Monoclonal antibody G250 (mAbG250) recognizes a determinant on carbonic anhydrase IX (CAIX). CAIX is expressed by virtually all renal cell carcinomas of the clear cell type (ccRCC), but expression in normal tissues is restricted. The homogeneous CAIX expression in ccRCC and excellent targeting capability of mAbG250 in animal models led to the initiation of the clinical evaluation of mAbG250 in (metastatic) RCC (mRCC) patients. Clinical studies confirmed the outstanding targeting ability of mAbG250 and cG250 PET imaging, as diagnostic modality holds great promise for the future, both in detecting localized and advanced disease. Confirmation of the results obtained in the non-randomized clinical trials with unmodified cG250 is needed to substantiate the value of cG250 treatment in mRCC. cG250-Based radio immuno-therapy (RIT) holds promise for treatment of patients with small-volume disease, and adjuvant treatment with unmodified cG250 may be of value in selected cases. In the upcoming years, ongoing clinical trials should provide evidence for these assumptions. Lastly, whether cG250-based RIT can be combined with tyrosine kinase inhibitors, which constitutes the current standard treatment for mRCC, needs to be established.

1. Introduction

Renal cell carcinoma (RCC) accounts for approximately 3% of all cancers and was estimated to be diagnosed in over 60,000 individuals in the United States in 2011 [1]. The most prominent subtype of RCC (~70%) is clear cell (ccRCC). In approximately 70% of patients, the tumor is confined to the kidney at presentation. In 30% of cases, patients present with or develop metastases at a later time point. Patients with advanced disease have a poor prognosis with an overall five-year survival of <10%. Based on the molecular insight that ccRCC is characterized by molecular aberrations that leads to high expression levels of amongst others VEGF, various anti-angiogenic therapies have been developed. For patients with metastatic RCC (mRCC), several anti-angiogenic therapies are available [2–7]. Implementation of these new treatment modalities has led to a significant increase in progression-free survival [8]. However, complete responses (CR) are rare, and long-lasting stable disease (SD) is often seen, but eventually all patients progress. Moreover, frequently significant toxicity can occur, which may lead to drug cessation or dose reduction.

Monoclonal antibody G250 (mAbG250) was isolated more than 25 years ago from a hybridoma produced from a splenocyte of a mouse immunized with a fresh human RCC [9]. Immunohistochemical analysis of renal tumors showed homogeneous expression in the vast majority (>80%) of primary RCC and about 70% of mRCC lesions. Analyses of non-RCC tumors revealed variable, non-homogeneous staining. Initial specificity analysis on normal human tissues revealed cross-reactivity with gastric mucosal cells and large bile ducts. Subsequent in-depth fine-specificity analysis revealed reactivity with epithelial cells of the upper gastrointestinal tract and pancreatic cells. Originally, no association with a particular histological RCC subtype was noted, but it is now clear that the antigen recognized by mAbG250 is almost ubiquitously expressed in ccRCC [10,11]. Based on this fine-specificity analysis, mAbG250 target antigen was readily suggested as a potential diagnostic and therapeutic target.

2. Cloning of G250 Antigen and Relation to ccRCC

The general occurrence of the antigen recognized by mAbG250 in RCC and absence from normal kidney suggested that the aberrant expression was inherently related to tumor development, possibly due to a common initiating event [9].

Cloning of the antigen recognized by mAbG250 showed that mAbG250 recognized a conformational determinant of carbonic anhydrase IX (CAIX), a gene originally identified in HeLa cells [12,13]. CAIX is a member of the carbonic anhydrase group of enzymes, has a transmembrane, as well as a cytosolic domain, and catalyzes the reaction: $CO_2 + H_2O \leftrightarrow HCO_3^- + H^+$. Extensive molecular studies of the CAIX promoter region demonstrated that HIF-1α binding was an absolute requirement for CAIX expression in ccRCC [14]. This finding uncovered a direct molecular link between the observed ccRCC-specificity of mAbG250 and

the molecular events leading to ccRCC. Elegant molecular studies in families suffering from Von Hippel-Lindau (VHL) syndrome, an autosomal dominant disease, showed that defects in the VHL gene were responsible for tumor development. These patients develop multiple tumors, including ccRCC. Studies in sporadic ccRCC demonstrated that also in these cases, VHL was mutated [15]. Subsequent studies showed that VHL is involved in the hypoxic response: under normoxic conditions, hypoxia-inducible factor-1α (HIF-1α) is hydroxylated by prolyl hydroxylase domain proteins and bound by pVHL, catalyzing the polyubiquitylation of prolyl hydroxylated HIF-1α for subsequent degradation via the 26S proteasome [16,17]. If pVHL is mutated, as in ccRCC, binding of HIF-1α by pVHL does not occur; the unbound HIF-1α is not degraded, but associates with the constitutively stable partner HIF-1β to form an active heterodimeric HIF-1 transcription factor, which binds to hypoxia-responsive elements located in the promoter/enhancer regions of numerous hypoxia-inducible genes. In view of the HIF-1α dependency of CAIX expression, the ubiquitous expression of the G250/CAIX antigen could be explained straightforwardly by nonfunctional VHL gene product in ccRCC (Figure 1).
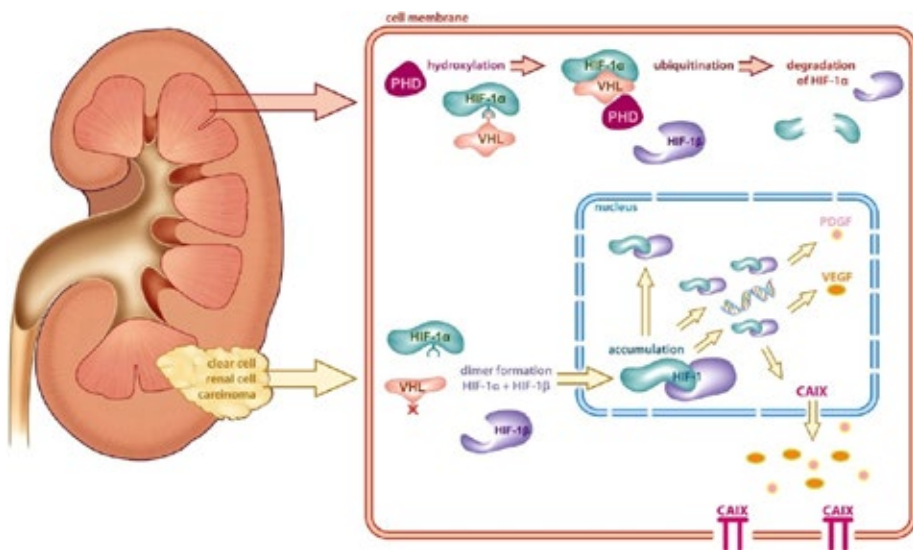
Figure 1. Schematic representation of regulation of carbonic anhydrase IX expression (CAIX) in kidney. In normal kidney tissue, hypoxia inducible factor-1α (HIF-1α) is hydroxylated by prolyl hydroxylase domain proteins (PHD) and bound by Von Hippel-Lindau protein (pVHL). Subsequently, the complex is ubiquitinated, which causes degradation of HIF-1α. In clear cell renal cell carcinoma (ccRCC), pVHL is mutated and binding with HIF-1α is prohibited. Subsequently HIF-1α forms a heterodimeric complex with HIF-1β, translocates to the nucleus, where it activates hypoxia inducible genes, such as vascular endothelial growth factor and CAIX, which is expressed on the tumor cell membrane. Reproduced with permission from Stillebroer *et al*., European Urology, published by Elsevier, July, 2010; 58(1):75–83 [20].

Elucidation of the molecular pathway of *CAIX* gene expression also readily explained the heterogeneous staining pattern in non-RCC tumors: this is the consequence of local hypoxia,

leading to HIF-1α stabilization and subsequent G250/CAIX expression. In fact, G250/CAIX is now regarded as an appropriate substitute hypoxia marker in various tumor types [18,19].

3. Clinical Studies with mAbG250

3.1. Imaging Studies

The incidental detection of renal lesions has increased up to 50% by improved radiologic imaging, such as contrast enhanced CT and positron emission tomography (PET) with fluorine-18 fluorodeoxyglucose (^{18}F-FDG) [21,22]. With increased possibilities for nephron-sparing surgery and the realization that around 20% of these masses are benign tumors, 25% are indolent tumors with limited metastatic potential and 54% represent the more potentially malignant ccRCC, it has become important to differentiate between these entities. However, conventional techniques have difficulties in differentiating between benign and malignant renal lesions. Therefore, surgical interventions are performed that could have been prevented. Consequently, new imaging techniques are needed to improve the differentiation between benign and malignant renal lesions. In view of the ccRCC specificity of mAbG250, multiple studies have addressed its ccRCC targeting capabilities.

Since its discovery, numerous preclinical targeting studies were performed in various mouse models [23–26] with various radionuclides, as well as in *ex vivo* perfusion experiments in tumor-bearing kidneys [27] with mAbG250. Selective and extraordinary high uptake of murine mAbG250 (mG250) in antigen-positive tumor xenografts was observed (e.g., up to more than 100% of the injected dose per gram tumor tissue at the lowest protein doses (up to 1 µg)). The combination of the restricted G250/CAIX expression in normal tissues, homogeneous G250/CAIX expression in RCC and excellent targeting capability in animal models provided a solid basis for the initiation of the clinical evaluation of mG250 in patients to investigate the possibility to use CAIX imaging as a new diagnostic tool.

The first clinical study with mouse mAbG250 (mG250) concerned a phase I presurgical protein dose-escalating study of ^{131}I-mG250 conducted to determine tumor uptake and mG250 distribution in patients suspect for RCC [28]. Apart from clear visualization of primary and metastatic (known and occult) RCC at protein doses >2 mg, occult metastases were imaged, immediately demonstrating the diagnostic potential. Levels of mG250 in tumor tissue samples reached levels of up to 0.1% of the injected dose per gram of tumor (%ID/g), these levels being among the highest reported in studies of solid tumors. Additionally, normal tissue uptake, actually limited to the liver, was saturable, encouraging future development of mG250 in RCC. Because histological confirmed CAIX-negative tumors did not image, it was concluded that mAbG250 accumulation was CAIX-specific. Since administration of murine G250 led to the formation of human-anti-mouse-antibodies (HAMA) in all patients, preventing multiple administrations [29], a chimeric variant of G250 (cG250) was constructed (see Table 1).

Table 1. Overview of imaging studies with mAbG250 in RCC patients

Ref.	Year	Agent	Number of patients	Patients	Outcome [#]	Remarks
Oosterwijk et al. [28]	1993	^{131}I-mG250	15	Primary RCC	12/12 pts	Phase I, dose escalation
Steffens et al. [30]	1997	^{131}I-cG250	16	Primary RCC	13/13 pts	Phase I, dose escalation
Steffens et al. [31]	1999	^{131}I-cG250 & ^{111}In-cG250	10	Primary RCC	10/10 pts	Dual label study
Brouwers et al. [32]	2002	^{131}I-cG250 vs. ^{18}F-FDG	20	M + RCC	^{131}I-cG250: 34/112 ^{18}F-FDG: 77/112 lesions	Comparative intrapatient study
Brouwers et al. [33]	2003	^{131}I-cG250 & ^{111}In-cG250	5	M + RCC	^{111}In-cG250: 47 lesions ^{131}I-cG250: 30 lesions	Comparative intrapatient study
Divgi et al. [34]	2007	[124]I-cG250	26	Primary RCC	15/16 ccRCC imaged	Prospective cG250-immunoPET
Divgi et al. [35]	2013	[124]I-cG250	226	Primary RCC	124/143 ccRCC imaged (sens. & spec. 86%)	Phase III, REDECT trial
Muselaers et al. [36]	2013	^{111}In-cG250	29	Primary RCC	15/16 ccRCC imaged	^{111}In-cG250 immunoSPECT

[#] outcome refers to diagnostic accuracy, i.e., number of positive images over total number of images mG250: mouse monoclonal antibody G250; cG250: chimeric monoclonal antibody G250; ccRCC: clear-cell renal cell carcinoma; ^{18}F-FDG: fluorine-18 fluorodeoxyglucose; M + RCC: metastatic renal cell carcinoma;

PET = positron emission tomography; SPECT: single-photon emission CT; sens.: sensitivity; spec.: specificity.

Because chimerization might lead to altered pharmacokinetic and pharmacodynamic behavior, a phase I protein dose-escalation trial of ^{131}I-cG250 identical to the phase I mG250 protein dose-escalation trial was necessary [30]. All patients with an antigen-positive tumor (*n* = 13) showed excellent targeting of radioactivity to all known tumor sites. Similar to mG250, previously undetected metastatic lesions (brain, bone and soft tissue) were detected. An example of the excellent cG250 uptake is shown in Figure 2. The performance of the chimerized G250 mAb was almost identical to the mouse mAbG250, including the optimal protein dose (5–10 mg) and very high focal uptake (up to 0.52% ID/g). The half-life (t½ β) of cG250 was comparable to mG250 (68.5 h *vs.* 47 h). ^{131}I-cG250 uptake in non-tumor tissues remained low. Most importantly, chimerization greatly diminished the immunogenicity of the antibody: in only two of 15 patients, low levels of human anti-chimeric antibody (HACA) were observed [30]. Thus, multiple administrations became feasible.
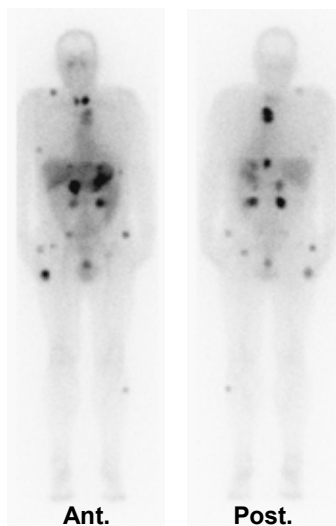
Figure 2. Whole body scan of a patient with multiple RCC metastases two weeks after infusion of 4144 MBq ^{131}I-cG250. **Ant.**: Anterior view; **Post.**: Posterior view. Note: thyroid uptake is due to non-specific accumulation, despite attempts to block thyroid uptake with intake of saturated potassium iodide.

Although very high uptake levels were observed, locally, cG250 tumor uptake was heterogeneous; this heterogeneity could not be explained by antigen expression alone. No consistent association with necrosis or vasculature was noted [37]. Since highly dynamic vascularization and intratumoral blood flow may contribute to this heterogeneous tumor

uptake, the impact of time on tumor uptake of cG250 was studied in a clinical setting. In this dual-label study, ten patients with a clinical diagnosis of primary RCC received two independent consecutive administrations of cG250, separated by four days. Post-surgery, the distribution of both administrations was mapped and analyzed. The study demonstrated that cG250 distribution did not differ between different administrations, indicating that intrinsic tumor factors, such as internalization and local differences in interstitial fluid pressure, played a prominent role in intra-tumoral heterogeneity of antibody distribution [31]. Initially, this explanation was felt to be improbable, because ^{131}I-cG250 tumor retention in patients was in the order of weeks, suggesting very low internalization rates [29].

To compare ^{131}I-cG250 radioimmunoscintigraphy (RIS) with ^{18}F-FDG PET, 20 mRCC patients were scanned using both techniques. Routine imaging modalities, performed before the experimental imaging techniques, revealed 79 metastases in these 20 patients. ^{18}F-FDG PET and ^{131}I-cG250 scintigraphy revealed 33 previously unknown lesions, of which 32 were PET positive and seven cG250-positive. Remarkably, ^{131}I-cG250 RIS detected only 30% (34/112) of documented metastases, whereas with ^{18}F-FDG PET, 69% (77/112) were detected [32]. The low percentage of RCC metastases detected by cG250-RIS in this study contrasts with the results of many other studies, where excellent visualization of all known metastases occurred and often new lesions were visualized, which were not seen using conventional imaging techniques. The inferiority of ^{131}I-cG250 RIS in detecting metastases might have been due to internalization of the radiolabeled mAb and subsequent excretion of ^{131}I by the tumor cells. Internalization and translocation of mAbG250 to the endocytic recycling compartment *in vitro* has been described before [38]. Alternatively, it is possible that many lesions were CAIX-negative, albeit that, in general, approximately 75% of ccRCC metastases are high in CAIX expression [39]. Unfortunately, we were unable to determine the CAIX expression in this trial, since lesions were unavailable.

The dual label clinical trial suggested that cG250 can be internalized by G250 antigen-expressing RCC cells. Indeed, follow-up animal experiments demonstrated that internalization can occur [40] and that accumulation in tumors of cG250 labeled with residualizing radionuclides, such as ^{111}In, might be higher than that of non-residualizing [131]I [25,41]. To investigate this phenomenon in detail in patients with RCC, a dual-label study was performed, with cG250 labeled with the residualizing radionuclide ^{111}In and non-residualizing radionuclide [131]I [33]. Four days post injection, the ^{111}In-cG250 images revealed more metastatic lesions ($n = 47$) than ^{131}I-cG250 ($n = 30$). Moreover, quantitative analysis of 25 metastases showed higher activities of ^{111}In-cG250 than of ^{131}I-cG250 in 20 of 25 lesions, thus ^{111}In-cG250 outperformed ^{131}I-cG250 for visualization of metastatic RCC lesions. This was partly due to the superior gamma camera characteristics of ^{111}In, but mainly because higher tumor:blood ratios were obtained.

ImmunoPET—that is, PET scanning that combines the favorable characteristics of PET (higher spatial resolution, three-dimensional imaging and superior quantitative analysis of images) with cG250—seems ideal for RCC imaging. However, the most commonly used positron emitters (^{11}C and ^{18}F) cannot be combined with the relatively slow pharmacokinetics

of intravenously injected radiolabeled mAb (optimal tumor uptake after several days), because of their too-short half-lives (2 min to 1.8 h). On the other hand, the positron emitters, [89]Zr and [124]I (half-lives 78 and 100 h, respectively), seem to be good candidates to match these slow kinetics. In the first cG250 immunoPET study, [124]I-cG250 (185 MBq, 10 mg) was evaluated in 26 patients with suspect renal masses to study whether ccRCC could be recognized unequivocally. In 15/16 patients with histological confirmed ccRCC after surgery, positive images were obtained (one patient received nonreactive antibody, due to technical problems). In addition, all nine non-clear cell renal masses were negative; hence, the sensitivity and specificity of [124]I-G250 PET for ccRCC was 94% and 100%, respectively. The negative (NPV) and positive predictive value (PPV) were 90% and 100%, respectively [34].

This proof of principle study suggested that immunoPET might help in clinical decision-making and might aid in the surgical management of patients with small renal masses scheduled for partial nephrectomy.

To substantiate whether cG250 immunoPET might be helpful in the clinical management of patients with suspect renal masses, a large multicenter phase III trial comparing [124]I-cG250 immuno PET/computed tomography (CT) ([124]I-Girentuximab/REDECTANE®) scanning to contrast enhanced CT (CECT) for the detection of ccRCC was performed. In total, 226 patients scheduled for partial or complete nephrectomy were enrolled in this study [35]. [124]I-girentuximab was well tolerated, and 195 patients were evaluable. The results of this trial confirmed the high specificity and sensitivity of [124]I-cG250 for ccRCC. Notably, the average sensitivity and specificity were higher for G250 PET/CT than for CECT (86.2% *vs*. 75.5% and 85.9% *vs*. 46.8%, respectively). The authors concluded that [124]I-girentuximab PET/CT can accurately and noninvasively identify ccRCC, with potential utility for designing best management approaches for patients with renal masses. One limitation of [124]I-based immunoPET is the limited availability of [124]I worldwide, requiring centralized production.

Because girentuximab labeled with the gamma-emitting radionuclide indium ^{111}In is easier to produce as an off-the-shelf agent, not requiring centralized production nor specialized equipment, and because dual labeling studies showed superior imaging of ^{111}In-cG250 in mRCC [33], we investigated this agent as a potential imaging modality. Similar to [124]I-girentuximab immunoPET, single-photon emission CT (SPECT) with ^{111}In-labeled girentuximab is non-invasive and does not require the use of intravenous contrast agents, which makes it suitable for patients with an impaired renal function. In this study, 29 patients with an incidentaloma of the kidney or having a history of ccRCC with lesions on follow-up imaging suspect for metastases were enrolled [36]. Distinct uptake of ^{111}In-girentuximab was seen in 16 of 22 patients presenting with a renal mass (Figure 3). All renal masses proven to be ccRCC after resection (*n* = 15) were detected with ^{111}In-girentuximab. In one of the 16 patients, a type 2 papillary RCC with histological proven CAIX expression was targeted with ^{111}In-girentuximab. In addition, no targeting was observed in six patients. Histopathological evaluation in 4/6 patients revealed two cases of benign oncocytoma, a chromophobe and a mucinous tubular spindle cell carcinoma subtype tumor. For the two remaining patients,

biopsy material was unavailable, but close monitoring with repeated CT scans did not reveal growth of the suspected mass in the follow-up period (>24 months). In this limited group of patients, the PPV of ^{111}In-girentuximab imaging for ccRCC was 94%. In addition, seven patients with a history of ccRCC and possible metastatic lesions on follow-up computed tomography scans were imaged with ^{111}In-girentuximab. In 4/7 patients, the lesions showed preferential uptake of ^{111}In-girentuximab and local or systemic treatment was initiated. In three other cases, no targeting was seen. During follow-up of these three patients, 1/3 showed progression, for which systemic treatment was started. In conclusion, cG250 immunoSPECT either labeled with [124]I or with ^{111}In can be used to detect ccRCC lesions in patients with a primary renal mass and to clarify the nature of lesions suspect for metastases in patients with a history of ccRCC.
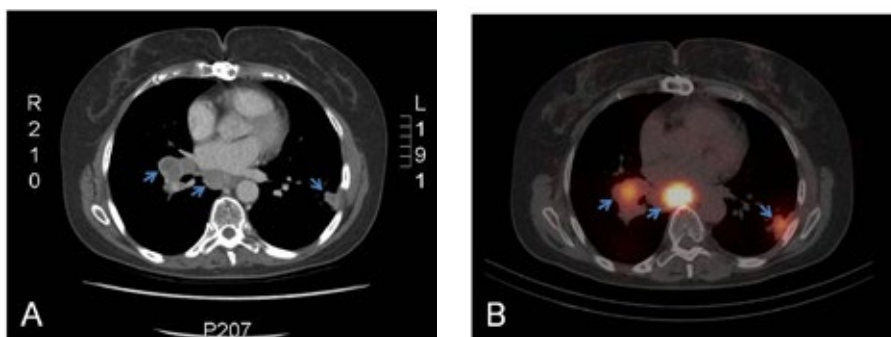
Figure 3. Images of a patient with metastatic RCC. Conventional CT (**A**) and ^{111}In-girentuximab immunoSPECT (**B**) images of a patient with metastatic ccRCC. Clear and preferential uptake of the radiolabeled antibody was observed in mediastinal and pleural lesions (arrows). The patient was enrolled in the phase II ^{177}Lu-girentuximab RIT trial.

3.2. Therapy Studies

The therapeutic potential of CAIX targeting with mAbG250 has been studied in numerous clinical trials (see Table 2). Roughly, these can be divided into trials with "naked" antibody alone or in combination with cytokines and radioimmunotherapy trials.

In the first dose escalating radioimmunotherapy (RIT) trial, ^{131}I-mG250 was administered to progressive patients with measurable, histological proven ccRCC [29]. In this trial, hepatic toxicity was observed, most likely the result of specific mG250 accumulation in the liver. Indeed, with higher doses, the liver uptake was decreased, suggesting saturation of G250 sites by the antibody. The toxicity was transient and not dose-limiting. As in all RIT studies with radiolabeled antibodies, dose-limiting toxicity (DLT) was hematopoietic. After determining the maximum tolerated dose (MTD) of ^{131}I-activity (3330 MBq/m^2), 15 patients were treated at the MTD level to determine efficacy, but no major responses were noted.

However, overall survival of patients treated with ^{131}I-mG250 seemed to be increased in comparison with that of historic control patients: 17/33 SD and two minor responses. As mentioned earlier, the development of high HAMA levels in all patients precluded retreatment, and all subsequent trials were carried out with cG250.

Following the protein dose-escalation trial with ^{131}I-cG250, which established the most favorable protein dose, a phase I ^{131}I-cG250 activity dose escalation was performed to establish DLT similar to the mG250 trial [42]. One major adjustment was the inclusion of an imaging dose (222 MBq of [131]I- labeled to 5 mg of cG250), before being allowed to advance to therapeutic dose (1665–2775 MBq of [131]I- labeled to 5 mg of cG250) to prevent infusion of high-dose ^{131}I-cG250 in CAIX-negative patients.

Only those patients showing targeting to tumor (*n* = 8) received the therapeutic infusion of ^{131}I-cG250 one week later. Unexpectedly, through the administration of the scout dose, liver toxicity was avoided, most likely because the liver compartment was saturated. Alternatively, hepatic uptake of chimeric mAbG250 is lower than murine mAbG250. At equal doses, liver uptake of mG250 [28] was 2–3-times higher than the liver uptake of cG250 [30]. Dose-limiting toxicity of ^{131}I-cG250 was at 2775 MBq ^{131}I-cG250/m^2, significantly lower than DLT observed for the murine version. The MTD was therefore set at 2220 MBq/m^2. Almost certainly, the extended serum half-life is responsible for the enhanced hematopoietic toxicity, since this leads to extended radiation of the bone marrow compartment.

In one patient, HACA was observed in the serum sample obtained prior to the injection of the radiolabeled antibody, as well as in subsequent serum samples. cG250 was rapidly cleared. The observed HACA was probably due to previous injections with mAbG250. This particular patient had participated four months beforehand in another clinical study and had received two injections of mAbG250, four days apart. Targeting of mAbG250 was observed in his primary tumor at that time. No HACA responses were detected in all other patients.

An antitumor response was observed in 2/8 patients; one SD for 3–6 months and one partial response (PR) >9 months. Both patients were treated at the 2220 MBq/m^2 dose level. However, quite disappointingly, all other patients showed progression of disease.

This first RIT trial with cG250 clearly showed that increased doses of radioactivity to the tumors were required to achieve more complete and lasting responses. In an effort to increase RIT efficacy, a fractionated dose RIT was performed, based on whole-body radiation absorbed dose [43].

Fractionated RIT is more effective than a single large amount and is associated with a lower toxicity profile in animal models. The primary objective of this trial was to determine the maximum tolerated whole-body radiation-absorbed dose of fractionated ^{131}I-cG250, with dose escalation referred to here as the escalation of average whole-body absorbed dose. Fifteen patients with measurable metastatic renal cancer were included. The majority of patients tolerated repeated injections with no change in kinetics, confirming the lack of immunogenicity of the antibody construct. Whole-body and serum kinetics varied significantly between patients, with estimated biologic clearance half-times ranging from 3.2 to 7.5 days

Table 2. Overview of Therapy studies with mAbG250 in RCC patients.

Ref	Year	Agent	Number of patients	Patients	Response	Duration Response	Remarks
Divgi et al. [29]	1998	^{131}I-mG250	33	M + RCC	17 SD; 16 PD	2–3 mo	Phase I/II
Steffens et al. [42]	1999	^{131}I-cG250	12	M + RCC	1 PR; 1 SD; 10 PD	9+; 3–6 mo	Phase I Activity dose
Divgi et al. [43]	2004	^{131}I-cG250	15	M + RCC	7 SD; 8 PD	2–11 mo	Phase I fractionated dose
Brouwers et al. [44]	2005	^{131}I-cG250 Two doses	27	M + RCC	5 SD; 22 PD	3–12 mo	Phase I two high doses
Stillebroer et al. [45]	2012	^{177}Lu-cG250 Multiple doses	23	M + RCC	1 PR; 17 SD	9+; 3+ mo	Phase I dose escalation
Davis et al. [46]	2007	cG250	12	M + RCC	1 CR; 8 SD; 3 PD	6–66 wk	Phase I
Bleumer et al. [47]	2004	cG250	36	M + RCC	1 CR; 1 PR; 8 SD; 26 PD	1–20+ wk	Phase II
ARISER [48]		cG250	864	High risk, after nephrectomy	No benefit *		Phase III
Davis et al. [49]	2007	cG250 + IL-2	9	M + RCC	2 SD; 7 PD	6, 12 wk	Phase I
Bleumer et al. [50]	2006	cG250 + IL-2	35	M + RCC	1 PR; 7 SD; 27 PD	95+; 24+ wk	Phase II
Siebels et al. [51]	2011	cG250 + IFN-2α	31	M + RCC	1 CR; 9 SD	17+; 24+ wk	Phase II

* No benefit for whole population, high CAIX expression correlated with risk of recurrence reduction. mG250: mouse monoclonal antibody G250; cG250: chimeric monoclonal antibody G250; ccRCC: clear-cell renal cell carcinoma; M + RCC: metastatic renal cell carcinoma; IL-2: interleukin-2; IFN: interferon; CR: complete response; PR: partial response; SD: stable disease; PD: progressive disease; mo: months; wk: weeks.

for the whole body and from 1.3 to >5 days for serum β–half-life (t½ β). In two of 15 patients, HACA was observed, which lead to a faster serum clearance. Similar to single dose, cG250 RIT, DLT was hematopoietic. In this logistically demanding fractionated administration regimen, sparing of the hematopoietic system was not observed. Moreover, the total dose that could be delivered was low, and efforts along these lines were abandoned.

In view of the minimal clinical response in single doses cG250 RIT, a study was performed with two sequential high-dose (at MTD) ^{131}I-cG250 treatments in patients with progressive mRCC [44]. After receiving a scout dose of 185 MBq/m^2 of ^{131}I-cG250 to demonstrate tumor targeting, 29 patients with adequate cG250 uptake received a therapeutic dose of 2220 MBq/m^2 ^{131}I-cG250. In the absence of grade 4 hematological toxicity, patients received a second cycle after three months, consisting of a diagnostic infusion and a second high dose injection of ^{131}I-cG250, escalated from 1110 MBq/m^2 to 1665 MBq/m^2. The MTD of the second RIT was 1665 MBq/m^2, with myelotoxicity as DLT. Four patients were excluded from the study, because they developed HACA after the first RIT dose (*n* = 2), after the second scout dose (*n* = 1) or after the second RIT dose. Those patients developed high HACA titers with enhanced clearance of injected mAbG250 (t½ β: 20–27 h). In an additional four patients, detectable HACA titers at low levels developed in the course of the study. In these patients, no enhanced clearance was observed (t½ β: 52–74 h). Of the 16 patients who completed the protocol at both MTDs, none demonstrated an objective response, but five previously progressive patients had stabilization of their disease lasting 3–12 months. The low efficacy was partly attributed to the bulky disease in these end-stage patients, as sufficiently high radiation doses of ^{131}I could not be delivered to these large tumor masses. An inverse correlation between the size of metastases and radiation-absorbed dose was observed, and dosimetric analyses showed that therapeutic radiation doses (>50 Gy) were only guided to lesions smaller than 5 g. Therefore, it was suggested that future RIT with cG250 should aim at treatment of small-volume disease or should be used in an adjuvant setting, or other more potent radionuclides should be used [52].

Preclinical animal studies performed with cG250 labeled with more potent radionuclides (^{177}Lu, ^{90}Y or ^{186}Re) for RIT showed that tumor growth was most effectively inhibited by ^{177}Lu-cG250, followed by ^{90}Y-, ^{186}Re- and ^{131}I-cG250 [41]. Metabolites labeled with metallic radionuclides, such as ^{111}In, ^{90}Y and ^{177}Lu, are trapped in the lysosomes and residualize after internalization of the mAb–antigen complex by the target cells. Intracellular ^{131}I-cG250 is metabolized, and tyrosine-^{131}I is rapidly excreted by the tumor cell upon internalization. These RIT studies clearly showed the superiority of ^{177}Lu- and ^{90}Y-based RIT, in line with other studies. The dual-label study discussed before [33] also supported that trapped radionuclides are superior to the non-trapped iodine. In view of this evidence, subsequent clinical studies have focused on the possibility to use ^{90}Y or ^{177}Lu in RIT [53].

Recently, the results of a phase I/II trial with ^{177}Lu-cG250 were published [45]. This trial was paralleled by a trial with ^{90}Y-cG250 at Memorial Sloan Kettering Cancer Centre, New York (clinicaltrials.gov/NCT00199875). In the ^{177}Lu-cG250 trial, 23 patients with progressive

mRCC with proven ccRCC received a diagnostic dose of ^{111}In-cG250 (185 MBq), to establish adequate tumor accumulation followed by a dose of ^{177}Lu-cG250 one week post ^{111}In-cG250 injection (start dose 1110 MBq/m^2 ^{177}Lu, increments of 370 MBq/m^2; three patients/dose level). In four patients, elevated HACA levels during treatment were observed. In two patients, these HACA levels precluded administration of a subsequent treatment cycle. In the absence of grade 4 toxicity, patients were eligible to receive a second (13/23) and a third cycle (4/23), at 75% of the dose level of the previous injection. Hematopoietic toxicity was dose-limiting, and MTD was set at 2405 MBq/m^2, ^{111}In-cG250 images were superimposable on the ^{177}Lu-cG250 images, illuminating the predictive value of ^{111}In-cG250 for ^{177}Lu-cG250 accumulation [45]. In one patient, grade IV toxicity was observed at the 1850 MBq/m^2 dose level. No significant toxicity was observed in the other patients treated at MTD, also not after the second or third treatment cycle. The majority of patients responded by stabilization of disease. In one patient (1850 MBq/m^2 dose level), a PR was documented that lasted for nine months. Dosimetric analyses indicated effective uptake after consecutive treatments. Observed hematologic toxicity, especially platelet toxicity, correlated significantly with the administered activity, whole-body absorbed dose and red marrow dose. The tumor-to-red marrow dose ratio was higher for RIT with ^{177}Lu-cG250 than for RIT with ^{90}Y-cG250, indicating that ^{177}Lu has a wider therapeutic window for RIT with cG250 than [90]Y. The authors concluded that in patients with metastasized renal cell carcinoma, higher radiation doses can be guided to the tumors with ^{177}Lu-cG250 than with ^{90}Y-cG250 [54]. The authors concluded that RIT with ^{177}Lu-cG250, targeting CAIX, may stabilize previously progressive metastatic ccRCC.

3.3. Therapeutic Studies with Unmodified cG250

Antibodies have the capacity to lyse cells by complement activation or by antibody-dependent cellular cytotoxicity (ADCC). *In vitro* studies established that cG250 could initiate cell lysis through ADCC of CAIX-positive cells [55,56]. Also, significant tumor growth reduction was noted when mice bearing human RCC xenografts were treated with naked mAbG250 [49]. Based on these results, a phase 1 study with escalating doses of 5–50 mg/m^2 of cG250 (Girentuximab/RENCAREX®), with weekly infusions for 6 weeks, was initiated. Treatment up to the highest dose was safe and well tolerated. Of the 11 mRCC patients treated, one patient showed a CR and nine patients had SD after one treatment cycle [46].

In the subsequent phase 2 study, 36 patients with advanced RCC were included, all received 50 mg of cG250 weekly for 12 weeks. Before treatment, 80% of patients were progressive. After one treatment cycle, 28% of previously progressive patients had SD for at least six months, suggesting a clinical benefit [47]. During follow-up, one CR and one PR were noted, which lasted >1 year. The median survival of 15 months with 41% of the 32 evaluable patients still alive after two years suggested that cG250 might be able to modulate the natural course of mRCC. One group of patients received extended treatment (an

additional eight weeks of treatment). These patients showed a median survival of 39 months, compared to 10 months in the discontinued group. Patients receiving extended treatment with cG250 showed a significantly longer survival rate than the nonresponsive patients (70% *vs*. 26%). The levels of mAbG250-mediated ADCC differed between the patients: 42% of the patients showed moderate ADCC (5%–25%), whereas in 33% of patients, no ADCC was demonstrated. There was no clear correlation between the *in vitro* levels of cytotoxicity and the clinical responses. In addition, no correlation between the proportion of NK cells and the level of mAbG250-mediated ADCC was observed. In this non-randomized setting, it has been difficult to evaluate the true effect of cG250 treatment on the disease course of patients, as the natural disease course of mRCC is highly variable and periods with SD and/or PR can occur, even in the absence of treatment.

Based on these results, an adjuvant double-blind, placebo controlled phase 3 trial was started (ARISER, Adjuvant RENCAREX® Immunotherapy Phase III trial to study efficacy in non-metastatic RCC), aiming at reducing the recurrence of disease in nephrectomized RCC patients who have a high risk of relapse (http://www.wilex.de/portfolio-english/rencarex/phase-III-ariser/) [48]. The trial recruited 864 patients with prior nephrectomy of primary ccRCC; patients received a once-weekly infusion of RENCAREX® or placebo for 24 weeks. Those patients receiving the active drug received a loading dose of 50 mg in week 1 and weekly doses of 20 mg during weeks 2–24.

Unfortunately, the trial did not meet its primary endpoint. The analysis showed no improvement in median DFS (approximately 72 months) following RENCAREX® treatment compared with placebo. However, preliminary results of a retrospective subanalysis appear to indicate that with increasing CAIX expression in tumor tissue, as quantified by a CAIX score, the treatment was more effective; DFS showed a clinically and statistically significant improvement in the patient population with a high CAIX level treated with cG250 compared to both placebo and patients with a low CAIX score (press release Wilex, 26 February, 2013). No other data are available at present. Therefore, an cG250-based immunotherapy for ccRCC in the adjuvant setting might still be an option in a highly defined subpopulation.

Since interleukin-2 (IL-2) has been known to enhance ADCC of mAbs, the combination of this cytokine with cG250 was evaluated. *In vitro* studies had demonstrated that cG250 ADCC was increased when cells from IL-2-treated patients were used, suggesting that the combination of cG250 with IL-2 might be superior to cG250 alone [55]. In a phase 2 trial, 35 patients with progressive mRCC received weekly intravenous infusions of 50 mg of cG250 and daily subcutaneous low-dose IL-2 for 11 weeks. Treatment was well tolerated with little toxicity, attributable to IL-2. Clinical benefit was noted in eight of 35 patients (23%), with one long-lasting PR (>95 weeks), six long-lasting SD (>24 weeks) and a mean survival of 24 months, with 45% of the 30 evaluable patients still alive after two years. The extended treatment group (an additional six weeks of treatment) showed a median survival of 41 months, compared with 13 months in the non-response group. Patients receiving extended treatment showed a significantly longer survival rate than the non-response patients (55% *vs*.

25%). The increased survival (as compared to historic controls) was deemed to be cG250-related and not related to the IL-2, as a six-fold decrease of the normal IL-2 dose was used [50]. The favorable outcome might have been due to a synergistic effect of cG250 and IL-2, as was observed in the *in vitro* studies.

The number of effector cells (CD3−/CD16+/CD56+) increased during treatment, but lytic capacity per cell did not increase and ADCC and clinical outcome did not correlate. Similar results were observed in the study performed by Davis *et al*. [49]. Yet again, because patients were not randomized, it is difficult to judge the value of this observation. A randomized trial is needed to determine the true effect of the IL-2/cG250 treatment.

Based on *in vitro* observations that with the addition of Interferons (IFNs), G250/CAIX expression was upregulated and that with Interferon gamma (IFN-γ), ADCC of cG250 was enhanced, the effect of cG250 combined with IFN-α was studied [56,57].

In a multicenter, open-label, prospective, single-arm phase I/II trial study, cG250 in combination with IFN-α 2a was studied in a total of 32 patients with stage IV progressive RCC [51]. Patients received 20 mg cG250 weekly for three months, combined with IFN-α 2a, three million international units (MIU), three times per week, subcutaneously. Twenty six of 31 patients were evaluable for response to treatment. Two patients showed a PR and 14 patients SD in week 16. One patient experienced a PR for at least eight months, and nine patients had long durable disease stabilization (≥24 weeks). Clinical benefit was obtained in 42% (11/26) of the patients. The overall median survival was 30 months for the 31 patients treated with WX-G250 and IFNα, with 57% of patients still alive after two years. The patients receiving extended treatment showed a median survival of 45 months compared with 10 months in the non-extended group. Patients receiving extended treatment with cG250 showed a significantly longer survival rate than the non-response patients (79% *vs.* 30%).

4. Future Prospects

Clinical studies have now firmly established that cG250 adequately targets ccRCC. However, to prove that cG250 imaging can be used to guide clinical management, more evidence is needed. Thus far, patients for whom surgery was part of their clinical management have been studied, but the question whether watchful waiting can be applied in patients in whom no cG250 targeting is seen remains to be answered. As suggested by Divgi *et al*. [35], the role of cG250 imaging in influencing outcome would perhaps be best assessed in a clinical trial carried out in patients with small renal mass tumors and associated comorbidities.

Another issue that needs further study is choice of radionuclide for imaging purposes. As discussed, ^{111}In-cG250 SPECT may provide the same information as [124]I-cG250 PET, but with the advantage that this can be produced as an off-the-shelf product that can be used on site. Alternatively, other radionuclides, such as [89]Zr, might provide a useful alternative: it is similar with respect to its chemical characteristics, but is PET imageable.

Although the adjuvant study in a group of high-risk patients did not reach its primary end-point, it is noteworthy to mention that in a subgroup analysis, patients with high CAIX expression as determined by IHC showed lower recurrence than patients negative or low in CAIX expression levels. Biomarker studies have demonstrated that CAIX staining correlates with survival, as well as with response to high dose IL-2 [58,59]. A cutoff of 85% CAIX staining provided the most accurate prediction of survival. Low CAIX (≤85%) staining was an independent poor prognostic factor for survival for patients with mRCC. For patients with non-metastatic RCC and at high risk for progression, low CAIX predicted a worse outcome similar to patients with metastatic disease. Intriguingly, CAIX expression correlated with response to high dose IL-2: survival >5 years was only seen in high CAIX expressers [60,61]. It is tempting to speculate that high-dose IL-2 treatment leads to expansion of CAIX-specific CTL, but characterization of 18 different TIL cultures suggested that anti-G250 reactivity is rare [13]. Patient stratification based on CAIX expression might lead to a (adjuvant) treatment strategy similar to, e.g., trastuzumab treatment of patients with breast cancer, where a very high correlation exists between HER2 expression and the success of trastuzumab, which targets HER2 [62].

In summary, mAbG250 has shown remarkable targeting ability, and the main value of the antibody at present appears to be as diagnostic and, also, as a delivery vehicle for RIT.

cG250 PET imaging holds great promise for the future, both in detecting localized and advanced disease, albeit that the radioisotope to use is still under investigation. In the near future, a clinical trial with PET tracer ^{89}Zr-girentuximab will be initiated in our center, which will provide additional information about the use of girentuximab-based immunoPET in ccRCC.

Clinical trials with unmodified cG250 suggest that treatment with cG250 can influence the disease course in mRCC patients. However, to validate whether cG250 treatment is of value, large, randomized trials are needed.

Besides the usefulness in radioimmunodetection, girentuximab is a potent carrier for RIT in ccRCC. However, there are still several hurdles to overcome before girentuximab-based RIT can be implemented as a standard treatment. As previously mentioned, it is not clear which patients benefit most from RIT. Past results indicate that RIT is mainly suitable for treatment of small-volume disease or, possibly, as adjuvant treatment in selected cases, and more evidence regarding this topic is expected from the ongoing clinical trials with ^{90}Y and ^{177}Lu-labeled girentuximab in the upcoming years. Besides better patient selection in the future, advances in dosimetric analysis will presumably contribute to the improvement of RIT, as the trade-off between efficacy and toxicity can be better tailored to the individual patient. Lastly, an important deficit in our current knowledge is how to optimally combine girentuximab-based RIT with the current standard of care in metastatic ccRCC.

CAIX has also been used as a target in gene therapy studies with modified autologous T-cells [63]. In these studies, patients with advanced RCC were infused with escalating doses of T-cells genetically retargeted with a chimeric antibody receptor (CAR) directed towards

carbonic anhydrase IX. Thus, the antigen-specific variable regions of mAbG250 (targeting to RCC) were linked to T-cell receptor signaling chains, leading to *CAIX* targeting in an MHC-independent context. Liver toxicity was observed at the lowest cell dose, illustrating the potency of the modified T-cells. The liver toxicity could be prevented by pre-dosing with cG250 before administering modified T-cells [64]. Given that similar to mAb studies, the observed "on"-target toxicity could be prevented by blocking antigenic sites in off-tumor organs, higher T-cell doses might be possible. Although this is a very intriguing approach, patient recruitment has been very slow, and the final results are awaited.

Finally, the clinical management of mRCC has changed significantly over the last few years. Implementation of various tyrosine kinase inhibitors (TKI) and mTOR inhibitors has led to improved progression-free survival. However, therapy resistance is a major issue, and these therapies are directed against the tumor vasculature and not against the tumor cells. Combination of TKI and cG250 might be beneficial: they attack different targets, and the combination might lead to synergistic effects. In a preclinical study, the biodistribution of cG250 was determined in TKI treated mice. TKI are known anti-angiogenic drugs, and thus, the accessibility of tumor cells is likely to be altered. In nude mice bearing human RCC xenografts treated orally with sunitinib, vandetanib or sorafenib, tumor uptake of cG250 decreased dramatically, and vascular density decreased considerably, as judged by various markers [65]. This is comparable to the TKI effects on tumors in patients: large central necrotic areas can develop in tumors when patients are treated with TKI. When treatment was stopped, robust neovascularization, mainly at the tumor periphery, became apparent. Consequently, cG250 uptake recovered, albeit that cG250 uptake appeared to be restricted to the tumor periphery, where vigorous neovascularization was visible. This animal study demonstrated that simultaneous administration of TKI and mAb cG250 is unlikely to improve therapy outcome. This was also demonstrated in patients; a markedly decreased uptake of ^{111}In-girentuximab after treatment with TKI sorafenib was observed [66]. Data from this study suggest that the effect of girentuximab-based RIT would be severely hampered if given during TKI treatment. However, the observation that shortly after discontinuation of TKI treatment, mAb accumulation was restored, suggested that sequential treatment strategies might be useful [65]. Because cG250 and TKI appear to be feasible in sequence only, studies were designed to determine the optimal interval between TKI treatment and cG250 administration. Biodistribution studies in two different animal models demonstrated that a 3-day time interval was sufficient to reach optimal antibody accumulation (manuscript in preparation). Because TKI are also given in cycles in patients (four week treatment followed by two weeks off treatment), it appears that, indeed, combination of Sunitinib with mAb cG250 is feasible in mRCC patients, but the optimal treatment schedule needs to be determined.

Anti-CAIX antibodies that combine inhibition of the enzymatic activity of CAIX with ADCC and/or CDC might be more potent than mAbG250, which does not inhibit the enzymatic activity of CAIX. Recently, a CAIX-specific antibody with an inhibitory effect on the carbonic anhydrase activity was described [67]. Up to 76% of CAIX activity was inhibited with the full-

length IgG antibody MSC8. The authors speculated that combining target specificity with enzymatic inhibition in one antibody molecule may have an additive effect on reducing tumor growth. This interesting hypothesis will need to be substantiated.

5. Conclusion

In summary, mAbG250 has shown outstanding targeting ability, and cG250 PET imaging holds great promise for the future, both in detecting localized and advanced disease, albeit that the most favorable radioisotope still needs to be determined.

Confirmation of the results obtained in the non-randomized clinical trials with unmodified cG250 is needed to substantiate the value of cG250 treatment in mRCC. Girentuximab-based RIT holds promise for treatment of patients with small-volume disease or, possibly, as adjuvant treatment in selected cases, and ongoing clinical trials in the upcoming years should provide evidence for this assumption. Lastly, whether combination of girentuximab-based RIT with the current TKI is possible needs to be established.

References

1. Jemal, A.; Siegel, R.; Ward, E.; Hao, Y.; Xu, J.; Thun, M.J. Cancer statistics, 2009. *CA Cancer J. Clin.* **2009**, *59*, 225–249.
2. Patard, J.J.; Pignot, G.; Escudier, B.; Eisen, T.; Bex, A.; Sternberg, C.; Rini, B.; Roigas, J.; Choueiri, T.; Bukowski, R.; *et al*. Icud-eau international consultation on kidney cancer 2010: Treatment of metastatic disease. *Eur. Urol.* **2011**, *60*, 684–690.
3. Motzer, R.J.; Rini, B.I.; Bukowski, R.M.; Curti, B.D.; George, D.J.; Hudes, G.R.; Redman, B.G.; Margolin, K.A.; Merchan, J.R.; Wilding, G.; *et al*. Sunitinib in patients with metastatic renal cell carcinoma. *JAMA* **2006**, *295*, 2516–2524.
4. Escudier, B.; Eisen, T.; Stadler, W.M.; Szczylik, C.; Oudard, S.; Siebels, M.; Negrier, S.; Chevreau, C.; Solska, E.; Desai, A.A.; *et al*. Sorafenib in advanced clear-cell renal-cell carcinoma. *N. Engl. J. Med.* **2007**, *356*, 125–134.
5. Rixe, O.; Bukowski, R.M.; Michaelson, M.D.; Wilding, G.; Hudes, G.R.; Bolte, O.; Motzer, R.J.; Bycott, P.; Liau, K.F.; Freddo, J.; *et al*. Axitinib treatment in patients with cytokine-refractory metastatic renal-cell cancer: A phase II study. *Lancet Oncol.* **2007**, *8*, 975–984.
6. Sternberg, C.N.; Davis, I.D.; Mardiak, J.; Szczylik, C.; Lee, E.; Wagstaff, J.; Barrios, C.H.; Salman, P.; Gladkov, O.A.; Kavina, A.; *et al.* Pazopanib in locally advanced or metastatic renal cell carcinoma: Results of a randomized phase III trial. *J. Clin. Oncol.* **2010**, *28*, 1061–1068.
7. Escudier, B.; Bellmunt, J.; Negrier, S.; Bajetta, E.; Melichar, B.; Bracarda, S.; Ravaud, A.; Golding, S.; Jethwa, S.; Sneller, V. Phase III trial of bevacizumab plus interferon alfa-2a in patients with metastatic renal cell carcinoma (avoren): Final analysis of overall survival. *J. Clin. Oncol.* **2010**, *28*, 2144–2150.
8. Coppin, C.; Kollmannsberger, C.; Le, L.; Porzsolt, F.; Wilt, T.J. Targeted therapy for advanced renal cell cancer (rcc): A cochrane systematic review of published randomised trials. *BJU Int.* **2011**, *108*, 1556–1563.
9. Oosterwijk, E.; Ruiter, D.J.; Hoedemaeker, P.J.; Pauwels, E.K.; Jonas, U.; Zwartendijk, J.; Warnaar, S.O. Monoclonal antibody g250 recognizes a determinant present in renal-cell carcinoma and absent from normal kidney. *Int. J. Cancer* **1986**, *38*, 489–494.
10. Uemura, H.; Nakagawa, Y.; Yoshida, K.; Saga, S.; Yoshikawa, K.; Hirao, Y.; Oosterwijk, E. Mn/ca ix/g250 as a potential target for immunotherapy of renal cell carcinomas. *Br. J. Cancer* **1999**, *81*, 741–746.
11. Bismar, T.A.; Bianco, F.J.; Zhang, H.; Li, X.; Sarkar, F.H.; Sakr, W.A.; Grignon, D.J.; Che, M. Quantification of g250 mrna expression in renal epithelial neoplasms by real-time reverse transcription-pcr of dissected tissue from paraffin sections. *Pathology* **2003**, *35*, 513–517.
12. Pastorek, J.; Pastorekova, S.; Callebaut, I.; Mornon, J.P.; Zelnik, V.; Opavsky, R.; Zat'ovicova, M.; Liao, S.; Portetelle, D.; Stanbridge, E.J.; *et al.* Cloning and characterization of mn, a human tumor-associated protein with a domain homologous to carbonic anhydrase and a putative helix-loop-helix DNA binding segment. *Oncogene* **1994**, *9*, 2877–2888.
13. Grabmaier, K.; Vissers, J.L.; de Weijert, M.C.; Oosterwijk-Wakka, J.C.; van Bokhoven, A.; Brakenhoff, R.H.; Noessner, E.; Mulders, P.A.; Merkx, G.; Figdor, C.G.; *et al.* Molecular cloning and immunogenicity of renal cell carcinoma-associated antigen g250. *Int. J. Cancer* **2000**, *85*, 865–870.
14. Grabmaier, K.; A de Weijert, M.C.; Verhaegh, G.W.; Schalken, J.A.; Oosterwijk, E. Strict regulation of caix (g250/mn) by hif-1alpha in clear cell renal cell carcinoma. *Oncogene* **2004**, *23*, 5624–5631.
15. Gnarra, J.R.; Tory, K.; Weng, Y.; Schmidt, L.; Wei, M.H.; Li, H.; Latif, F.; Liu, S.; Chen, F.; Duh, F.M.; *et al.* Mutations of the vhl tumour suppressor gene in renal carcinoma. *Nat. Genet.* **1994**, *7*, 85–90.
16. Jaakkola, P.; Mole, D.R.; Tian, Y.M.; Wilson, M.I.; Gielbert, J.; Gaskell, S.J.; von Kriegsheim, A.; Hebestreit, H.F.; Mukherji, M.; Schofield, C.J.; *et al.* Targeting of hif-alpha to the von hippel-lindau ubiquitylation complex by o2-regulated prolyl hydroxylation. *Science* **2001**, *292*, 468–472.
17. Schofield, C.J.; Ratcliffe, P.J. Signalling hypoxia by hif hydroxylases. *Biochem. Biophys. Res. Commun.* **2005**, *338*, 617–626.
18. Ivanov, S.; Liao, S.Y.; Ivanova, A.; Danilkovitch-Miagkova, A.; Tarasova, N.; Weirich, G.; Merrill, M.J.; Proescholdt, M.A.; Oldfield, E.H.; Lee, J.; *et al.* Expression of hypoxia-inducible cell-surface transmembrane carbonic anhydrases in human cancer. *Am. J. Pathol.* **2001**, *158*, 905–919.
19. Potter, C.; Harris, A.L. Hypoxia inducible carbonic anhydrase ix, marker of tumour hypoxia, survival pathway and therapy target. *Cell Cycle* **2004**, *3*, 164–167.

20. Stillebroer, A.B.; Mulders, P.F.; Boerman, O.C.; Oyen, W.J.; Oosterwijk, E., Carbonic anhydrase ix in renal cell carcinoma: Implications for prognosis, diagnosis, and therapy. European urology **2010**, 58, 75-83.
21. Poeppel, T.D.; Krause, B.J.; Heusner, T.A.; Boy, C.; Bockisch, A.; Antoch, G. Pet/ct for the staging and follow-up of patients with malignancies. *Eur. J. Radiol.* **2009**, *70*, 382–392.
22. Patard, J.J. Incidental renal tumours. *Curr. Opin. Urol.* **2009**, *19*, 454–458.
23. Van Dijk, J.; Zegveld, S.T.; Fleuren, G.J.; Warnaar, S.O. Localization of monoclonal antibody g250 and bispecific monoclonal antibody cd3/g250 in human renal-cell carcinoma xenografts: Relative effects of size and affinity. *Int. J. Cancer* **1991**, *48*, 738–743.
24. Kranenborg, M.H.; Boerman, O.C.; de Weijert, M.C.; Oosterwijk-Wakka, J.C.; Corstens, F.H.; Oosterwijk, E. The effect of antibody protein dose of anti-renal cell carcinoma monoclonal antibodies in nude mice with renal cell carcinoma xenografts. *Cancer* **1997**, *80*, 2390–2397.
25. Steffens, M.G.; Kranenborg, M.H.; Boerman, O.C.; Zegwaart-Hagemeier, N.E.; Debruyne, F.M.; Corstens, F.H.; Oosterwijk, E. Tumor retention of 186re-mag3, 111in-dtpa and 125i labeled monoclonal antibody g250 in nude mice with renal cell carcinoma xenografts. *Cancer Biother. Radiopharm.* **1998**, *13*, 133–139.
26. Steffens, M.G.; Oosterwijk, E.; Kranenborg, M.H.; Manders, J.M.; Debruyne, F.M.; Corstens, F.H.; Boerman, O.C. *In vivo* and *in vitro* characterizations of three 99mtc-labeled monoclonal antibody g250 preparations. *J. Nucl. Med.* **1999**, *40*, 829–836.
27. Van Dijk, J.; Oosterwijk, E.; van Kroonenburgh, M.J.; Jonas, U.; Fleuren, G.J.; Pauwels, E.K.; Warnaar, S.O. Perfusion of tumor-bearing kidneys as a model for scintigraphic screening of monoclonal antibodies. *J. Nucl. Med.* **1988**, *29*, 1078–1082.
28. Oosterwijk, E.; Bander, N.H.; Divgi, C.R.; Welt, S.; Wakka, J.C.; Finn, R.D.; Carswell, E.A.; Larson, S.M.; Warnaar, S.O.; Fleuren, G.J.; *et al.* Antibody localization in human renal cell carcinoma: A phase i study of monoclonal antibody g250. *J. Clin. Oncol.* **1993**, *11*, 738–750.
29. Divgi, C.R.; Bander, N.H.; Scott, A.M.; O'Donoghue, J.A.; Sgouros, G.; Welt, S.; Finn, R.D.; Morrissey, F.; Capitelli, P.; Williams, J.M.; *et al.* Phase i/ii radioimmunotherapy trial with iodine-131-labeled monoclonal antibody g250 in metastatic renal cell carcinoma. *Clin. Cancer Res.* **1998**, *4*, 2729–2739.
30. Steffens, M.G.; Boerman, O.C.; Oosterwijk-Wakka, J.C.; Oosterhof, G.O.; Witjes, J.A.; Koenders, E.B.; Oyen, W.J.; Buijs, W.C.; Debruyne, F.M.; Corstens, F.H.; *et al.* Targeting of renal cell carcinoma with iodine-131-labeled chimeric monoclonal antibody g250. *J. Clin. Oncol.* **1997**, *15*, 1529–1537.
31. Steffens, M.G.; Boerman, O.C.; Oyen, W.J.; Kniest, P.H.; Witjes, J.A.; Oosterhof, G.O.; van Leenders, G.J.; Debruyne, F.M.; Corstens, F.H.; Oosterwijk, E. Intratumoral distribution of two consecutive injections of chimeric antibody g250 in primary renal cell carcinoma: Implications for fractionated dose radioimmunotherapy. *Cancer Res.* **1999**, *59*, 1615–1619.
32. Brouwers, A.H.; Dorr, U.; Lang, O.; Boerman, O.C.; Oyen, W.J.; Steffens, M.G.; Oosterwijk, E.; Mergenthaler, H.G.; Bihl, H.; Corstens, F.H. ^{131}I-cg250 monoclonal antibody immunoscintigraphy *vs.* [18F]fdg-pet imaging in patients with metastatic renal cell carcinoma: A comparative study. *Nucl. Med. Commun.* **2002**, *23*, 229–236.
33. Brouwers, A.H.; Buijs, W.C.; Oosterwijk, E.; Boerman, O.C.; Mala, C.; de Mulder, P.H.; Corstens, F.H.; Mulders, P.F.; Oyen, W.J. Targeting of metastatic renal cell carcinoma with the chimeric monoclonal antibody g250 labeled with ^{131}I or [111]In: An intrapatient comparison. *Clin. Cancer Res.* **2003**, *9*, 3953S–3960S.
34. Divgi, C.R.; Pandit-Taskar, N.; Jungbluth, A.A.; Reuter, V.E.; Gonen, M.; Ruan, S.; Pierre, C.; Nagel, A.; Pryma, D.A.; Humm, J.; *et al.* Preoperative characterisation of clear-cell renal carcinoma using iodine-124-labelled antibody chimeric g250 ([124]I-cg250) and pet in patients with renal masses: A phase i trial. *Lancet Oncol.* **2007**, *8*, 304–310.
35. Divgi, C.R.; Uzzo, R.G.; Gatsonis, C.; Bartz, R.; Treutner, S.; Yu, J.Q.; Chen, D.; Carrasquillo, J.A.; Larson, S.; Bevan, P.; *et al.* Positron emission tomography/computed tomography identification of clear cell renal cell carcinoma: Results from the redect trial. *J. Clin. Oncol.* **2013**, *31*, 187–194.
36. Muselaers, C.H.; Boerman, O.C.; Oosterwijk, E.; Langenhuijsen, J.F.; Oyen, W.J.; Mulders, P.F. Indium-111-labeled girentuximab immunospect as a diagnostic tool in clear cell renal cell carcinoma. *Eur. Urol.* **2013**, doi:10.1016/j.eururo.2013.02.022.
37. Steffens, M.G.; Oosterwijk, E.; Zegwaart-Hagemeier, N.E.; van't Hof, M.A.; Debruyne, F.M.; Corstens, F.H.; Boerman, O.C. Immunohistochemical analysis of intratumoral heterogeneity of [131I]cg250 antibody uptake in primary renal cell carcinomas. *Br. J. Cancer* **1998**, *78*, 1208–1213.
38. Durrbach, A.; Angevin, E.; Poncet, P.; Rouleau, M.; Chavanel, G.; Chapel, A.; Thierry, D.; Gorter, A.; Hirsch, R.; Charpentier, B.; *et al.* Antibody-mediated endocytosis of g250

tumor-associated antigen allows targeted gene transfer to human renal cell carcinoma *in vitro*. *Cancer Gene Ther.* **1999**, *6*, 564–571.

39. Genega, E.M.; Ghebremichael, M.; Najarian, R.; Fu, Y.N.; Wang, Y.H.; Argani, P.; Grisanzio, C.; Signoretti, S. Carbonic anhydrase ix expression in renal neoplasms correlation with tumor type and grade. *Am. J. Clin. Pathol.* **2010**, *134*, 873–879.

40. Van Schaijk, F.G.; Broekema, M.; Oosterwijk, E.; van Eerd, J.E.; McBride, B.J.; Goldenberg, D.M.; Corstens, F.H.; Boerman, O.C. Residualizing iodine markedly improved tumor targeting using bispecific antibody-based pretargeting. *J. Nucl. Med.* **2005**, *46*, 1016–1022.

41. Brouwers, A.H.; van Eerd, J.E.; Frielink, C.; Oosterwijk, E.; Oyen, W.J.; Corstens, F.H.; Boerman, O.C. Optimization of radioimmunotherapy of renal cell carcinoma: Labeling of monoclonal antibody cg250 with ^{131}I, ^{90}Y, ^{177}Lu, or ^{186}Re. *J. Nucl. Med.* **2004**, *45*, 327–337.

42. Steffens, M.G.; Boerman, O.C.; de Mulder, P.H.; Oyen, W.J.; Buijs, W.C.; Witjes, J.A.; van den Broek, W.J.; Oosterwijk-Wakka, J.C.; Debruyne, F.M.; Corstens, F.H.; *et al.* Phase I radioimmunotherapy of metastatic renal cell carcinoma with ^{131}I-labeled chimeric monoclonal antibody g250. *Clin. Cancer Res.* **1999**, *5*, 3268S–3274S.

43. Divgi, C.R.; O'Donoghue, J.A.; Welt, S.; O'Neel, J.; Finn, R.; Motzer, R.J.; Jungbluth, A.; Hoffman, E.; Ritter, G.; Larson, S.M.; *et al.* Phase I clinical trial with fractionated radioimmunotherapy using ^{131}I-labeled chimeric g250 in metastatic renal cancer. *J. Nuclear Med.* **2004**, *45*, 1412–1421.

44. Brouwers, A.H.; Mulders, P.F.; de Mulder, P.H.; van den Broek, W.J.; Buijs, W.C.; Mala, C.; Joosten, F.B.; Oosterwijk, E.; Boerman, O.C.; Corstens, F.H.; *et al.* Lack of efficacy of two consecutive treatments of radioimmunotherapy with ^{131}I-cg250 in patients with metastasized clear cell renal cell carcinoma. *J. Clin. Oncol.* **2005**, *23*, 6540–6548.

45. Stillebroer, A.B.; Boerman, O.C.; Desar, I.M.; Boers-Sonderen, M.J.; van Herpen, C.M.; Langenhuijsen, J.F.; Smith-Jones, P.M.; Oosterwijk, E.; Oyen, W.J.; Mulders, P.F. Phase 1 radioimmunotherapy study with lutetium 177-labeled anti-carbonic anhydrase IX monoclonal antibody girentuximab in patients with advanced renal cell carcinoma. *Eur. Urol.* **2012**, doi:10.1016/j.eururo.2012.08.024.

46. Davis, I.D.; Wiseman, G.A.; Lee, F.T.; Gansen, D.N.; Hopkins, W.; Papenfuss, A.T.; Liu, Z.; Moynihan, T.J.; Croghan, G.A.; Adjei, A.A.; *et al.* A phase i multiple dose, dose escalation study of cg250 monoclonal antibody in patients with advanced renal cell carcinoma. *Cancer Immun.* **2007**, *7*, 13.

47. Bleumer, I.; Knuth, A.; Oosterwijk, E.; Hofmann, R.; Varga, Z.; Lamers, C.; Kruit, W.; Melchior, S.; Mala, C.; Ullrich, S.; *et al.* A phase ii trial of chimeric monoclonal antibody g250 for advanced renal cell carcinoma patients. *Br. J. Cancer* **2004**, *90*, 985–990.

48. WILEX Ariser, adjuvant rencarex® immunotherapy phase iii trial to study efficacy in non-metastatic rcc. http://www.wilex.de/portfolio-english/rencarex/phase-iii-ariser/

49. Davis, I.D.; Liu, Z.; Saunders, W.; Lee, F.T.; Spirkoska, V.; Hopkins, W.; Smyth, F.E.; Chong, G.; Papenfuss, A.T.; Chappell, B.; *et al.* A pilot study of monoclonal antibody cg250 and low dose subcutaneous il-2 in patients with advanced renal cell carcinoma. *Cancer Immun.* **2007**, *7*, 14.

50. Bleumer, I.; Oosterwijk, E.; Oosterwijk-Wakka, J.C.; Voller, M.C.; Melchior, S.; Warnaar, S.O.; Mala, C.; Beck, J.; Mulders, P.F. A clinical trial with chimeric monoclonal antibody wx-g250 and low dose interleukin-2 pulsing scheme for advanced renal cell carcinoma. *J. Urol.* **2006**, *175*, 57–62.

51. Siebels, M.; Rohrmann, K.; Oberneder, R.; Stahler, M.; Haseke, N.; Beck, J.; Hofmann, R.; Kindler, M.; Kloepfer, P.; Stief, C. A clinical phase I/II trial with the monoclonal antibody cg250 (rencarex(r)) and interferon-alpha-2a in metastatic renal cell carcinoma patients. *World J. Urol.* **2011**, *29*, 121–126.

52. Brouwers, A.H.; Buijs, W.C.; Mulders, P.F.; de Mulder, P.H.; van den Broek, W.J.; Mala, C.; Oosterwijk, E.; Boerman, O.C.; Corstens, F.H.; Oyen, W.J. Radioimmunotherapy with [131I]cg250 in patients with metastasized renal cell cancer: Dosimetric analysis and immunologic response. *Clin. Cancer Res.* **2005**, *11*, 7178S–7186S.

53. Sharkey, R.M.; Behr, T.M.; Mattes, M.J.; Stein, R.; Griffiths, G.L.; Shih, L.B.; Hansen, H.J.; Blumenthal, R.D.; Dunn, R.M.; Juweid, M.E.; *et al.* Advantage of residualizing radiolabels for an internalizing antibody against the b-cell lymphoma antigen, cd22. *Cancer Immunol. Immunother.* **1997**, *44*, 179–188.

54. Stillebroer, A.B.; Zegers, C.M.; Boerman, O.C.; Oosterwijk, E.; Mulders, P.F.; O'Donoghue, J.A.; Visser, E.P.; Oyen, W.J. Dosimetric analysis of ^{177}Lu-cg250 radioimmunotherapy in renal cell carcinoma patients: Correlation with myelotoxicity and pretherapeutic absorbed dose predictions based on ^{111}In-cg250 imaging. *J. Nucl. Med.* **2012**, *53*, 82–89.

55. Surfus, J.E.; Hank, J.A.; Oosterwijk, E.; Welt, S.; Lindstrom, M.J.; Albertini, M.R.; Schiller, J.H.; Sondel, P.M. Anti-renal-cell carcinoma chimeric antibody g250 facilitates antibody-dependent

cellular cytotoxicity with *in vitro* and in vivo interleukin-2-activated effectors. *J. Immunother. Emphasis Tumor Immunol.* **1996**, *19*, 184–191.

56. Liu, Z.; Smyth, F.E.; Renner, C.; Lee, F.T.; Oosterwijk, E.; Scott, A.M. Anti-renal cell carcinoma chimeric antibody g250: Cytokine enhancement of *in vitro* antibody-dependent cellular cytotoxicity. *Cancer Immunol. Immunother.* **2002**, *51*, 171–177.

57. Brouwers, A.H.; Frielink, C.; Oosterwijk, E.; Oyen, W.J.; Corstens, F.H.; Boerman, O.C. Interferons can upregulate the expression of the tumor associated antigen g250-mn/ca IX, a potential target for (radio)immunotherapy of renal cell carcinoma. *Cancer Biother. Radiopharm.* **2003**, *18*, 539–547.

58. Bui, M.H.; Seligson, D.; Han, K.R.; Pantuck, A.J.; Dorey, F.J.; Huang, Y.; Horvath, S.; Leibovich, B.C.; Chopra, S.; Liao, S.Y.; *et al.* Carbonic anhydrase IX is an independent predictor of survival in advanced renal clear cell carcinoma: Implications for prognosis and therapy. *Clin. Cancer Res.* **2003**, *9*, 802–811.

59. Bui, M.H.; Visapaa, H.; Seligson, D.; Kim, H.; Han, K.R.; Huang, Y.; Horvath, S.; Stanbridge, E.J.; Palotie, A.; Figlin, R.A.; *et al.* Prognostic value of carbonic anhydrase IX and ki67 as predictors of survival for renal clear cell carcinoma. *J. Urol.* **2004**, *171*, 2461–2466.

60. Atkins, M.; Regan, M.; McDermott, D.; Mier, J.; Stanbridge, E.; Youmans, A.; Febbo, P.; Upton, M.; Lechpammer, M.; Signoretti, S. Carbonic anhydrase ix expression predicts outcome of interleukin 2 therapy for renal cancer. *Clin. Cancer Res.* **2005**, *11*, 3714–3721.

61. Dudek, A.Z.; Yee, R.T.; Manivel, J.C.; Isaksson, R.; Yee, H.O. Carbonic anhydrase ix expression is associated with improved outcome of high-dose interleukin-2 therapy for metastatic renal cell carcinoma. *Anticancer Res.* **2010**, *30*, 987–992.

62. Smith, I.; Procter, M.; Gelber, R.D.; Guillaume, S.; Feyereislova, A.; Dowsett, M.; Goldhirsch, A.; Untch, M.; Mariani, G.; Baselga, J.; *et al.* 2-year follow-up of trastuzumab after adjuvant chemotherapy in her2-positive breast cancer: A randomised controlled trial. *Lancet* **2007**, *369*, 29–36.

63. Lamers, C.H.; Sleijfer, S.; Vulto, A.G.; Kruit, W.H.; Kliffen, M.; Debets, R.; Gratama, J.W.; Stoter, G.; Oosterwijk, E. Treatment of metastatic renal cell carcinoma with autologous t-lymphocytes genetically retargeted against carbonic anhydrase IX: First clinical experience. *J. Clin. Oncol.* **2006**, *24*, e20–e22.

64. Lamers, C.H.; Sleijfer, S.; van Steenbergen, S.; van Elzakker, P.; van Krimpen, B.; Groot, C.; Vulto, A.; den Bakker, M.; Oosterwijk, E.; Debets, R.; *et al.* Treatment of metastatic renal cell carcinoma with caix car-engineered t cells: Clinical evaluation and management of on-target toxicity. *Mol. Ther.* **2013**, *21*, 904–912.

65. Oosterwijk-Wakka, J.C.; Kats-Ugurlu, G.; Leenders, W.P.; Kiemeney, L.A.; Old, L.J.; Mulders, P.F.; Oosterwijk, E. Effect of tyrosine kinase inhibitor treatment of renal cell carcinoma on the accumulation of carbonic anhydrase IX-specific chimeric monoclonal antibody cg250. *BJU Int.* **2011**, *107*, 118–125.

66. Muselaers, S.; Boerman, O.; Stillebroer, A.; Desar, I.; Sonderen, M.; van Herpen, C.; Oosterwijk, E.; Leenders, W.; Mulders, P.; Oyen, W. Sorafenib decreases indium-111-girentuximab tumor uptake in clear cell renal cell carcinoma patients. *J. Nuc. Med.* **2012**, *53*, 27.

67. Murri-Plesko, M.T.; Hulikova, A.; Oosterwijk, E.; Scott, A.M.; Zortea, A.; Harris, A.L.; Ritter, G.; Old, L.; Bauer, S.; Swietach, P.; *et al.* Antibody inhibiting enzymatic activity of tumour-associated carbonic anhydrase isoform IX. *Eur. J. Pharmacol.* **2011**, *657*, 173–183.

Chapter 3

Targeted Therapy
of Renal Cell Carcinoma:
Synergistic Activity of cG250-TNF
and IFNγ

Jeannette C. Oosterwijk-Wakka[1*], Stefan Bauer[2*], Nicole Adrian[3],
Egbert Oosterwijk[1], Eliane Fischer[2], Thomas Wüest[2], Frank Stenner[2], Angelo Perani,
Leonard Cohen[5], Alexander Knuth[2], Chaitanya Divgi[6], Dirk Jäger[7], Andrew M. Scott[4],
Gerd Ritter[5], Lloyd J. Old[5] and Christoph Renner[2]

[1] Department of Urology, Radboud university medical center, Nijmegen, The Netherlands, [2] Department of
Oncology, UniversitätsSpital Zürich, Zürich, Switzerland, [3] Department of Internal Medicine, Universität des
Saarlandes, Homburg/Saar, Germany, [4] Department of Nuclear Medicine and Centre for P.E.T., Ludwig Institute for
Cancer Research, Melbourne Centre, Austin Hospital, Victoria, Australia, [5] Ludwig Institute for Cancer Research,
New York Branch, Memorial Sloan Kettering Cancer Center, New York, United States, [6] Department of Nuclear
Medicine and Clinical Molecular Imaging, University of Pennsylvania, Philadelphia, United States, [7] Department
of Medical Oncology, University of Heidelberg, National Center for Tumour Diseases, Heidelberg, Germany

* JCOW and SB contributed equally to this manuscript

Abstract

Immunotherapeutic targeting of G250/Carbonic anhydrase IX (CA-IX) represents a promising strategy for treatment of renal cell carcinoma (RCC). The well characterized human-mouse chimeric G250 (cG250) antibody has been shown in human studies to specifically enrich in CA-IX positive tumors and was chosen as a carrier for site specific delivery of TNF in form of our IgG-TNF-fusion protein (cG250-TNF) to RCC xenografts. Genetically engineered TNF constructs were designed as CH2/CH3 truncated cG250-TNF fusion proteins and eucariotic expression was optimized under serum-free conditions. *In-vitro* characterization of cG250-TNF comprised biochemical analysis and bioactivity assays, alone and in combination with Interferon-γ (IFNγ). Biodistribution data on radiolabeled [125-I] cG250-TNF and antitumor activity of cG250-TNF, alone and in combination with IFNγ, were measured on RCC xenografts in BALB/c nu/nu mice. Combined administration of cG250-TNF and IFNγ caused synergistic biological effects that represent key mechanisms displaying antitumor responses. Biodistribution studies demonstrated specific accumulation and retention of cG250-TNF at CA-IX-positive RCC resulting in growth inhibition of RCC and improved progression free survival and overall survival. Antitumor activity induced by targeted TNF-based constructs could be enhanced by coadministration of low doses of nontargeted IFNγ without significant increase in side effects. Administration of cG250-TNF and IFNγ resulted in significant synergistic tumoricidal activity. Considering the poor outcome of renal cancer patients with advanced disease, cG250-TNF-based immunotherapeutic approaches warrant clinical evaluation.

Introduction

Renal cell carcinoma (RCC) accounts for 2% of all cancers, leading to 20,000 annual deaths in Europe and 12,000 in the United States [1,2]. Although advances in understanding the biology of RCC led to novel approaches for the treatment of metastatic disease [3] with subsequent increase of progression-free and overall-survival rates, the prognosis for these patients is poor with a 5-year survival rate of less than 10% [4]. The predominant histological type of RCC is clear-cell carcinoma, comprising more than 85% of metastatic disease. Both, sporadic and inherited forms of clear cell RCC are associated with mutations in the von Hippel-Lindau (VHL) tumor suppressor gene [5]. Elucidation of its role in up-regulating growth factors associated with angiogenesis as well as the hypoxia-induced carbonic anhydrase IX (CA-IX) defined a series of potential targets for novel treatment strategies. Among them, targeting of a surface expressed epitope of CA-IX (called G250) using chimeric G250 monoclonal antibody (cG250) is a promising immunotherapeutic approach [6]. Safe administration with excellent tumor targeting properties of the radio-labeled [131]I- and [124]I-cG250 antibody has been demonstrated in phase I clinical trials in patients with metastatic clear cell RCC [7–10]. Additional studies showed that multiple doses of cG250 were well tolerated and combination with low dose IL-2 resulted in disease stabilization [11,12]. These encouraging clinical features prompted us to optimize effector functions of cG250 to further improve its antitumor properties.

We have previously reported on a strategy to promote the therapeutic efficacy of tumor specific antibodies by genetic fusion to tumor necrosis factor (TNF) [13]. The soluble form of TNF occurs mainly as a trimer of 3 identical subunits. TNF was first identified as a mediator of hemorrhagic tumor necrosis mediating regression of murine [14] and xenotransplanted human tumors [15]. Subsequent research revealed that Interferon gamma (IFNγ) plays a substantial role in TNF-mediated tumor rejection processes [16,17]. Many IFNγ-mediated mechanisms have been proposed to promote antitumor responses including antiproliferative and proapoptotic activity on tumor cells [18], inhibition of angiogenesis within tumors [19,20] or activation of innate [21,22] and adapted immune responses [23,24]. Thus, both TNF and IFNγ exert pleiotropic mechanisms on a variety of cell types and coadministration of both cytokines even results in synergistic antitumor activities [25–27]. However, because of its life-threatening systemic toxicity [28] caused by affection of normal endothelial cells in peripheral blood vessels [29,30], the clinical use of TNF in combination with IFNγ as an anticancer drug is restricted to loco-regional treatment (e.g. isolated limb perfusion) [31,32]. However, we established a 2-step approach to enlarge the therapeutic window of the cytokine: TNF molecules were genetically fused to a tumor-specific antibody to focus TNF at the tumor site. In addition, TNF subunits were forced to form a dimer to reduce their activity in peripheral blood vessels outside the tumor compartment [13]. Abandoning the natural homotrimeric symmetry of TNF resulted in significantly reduced toxicity as seen both in immunodeficient and immunocompetent mouse strains [33]. The dimeric IgG-TNF molecules displayed significantly stronger antitumor activity *in-vivo* than wild type TNF or trimeric TNF-antibody

conjugates. Dose escalation increased the therapeutic index of IgG-TNF and repeated administration additionally delayed tumor growth with tolerable side effects [33].

Here, we describe the construction, expression and purification of a cG250-TNF fusion protein and its preclinical evaluation in a RCC mouse model. Biodistribution studies in G250/CA-IX-positive RCC xenografted BALB/c nu/nu mice showed a significant increase of tumor-to-blood ratio over time with specific accumulation and retention of cG250-TNF in the tumor resulting in growth control of established RCC. Furthermore, a combination regimen with clinically well-tolerated doses of non-targeted IFNγ-induced synergistic activation of different tumoricidal pathways and increased significantly the antitumor response *in vivo*. Considering the poor outcome of patients with advanced renal cell cancer, cG250-TNF-based immunotherapeutic approaches could be a valuable therapeutic option.

Material and methods

Cell lines and reagents

RPMI 1640 medium [supplemented with 10% (v/v) heat-inactivated fetal bovine serum, penicillin (100 units/ml), streptomycin (0.1 mg/ml) and glutamine (0.3 mg/ml)] (all Gibco, Karlsruhe, Germany) was used as standard medium for all cell lines if not indicated otherwise. Human renal carcinoma cell lines NU-12, SK-RC-52 (high G250 expression level), SK-RC-17 (G250-negative), the cervix carcinoma cell line Me-180, and mouse fibrosarcoma cell lines WEHI-164 S (TNF sensitive) and the WEHI-164 R (TNF resistant; a WEHI-164 variant, cloned under the exposure to TNF) were supplied by Ludwig Institute for Cancer Research. HUVEC-c endothelial cell supplemented growth medium was obtained from PromoCell (Heidelberg, Germany). For selective cell culture mouse myeloma NSO cells were grown in Glutamine- free DMEM supplied by SAFC Biosciences (Lennexa, KS) according to Lonza's manual of operating procedures (Lonza, NH). Human recombinant TNF, human recombinant IFNγ, murine recombinant IFNγ and soluble TNF-R1 were purchased from Genzyme (Neu-Isenburg, Germany). Anti-FAP-TNF has been described previously [13]. Antibodies were obtained from the following sources: rabbit antihuman tissue factor from American Diagnostica (Pfungstadt, Germany), rabbit antihuman ICAM-1 from Santa Cruz Biotechnology (Heidelberg, Germany), rabbit antihuman actin from Sigma (St. Louis, MO) PE-conjugated goat anti- rabbit from Dako (Glostrup, Denmark), murine anti-idiotypic anti-G250 and the chimeric G250 mAb were previously described.

Construction of cG250-TNF fusion protein

Reverse transcription-PCR on mRNA isolated from peripheral blood mononuclear cells for amplification of the mature human TNF cDNA sequence was previously described [13]. The cDNA sequence coding for the cG250 variable heavy (HC) and light (LC) chain sequence was subcloned into pEAK8 mammalian cell expression vector (Edge BioSystems, Gaithersburg, MA) with the HC-expression vector containing the previously described human

CH2/CH3-truncated IgG1 TNF [13] C-terminally fused to His6 tag. cG250 LC was amplified by PCR with the forward primer (GAACC CGGGG CCGCC ACCAT GGGCA AGATG GAGTT TCATA CT) containing Kozak's sequence and a Sma I restriction side and the reverse primers containing the stop codon and a EcoR I restriction enzyme sequence. Amplification of the cG250 IgG1 CH1 TNF H6 sequence was done by sequential use of two reverse primers (CAAAG ATCTC AGGGC AATGA TCCCA AAGTA GAC and CAAGA ATTCT CAGTG ATGGT GATGG TGATG CAGGG CAATG ATCCC) and the forward primer introducing either the Kozak's and the Sma I restriction side sequence (GAACC CGGGG CCGCC ACCAT GAACT TCGGG CTCAG ATTG). Variable cG250 LC sequence was cloned into mammalian expression vector pEE12.4 by Sma I/EcoR I and, respectively, the H6-tagged HC-TNF sequence by Sal I/Not I in pEE6.4 (Lonza, Portsmouth, USA). The double-gene vector encoding the cG250-TNF fusion protein was created by digestion of both vectors with Not I and Sal I restriction enzymes and ligation of the pEE6.4 fragment into the larger pEE12.4 fragment according to Lonza's manual of operating procedures.

Generation of stable transfected cell lines, expression, purification and characterization of cG250-TNF fusion protein

Stable transfected NSO cell lines were established by electroporation of Pvu I linearized DNA using a GENPULSER (BioRad, Munich, Germany) according to manufacturer's instructions. Transfected cells are selected for their ability to grow in glutamine-free medium. Stable cell lines producing high level of antibodies were expanded, weaned off FCS and transferred into a Technomouse system (Integra Biosciences, Fernwald, Germany) for large scale production. Antibody supernatant from the Technomouse system was dialyzed against PBS (phosphate buffered saline, pH 7.2) overnight (4°C). The dialyzed sample was passed over Protein A and G sepharose columns (Pharmacia, Freiburg, Germany) in a 2-step procedure. Fusion proteins bound to Protein G were stepwise eluted by adding 0.1 M glycine/HCl (pH 3.5) and samples were rapidly neutralized by the addition of 1 M Tris buffer (pH 8.0). Endotoxin contamination of the final product was excluded by Limulus amebocyte assay (QCL 1000, BioWhittacker, Walkersville, MD). The size of the fusion protein was analyzed in reducing condition on SDS–PAGE and in native condition by FPLC-gel filtration on a Superdex S-200 chromatography column (Amersham Pharmacia, Freiburg, Germany).

Integrity of cG250-TNF in vitro

Structural integrity of cG250-TNF was assessed by sandwich-ELISA as described [13]. In brief, 96-well flat-bottom microtiter plates were coated overnight (4°C) with Infliximab (antihuman TNF antibody), plates were blocked with 1.5% gelatine in PBS and the indicated reagents solved in PBS were added in serial dilutions (60 min, RT) and the bound cG250-TNF using a murine anti-cG250 anti-idiotypic antibody (1 μg/ml, 1 hr, room temperature) as described previously [13].

TNF-receptor 1 mediated apoptosis was investigated on TNF- sensitive ''WEHI-164 S'' and on partially TNF-resistant [34] ''WEHI-164 R'' as described [13]. 5 x 10^5 WEHI cells were cultured in 96-well plates in the presence of the indicated reagents. Apoptotic cells were identified by annexin V staining by flow staining as described [13].

Synergistic bio-activity of cG250-TNF and IFNγ in vitro

Synergistic cytotoxic interaction of cG250-TNF and IFNγ was demonstrated by reduction of Me-180 cervical carcinoma cell viability as described [25,35]. Measurement of H_2O_2 release by stimulated human polymorphonuclear leukocytes (PMN) prepared from venous blood of healthy donors was done as described [13]. Samples were taken at selected time points after incubation with triggering agents (37°C over 180 min in air). Activation of HUVEC endothelial cells cultured at second or third passage was done by incubation (6–24 hr at 37°C) with effectors at indicated dilutions and harvested as described [13]. IP-10 expression levels were analyzed by RT-PCR (forward: AATCA AACTG CGATT CTGAT TTGC; reverse: AGGAG ATCTT TTAGA CATTT CCTT) and GADPH (forward: GTGAA GGTCG GAGTC AACGG ATTT; reverse: CTCCT TGGAG GCCAT GTGGG CCAT). Expression levels of tissue factor and ICAM-1 were detected by Western blot analysis.

Xenograft models, biodistribution and treatment protocols

Biodistribution and efficacy studies were done on xenografted 6–8-week-old athymic BALB/c *nu/nu* mice (Charles River Laboratories, Central Animal Facility, University Medical Center Nijmegen, The Netherlands). Renal cell tumor engraftment was achieved by subcutaneous injection of 5 x 10^6 SK-RC-17, SK-RC-52, or transplantation of NU-12 xenografts. The studies were approved by the local Animal Welfare Committee and performed in accordance with their guidelines.

Protein was radioiodinated with ^{131}I or [125]Iodine (MDS Nordion, Fleurus, Belgium) according to the IodoGen method and the immune-reactive fraction of the radiolabeled preparations was determined by Lindmo analysis with minor modifications as described [7] and was 80–95%. Mice bearing subcutaneously established tumors were intravenously injected with 5, 25, or 50 μg of radioiodinated constructs. Cohorts of animals were sacrificed at predetermined timepoints after injection and tissues harvested, weighted and the uptake of ^{125}I-cG250-TNF or ^{131}I-cG250, respectively, was determined in a gamma-counter as described [36]. Therapeutic efficacy of cG250-TNF alone or in combination with IFNγ was investigated in mice xenografted with G250-positive or -negative or both renal cell carcinomas and analyzed by daily monitoring of health and body weight of mice and measurement of tumor size on treatment days. Differences between treatment groups were tested for statistical significance by Student's *t* test.

Results

Production and characterization of cG250-TNF

We established an antibody fusion protein named cG250-TNF that consists of human TNF and chimeric antibody cG250. The N- terminal domain of human TNF was linked to the IgG hinge region as described [13]. The variable domains of cG250 were inserted through specific restriction sites into the pEE6.4 and pEE12.4 plasmids. The vector construct was confirmed by DNA sequencing (Fig. 1a). High-level expression of the recombinant fusion protein using NSO cells was achieved with about a 270 mg/l of culture supernatant and a specific productivity of 12.46 pg/cell/day (data not shown). The immunocytokine was purified using a sequential 2-step affinity chromatography with Protein A (flow-through) and Protein G (capture), respectively. Deletion of the CH2- and the CH3-domains of cG250 and their replacement with TNF-molecules reduced substantially the affinity of cG250-TNF to Protein A. During the first pass of the dialyzed sample over Protein A column, contaminating residual bovine globulins were captured. The flow through still contained the cG250-TNF fraction, and the construct was captured by a second pass over Protein G column. Fractions corresponding to dimeric species were collected during gel-filtration chromatography (Fig. 1b). Purity and identity of parental cG250 (Fig. 1b: lanes 1, 3, 5, 7) and cG250-TNF (Fig. 1b: lanes 2, 4, 6, 8) were characterized using SDS-PAGE under reducing and nonreducing conditions and Western blotting with anti-TNF. The recombinant heavy chain of cG250-TNF migrates with an apparent molecular weight of 47 kDa (Fig. 1b, lane 2) and is slightly smaller than a natural IgG heavy chain (Fig. 1b, lane 1). The human light chain is not altered with an apparent MW of 28 kDa. Western blotting of SDS-PAGE gels under both conditions and subsequent staining with anti-TNF identifies the heavy-chain of cG250-TNF (Fig. 1b, lanes 4 and 8). As expected, staining with anti-TNF failed to detect cG250 (Fig. 1b, Lanes 3 and 7). Correct folding of cG250-TNF hybrid protein was confirmed by sandwich ELISA with recognition of the TNF-part by Infliximab (antihuman TNF antibody) and by binding of the antibody part to an anti-cG250 anti-idiotypic antibody (Fig. 1c). The affinity constant for the targeted G250 antigen was identical for the cG250-TNF (Ka = 2.5 x 10^9 M^{-1}) and parental cG250 (Ka = 2.2 x 10^9 M^{-1}) construct as measured by ELISA and Scatchard analysis (data not shown). The capacity of dimerized TNF subunits in triggering TNF-receptor 1 (TNF-R1) dependent signaling was determined by WEHI-164 cytotoxicity assay system. With regard to different molarities of cG250-fused dimeric TNF and recombinant trimeric TNF, assays were performed at TNF-equivalent doses. In agreement with our previous results on dimeric TNF fusion proteins, TNF-R1 mediated cytotoxicity of cG250-TNF was approximately 10-fold lower when compared with trimerized, commercially available recombinant human TNF (rhTNF; Fig. 1d).
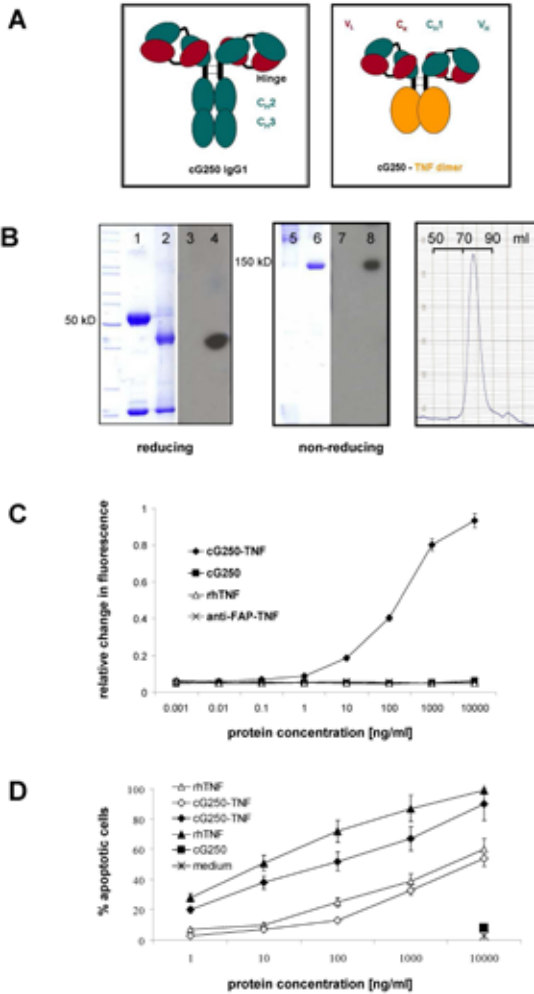
Figure 1. Schematic model, expression and functional characterization of cG250-TNF. **(a)** The Fc-region (CH2 and CH3) of the parental chimeric G250-IgG antibody has been replaced by two human TNF molecules. **(b)** Coomassie Brillant Blue staining of SDS–PAGE Gel of purified cG250 (Lanes 1 and 5) and cG250-TNF (Lanes 2 and 6) and Western Blot analysis under reducing (left) and nonreducing (middle) conditions stained with anti-TNF antibodies (Lanes 3 and 7 for cG250, Lanes 4 and 8 for cG250-TNF). Fast protein liquid chromatography elution profile of cG250-TNF after sequential Protein A and Protein G purification (right). **(c)** Structural integrity of purified cG250-TNF was studied by sandwich ELISA. Complexes of dimeric cG250-TNF and coated antihuman TNF antibody were visualized using a murine anti-cG250 anti-idiotypic antibody. cG250, rhTNF, and anti-FAP-TNF served as control as indicated. Standard deviations are indicated by bars. **(d)** TNF-receptor 1 mediated activity of cG250-TNF was investigated on TNF-sensitive (closed symbols) or TNF-resistant (open symbols) WEHI cells. Cells were incubated with indicated amount of reagents for 12 hr at TNF-equivalent doses and numbers of apoptotic cells were analyzed by annexin V staining. Standard deviation is indicated by bars.

Synergistic biological activity of cG250-TNF and IFNγ in vitro

We next determined the capacity of dimeric cG250-TNF to induce tumoricidal activities with IFNγ in synergistic manner, as it is known for IFNγ and homotrimeric physiological TNF [26]. As expected, incubation of the human cervical cancer cell line Me-180 with either IFNγ or cG250-TNF as single substances was rather ineffective even at high concentrations [25,35], but combined incubation with IFNγ and cG250-TNF resulted in dose-dependent cell death (Fig. 2a). However, the efficacy of the combined administration of TNF and IFNγ as antitumor strategy depends rather on its effects on tumor vessels [27] than on lysis of the malignant cells themselves. We, therefore, investigated the effect of cG250-TNF and IFNγ on key regulators of early and late events in vessel destruction. Activated polymorphonuclear leukocytes (PMN) participate in endothelial cell injury through generation of reactive oxygen species. On stimulation with hydrogen peroxide (H_2O_2) and under direct influence of TNF and IFNγ, endothelial cells upregulate expression of adhesion molecules such as ICAM-1 (inter
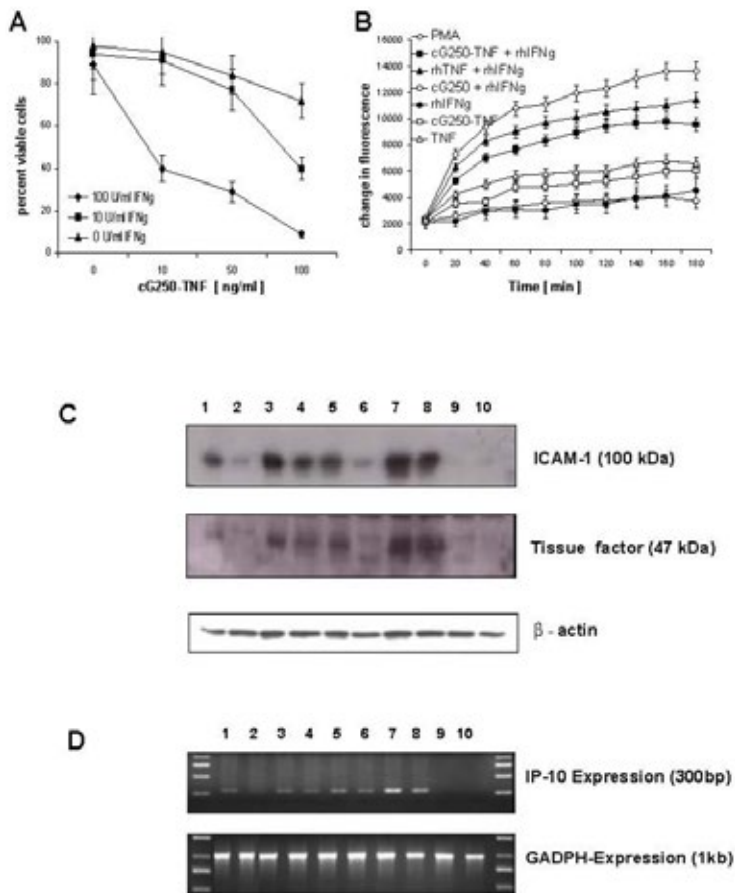
Figure 2. Synergistic effects of cG250-TNF and IFNγ. **(a)** Me-180 cervix carcinoma cells were incubated with indicated concentrations of IFNγ and cG250-TNF (37°C, 24 hr). Viable cells were visualized by trypan blue exclusion. Standard deviation is indicated by bars. **(b)** Activation of adherent human granulocytes from healthy donors were stimulated with indicated amount of reagents and H_2O_2-release was measured at 37°C over 3 hr as described [13]. IFNγ was used at a concentration of 100 U/ml, all other reagents at 10 μg/ml. PMA served as positive control. Standard deviations are indicated by bars. HUVEC endothelial cells were treated with cG250-TNF and IFNγ and the expression level of ICAM-1 and tissue factor was analyzed by Western Blotting **(c)** and IP-10 by RT-PCR **(d)**. HUVEC endothelial cells were incubated over 6 hr (tissue factor), 12 hr (IP-10) or 24 hr (ICAM-1) respectively at 37°C with (1) rhu TNF (1 ng/ml), (2) cG250-TNF (1 ng/ml), (3) rhu TNF (100 ng/ml), (4) cG250-TNF (100 ng/ml), (5) rhu TNF (1 ng/ml) plus IFNγ (100 IE), (6) cG250-TNF (1 ng/ml) plus IFNγ (100 IE), (7) rhu TNF (100 ng/ml) plus IFNγ (100 IE), (8) cG250-TNF (100 ng/ml) plus IFNγ (100 IE), (9) IFNγ (100 IE) and (10) culture medium without effectors.

cellular adhesion molecule 1) on their surface, thus rendering endothelial cells more susceptible to neutrophil-mediated endothelial cell injury. Combined incubation of PMN with cG250-TNF and IFNγ-induced persistent generation of H_2O_2 to a significant higher extend, when compared with single TNF activity and H_2O_2 release induced by single IFNγ treatment was negligible (Fig. 2b). Addition of IFNγ to HUVEC endothelial cells incubated with TNF or cG250-TNF also enhanced up-regulation of ICAM-1 expression (Fig. 2c, Lanes 7 and 8).

Staining of ICAM-1 was more intensive, after stimulation of HUVEC cells using trimeric TNF (Lanes 1, 3, 5, 7) when compared with cG250-fused dimeric TNF (Lanes 2, 4, 6, 8). This effect was evident following treatment with single substances and using the combination regimen. Different levels of TNF-R1-mediated up-regulation of key regulators in response to receptor triggering by dimeric or trimeric TNF confirm our results obtained from the WEHI assay system. In addition to the activation loop between PMN and endothelial cells, we investigated the effects of the combined regimen on endothelial expression of IP-10 and tissue factor. IP-10 contributes to IFNγ-dependent tumor angiostasis promoting tumor rejection by inhibition of neo-vascularization, while endothelial tissue factor represents the key event for the activation of the extrinsic coagulation cascade initiating thrombotic infarction of established tumor vessels. Treatment with cG250-TNF or with rhuTNF in combination with IFNγ resulted in synergistic upregulation of IP-10 (Fig. 2c) and tissue factor (Fig. 2d). In addition to this procoagulant activity, endothelial cells undergo striking morphological changes [37] together with changes. in vascular permeability following exposure to TNF and
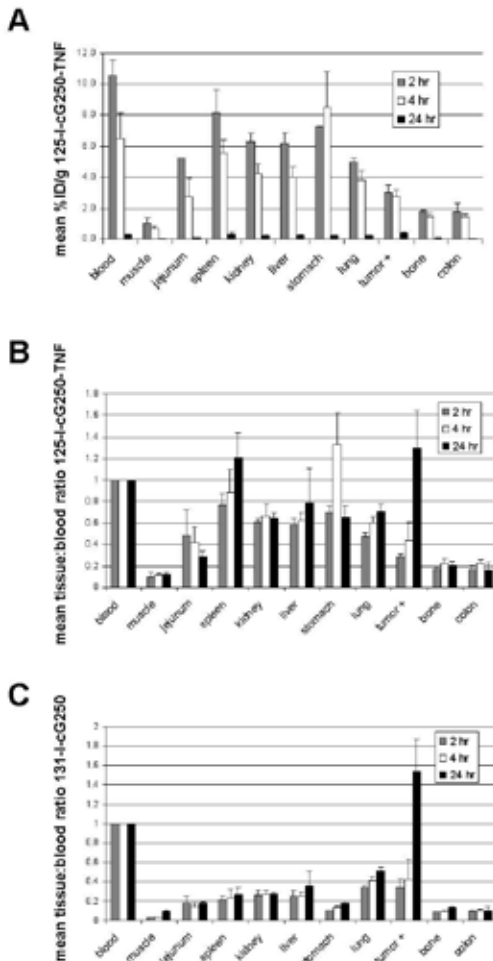
Figure 3. Biodistribution of radiolabeled cG250-TNF in BALB/c *nu/nu* mice xenografted with RCC tumors. In all biodistribution experiments, indicated tissue (n = 3 animals) was analyzed at each time point and bars indicate standard deviation. **(a)** 5 µg of I-125 labeled cG250-TNF were administered and percent of injected dose (%ID/g) was measured within 24 hr. Tissue-to-blood ratios were calculated for applied 125-I-cG250-TNF **(b)** and 131-I-cG250 **(c)** to compare the respective biodistribution profiles. Tumor uptake was similar for radiolabeled cG250-TNF and cG250. Transient accumulation of I-125-cG250-TNF in the stomach was because of free iodide accumulation.

IFNγ [27]. Combined treatment of HUVEC cells with cG250-TNF and IFNγ changed cell morphology from a confluent cobblestone mono-layer to a spindle endothelial cell morphology with interrupted confluence (data not shown). In summary, the combination regimen of dimeric TNF fused to cG250 and IFNγ induced important cellular response programs displaying antitumor activities in a synergistic manner.

A
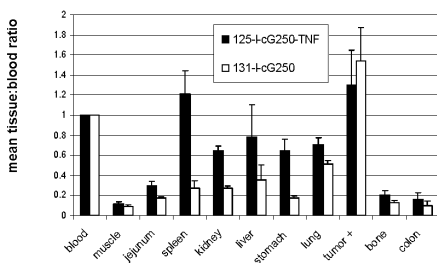
B

Figure 4. Dual labeling experiments to evaluate the impact of CH2/CH3 exchange by TNF molecules on half-life of the constructs. **(a)** Similar tumor-to-blood ratios could be reached for simultaneously applied 131-I-cG250 and 125-I-cG250-TNF at 5 µg doses. **(b)** %ID/g of 125-I-cG250-TNF was much lower when compared with 131-I-cG250. Distribution profiles show comparable targeting properties for both agents with a shortened half-life of the CH2/CH3-deleted TNF-construct. Indicated tissue of animals (n = 3)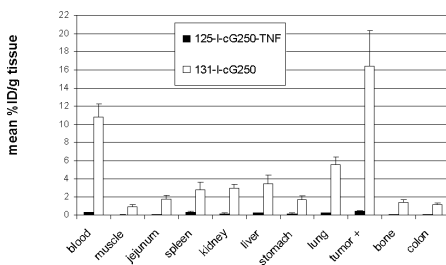 grafted with RCC tumors was analyzed following simultaneous application of differently labeled antibodies and standard deviations are indicated by bars.

Biodistribution of cG250-TNF in vivo

To investigate the *in-vivo* behavior of cG250-TNF, biodistribution experiments were performed in BALB/c *nu/nu* mice grafted with NU-12 solid renal cell carcinomas as described [38]. On the basis of our experience with cG250 IgG, each animal received 5 µg of radiolabeled antibody. Because the half-life of IgG is mainly determined by the CH2/CH3 constant regions, exchange of these by TNF was expected to lead to a dramatic alteration of the clearance rate. Mice were sacrificed within 24 hr post injection, tissues were harvested and uptake of ^{125}I-cG250-TNF was measured. cG250-TNF tissue levels were no greater than those in blood, with a rapid decrease of percent of injected dose per gram tissue (%ID/g) and similar tissue-to-blood ratios over time (Fig. 3a). In contrast, tumor-to-blood ratios increased over time, demonstrating specific accumulation and retention of both cG250-TNF (Fig. 3b) and the parental cG250 antibody (Fig. 3c) at the tumor site. To determine whether similar tumor-to-blood ratios could be reached for cG250-TNF and cG250 antibody, dual labeling

experiments were performed with ^{131}I-labeled cG250 IgG and ^{125}I-cG250-TNF. Indeed, tumor-to-blood ratios of the parental cG250 IgG and the cG250-TNF fusion protein were similar (Fig. 4a), though %ID/g for cG250-TNF was much lower (Fig. 4b). These effects are due to the shorter half-life and the accelerated clearance of cG250-TNF leading to a short time period where cG250-TNF can accumulate at the tumor environment. In view of the rapid blood clearance, we performed a dose-escalation study, because higher cG250-TNF doses might result in higher tumor uptake levels. Cohorts of animals received 5, 25 or 50 µg radioiodinated cG250-TNF. Tissue-to-blood ratios remained stable at all dose levels and for almost all tissues, with exception of stomach uptake, attributed to free iodine in gastric mucosa (Fig. 5a). In contrast, relative as well as absolute amounts of cG250-TNF more than doubled in the tumors with increasing protein doses, reaching absolute levels comparable with the parental cG250 IgG (Fig. 3c). To ensure G250-antigen specific targeting, we performed a complementary biodistribution study in BALB/c *nu/nu* mice simultaneously grafted with solid G250-negative renal cell carcinoma. Minimal but not significant uptake of cG250-TNF was seen in antigen-negative tumors. Biodistribution in organs did not differ between animals carrying G250-positive or G250-negative tumors. Most notably, tumor-to-blood ratios were significantly lower for G250-negative than for antigen-positive tumors, demonstrating G250-antigen specific accumulation (Fig. 5c).
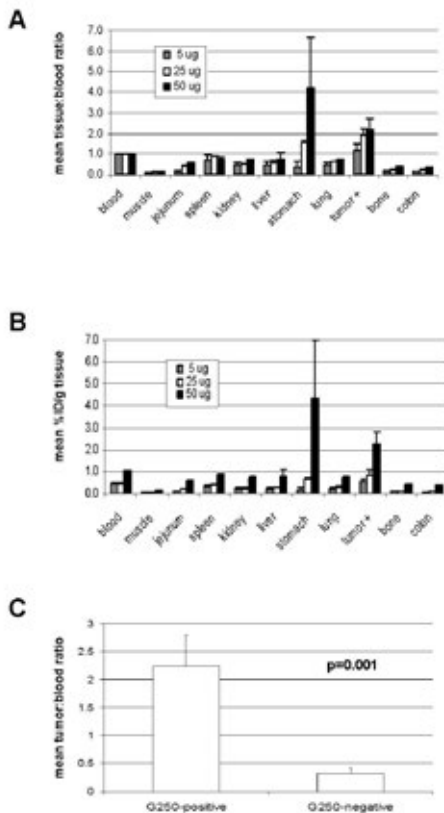
Figure 5. Effect of dose escalation on tumor targeting and construct enrichment. Cohorts of n = 3 animals received 5, 25, or 50 µg cG250-TNF and tissues were harvested, counted and weighed 24 hr after administration of radioiodinated construct. Standard deviation is indicated by bars. **(a)** Tissue-to-blood ratios remained stable for almost all tissues, with exception of stomach uptake, again attributed to free iodine in gastric mucosa. **(a)** Relative as well as **(b)** absolute amount of cG250-TNF accumulated in the tumors more than doubled with increasing protein dose, reaching absolute levels comparable to cG250. **(c)** Tumor uptake of radiolabeled cG250-TNF was investigated in mice simultaneously xenotransplanted with G250-positive and G250-negative renal cell carcinomas. Enrichment of the radiolabeled fusion protein was dependent on the presence of the targeted antigen. Standard deviations are indicated by bars.

Efficacy of combined immunotherapy *in vivo*

To compare the bioactivity of cG250-TNF with rhTNF at equimolar levels, we performed experiments at TNF-equivalent doses (30 µg of recombinant human TNF vs. 100 µg of cG250-TNF). Initial studies revealed that the toxicity profile of cG250-TNF was analogous to our previously defined LD50 of dimeric-TNF-fusion proteins such as anti-FAP-TNF for BALB/c *nu/nu* mice [33]. Tumor-bearing mice treated with 30 µg of rhTNF all died within 24 hr and could not be challenged with a second injection. Mice treated with 100 µg of cG250-TNF showed some signs of stress but all completed treatment without any lethal side effects. Further dose escalation of cG250-TNF led to significant weight loss and alteration of behavior when applied in combination with IFNγ without improvement of therapeutic efficacy (data not shown). Animals were simultaneously xenografted with solid growing G250-positive (SK-RC-52) and G250-negative (SK-RC-17) renal cell carcinomas on the opposite flanks and therapeutic agents were administered three times per week. Repeated i.v. injections of 100 µg of cG250-TNF resulted in a significant growth retardation of G250- expressing RCC when compared with treatment with parental cG250 IgG at the 100 µg dose or to treatment with 100 µg of control construct anti-FAP-TNF (p = 0.0001). Tumor size was controlled and remained stable during antigen-specific treatment without achieving complete remissions and tumor regrowth was only measurable after termination of cG250-TNF administration. In accordance to G250 antigen-restricted enrichment of radiolabeled cG250-TNF (Fig. 5c), the therapeutic activity of the unlabeled construct was also dependent on the presence of the targeted antigen as no therapeutic effect was seen on G250-negative tumors (Fig. 6a). A control fusion protein (anti-FAP-TNF) which does not recognize a relevant antigen in this model as well as the parental cG250 IgG failed to induce significant antitumor responses (Fig. 6a). Combined application of cG250-TNF i.v. and low-dose IFNγ s.c. was significantly superior to monotherapy (p = 0.01) as additional down-sizing of established xenografts could be induced. The groups receiving cG250-TNF or cG250-TNF in combination with IFNγ showed only progressive disease after termination of the treatment (Fig. 6b). Treatment at these dose levels could be completed without severe side effects. This clearly demonstrates that low dose IFNγ has a synergistic effect on cG250-TNF therapy *in vivo* and is well tolerated in combination with therapeutic cG250-TNF concentrations.

Discussion

Human clear cell carcinoma is the most common and aggressive renal tumor type. The recognition of hypoxia-inducible factor (HIF) related pathways involved in clear-cell RCC was the major breakthrough for the development of novel targeted therapies [4]. Activation of the HIF cascade leads to up-regulation of membrane bound G250/CAIX in more than 94% of clear-cell RCC [39]. Positron emission tomography (PET) imaging of patients with renal masses using [124]I-cG250 could identify aggressive clear-cell RCC with 100% specificity and positive predictive accuracy [10]. According to previous clinical trials using iodinated cG250,
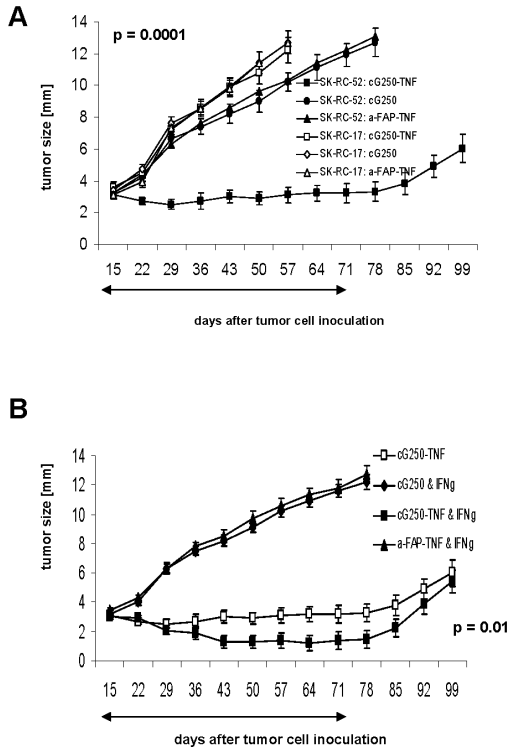
A

B

Figure 6. Treatment of BALB/c *nu/nu* mice simultaneously xenografted with G250-antigen positive (SK-RC-52) and -negative (SK-RC-17) renal cell carcinomas. Groups of n = 7 mice were treated every three days with i.v. injections cG250-TNF (100 µg), uncoupled cG250 antibody (100 µg) or with anti-FAP-TNF (100 µg) and tumor diameters were measured (mm). Treatment period is indicated by arrow (day 15 to day 78). **(a)** Therapeutic efficacy was dependent on the presence of the targeted G250-antigen and application of cG250-TNF and resulted in significant remission of established xenografts during treatment period. **(b)** Response to treatment was significantly improved by combined application of IFNg (300 ng) s.c., every 3 days and cG250-TNF (p = 0.01). Standard deviations are indicated by bars.

even metastatic spread of the disease could be visualized [8,10]. These prospective trials support the potency of cG250 for tumor detection and the preclinical study presented here establishes cG250 for the targeted delivery of TNF to xenotransplanted renal cell carcinoma. The cG250-based TNF fusion protein was designed in analogy to a previously generated IgG-TNF construct allowing for efficient systemic TNF administration [13,33]. Intensity of TNF-R1 mediated signaling *in vitro* using the cytotoxicity assay system was comparable with the well-known range of the formerly characterized dimeric TNF-construct [13] Overall, cG250-TNF displays bioactivity in tumoricidal effector systems *in vitro* like induction of respiratory burst and triggering of endothelial cell injury. These effects, which play an important role in the antitumor efficacy of TNF *in vivo*, are further up-regulated by IFNγ leading to synergistic rather than additive stimulation of key regulators responsible for antitumor effectiveness *in vivo*. Biodistribution studies in xenografted nude mice demonstrated the tumor-vasculature specific uptake of cG250-TNF and its enrichment over time exclusively at the tumor site. The labeling did not affect the immuno-reactivity of the protein, i.e., the pharmacokinetic behavior as measured by counting the radioactivity in harvested organs was a representation of true cG250-TNF targeting. Of note, part of the purified labeled material consisted of aggregates and thus, some uptake of aggregated material in liver and spleen was anticipated. The radioactivity measured in stomach was

likely due to free iodide accumulation in this tissue [40]. We conclude that the shorter clearance time of cG250-TNF in comparison to the full-size IgG-format together with its lower TNF activity because of the dimeric TNF-structure led to the favorable low-toxicity profile. These properties allowed for the present dose dense application regimen and targeting TNF as a truncated IgG-construct induced significant antitumor responses in the xenograft RCC nude mouse model. Moreover, therapeutic potency of cG250-TNF could circumvent previously reported limitations of TNF-based immunotherapy in nude mice: Preclinical and clinical data suggest production of endogenous IFNγ as a central triggering antitumor mechanism in response to treatment with TNF [41,42]. As activated T cells seem to play the major role for triggering synergistic endogenous IFNγ release, nontargeted TNF alone, or even in combination with chemotherapy failed to induce antitumor effects in athymic nude mice bearing human xenografts [43]. Similarly, no antitumor effect was observed for the combination of targeted trimeric TNF at lower doses and an alkylating agent. Only the additional application of exogenous IFNγ improved the response rate to targeted TNF in these trials [44]. In this study, however, the dose dense administration schedule of cG250-TNF resulted in significant size reduction of xenotransplanted renal cell carcinomas and led to disease control during treatment. The combination of IFNγ and cG250-TNF could even improve treatment efficacy further resulting in a significant advantage of the combination regimen when compared to cG250-TNF monotherapy. Other trials reported up-regulation and enhanced shedding of TNF-receptors in response to IFNγ or TNF treatment [45,46]. Thus, the release of TNF receptors represents a counter-regulatory mechanism potentially contributing to a decrease in therapeutic TNF activity [47]. Antitumor efficacy of single agent treatment with cG250-TNF was not limited by such undesirable effects. Furthermore, addition of IFNγ at clinically well-tolerated doses used in our trial was already sufficient to further improve the good results obtained from the single agent treatment and alteration of soluble TNF-R1 levels is almost negligible in response to such low doses of IFNγ [45]. Furthermore, the TNF part of cG250-TNF consists of two human TNF subunits thereby circumventing murine TNF-R2 binding with concomitant inhibition [48]. In summary, administration of cG250-TNF alone or in combination with IFNγ displayed impressive therapeutic efficacy. Initial reduction in tumor size and therapeutic control over established renal cell carcinomas was observed throughout continued administration of cG250-TNF. The phenomenon that withdrawal of targeted therapy provoked tumor regrowth is a common feature also observed in other therapeutic tumor vascular targeting settings [49]. The schedule of treatment and dosage of combined drugs is very critical for biological effects of applied cytokines [50]. The large therapeutic window and its antitumor efficacy qualify cG250-TNF for further trials with potent co-effectors. Moreover, the very limited progression-free survival of patients suffering from metastatic disease promotes treatment strategies basing on cG250-TNF [51]. The encouraging targeting and antitumor properties of cG250-TNF and the strong and stable expression pattern of CAIX/G250 in sporadic and inherited forms of RCC warrant clinical evaluation of this construct.

Acknowledgements

References

1. Parkin DM, Bray F, Ferlay J, Pisani P. Global cancer statistics, 2002. CA Cancer J Clin 2005;55:74–108.
2. Levi F, Lucchini F, Negri E, La Vecchia C. Declining mortality from kidney cancer in Europe. Ann Oncol 2004;15: 1130–5
3. Motzer RJ, Bukowski RM. Targeted therapy for metastatic renal cell carcinoma. J Clin Oncol 2006;24:5601–8.
4. Ravaud A, Wallerand H, Culine S, Bernhard JC, Fergelot P, Bensalah K, Patard JJ. Update on the medical treatment of metastatic renal cell carcinoma. Eur Urol 2008;54:315–25.
5. Latif F, Tory K, Gnarra J, Yao M, Duh FM, Orcutt ML, Stackhouse T, Kuzmin I, Modi W, Geil L. Identification of the von Hippel-Lindau disease tumor suppressor gene. Science 1993;260: 1317–20.
6. Uemura H, Nakagawa Y, Yoshida K, Saga S, Yoshikawa K, Hirao Y, Oosterwijk E. MN/CA IX/G250 as a potential target for immunotherapy of renal cell carcinomas. Br J Cancer 1999;81:741–6.
7. Steffens MG, Boerman OC, Oosterwijk-Wakka JC, Oosterhof GO, Witjes JA, Koenders EB, Oyen WJ, Buijs WC, Debruyne FM, Corstens FH, Oosterwijk E. Targeting of renal cell carcinoma with iodine- 131-labeled chimeric monoclonal antibody G250. J Clin Oncol 1997;15:1529–37.
8. Steffens MG, Boerman OC, de Mulder PH, Oyen WJ, Buijs WC, Witjes JA, van den Broek WJ, Oosterwijk-Wakka JC, Debruyne FM, Corstens FH, Oosterwijk E. Phase I radioimmunotherapy of metastatic renal cell carcinoma with 131I-labeled chimeric monoclonal antibody G250. Clin Cancer Res 1999;5:s3268–s74.
9. Davis ID, Wiseman GA, Lee FT, Gansen DN, Hopkins W, Papenfuss AT, Liu Z, Moynihan TJ, Croghan GA, Adjei AA, Hoffman EW, Ingle JN, et al. A phase I multiple dose, dose escalation study of cG250 monoclonal antibody in patients with advanced renal cell carcinoma. Cancer Immun 2007;7:13.
10. Divgi CR, Pandit-Taskar N, Jungbluth AA, Reuter VE, Gonen M, Ruan S, Pierre C, Nagel A, Pryma DA, Humm J, Larson SM, Old LJ, et al. Preoperative characterisation of clear-cell renal carcinoma using iodine-124-labelled antibody chimeric G250 (124I-cG250) and PET in patients with renal masses: a phase I trial. Lancet Oncol 2007;8:304–10.
11. Bleumer I, Oosterwijk E, Oosterwijk-Wakka JC, Voller MC, Melchior S, Warnaar SO, Mala C, Beck J, Mulders PF. A clinical trial with chimeric monoclonal antibody WX-G250 and low dose interleukin-2 pulsing scheme for advanced renal cell carcinoma. J Urol 2006; 175:57–62.
12. Davis ID, Liu Z, Saunders W, Lee FT, Spirkoska V, Hopkins W, Smyth FE, Chong G, Papenfuss AT, Chappell B, Poon A, Saunder TH, et al. A pilot study of monoclonal antibody cG250 and low dose subcutaneous IL-2 in patients with advanced renal cell carcinoma. Cancer Immun 2007;7:14.
13. Bauer S, Adrian N, Williamson B, Panousis C, Fadle N, Smerd J, Fet- tah I, Scott AM, Pfreundschuh M, Renner C. Targeted bioactivity of membrane-anchored TNF by an antibody-derived TNF fusion protein. J Immunol 2004;172:3930–9.
14. Carswell EA, Old LJ, Kassel RL, Green S, Fiore N, Williamson B. An endotoxin-induced serum factor that causes necrosis of tumors. Proc Natl Acad Sci USA 1975;72:3666–70.
15. Creasey AA, Reynolds MT, Laird W. Cures and partial regression of murine and human tumors by recombinant human tumor necrosis factor. Cancer Res 1986;46:5687–90.
16. Dighe AS, Richards E, Old LJ, Schreiber RD. Enhanced in vivo growth and resistance to rejection of tumor cells expressing dominant negative IFN gamma receptors. Immunity 1994;1:447–56.
17. Muller-Hermelink N, Braumuller H, Pichler B, Wieder T, Mailhammer R, Schaak K, Ghoreschi K, Yazdi A, Haubner R, Sander CA, Mocikat R, Schwaiger M, et al. TNFR1 signaling and IFN-gamma signaling determine whether T cells induce tumor dormancy or promote multistage carcinogenesis. Cancer Cell 2008;13:507–18.
18. Ikeda H, Old LJ, Schreiber RD. The roles of IFN gamma in protection against tumor development and cancer immunoediting. Cytokine Growth Factor Rev 2002;13:95–109.
19. Angiolillo AL, Sgadari C, Taub DD, Liao F, Farber JM, Maheshwari S, Kleinman HK, Reaman GH, Tosato G. Human interferon-inducible protein 10 is a potent inhibitor of angiogenesis in vivo. J Exp Med 1995;182:155–62.
20. Sgadari C, Angiolillo AL, Cherney BW, Pike SE, Farber JM, Koniaris LG, Vanguri P, Burd PR, Sheikh N, Gupta G, Teruya-Feldstein J, Tosato G. Interferon-inducible protein-10 identified as a mediator of tumor necrosis in vivo. Proc Natl Acad Sci USA 1996;93: 13791–6.

21. Schreiber RD, Hicks LJ, Celada A, Buchmeier NA, Gray PW. Monoclonal antibodies to murine gamma-interferon which differentially modulate macrophage activation and antiviral activity. J Immunol 1985;134:1609–18.
22. MacMicking J, Xie QW, Nathan C. Nitric oxide and macrophage function. Annu Rev Immunol 1997;15:323–50.
23. Shankaran V, Ikeda H, Bruce AT, White JM, Swanson PE, Old LJ, Schreiber RD. IFNgamma and lymphocytes prevent primary tumour development and shape tumour immunogenicity. Nature 2001;410: 1107–11.
24. Marincola FM, Jaffee EM, Hicklin DJ, Ferrone S. Escape of human solid tumors from T-cell recognition: molecular mechanisms and functional significance. Adv Immunol 2000;74:181–273.
25. Williamson BD, Carswell EA, Rubin BY, Prendergast JS, Old LJ. Human tumor necrosis factor produced by human B-cell lines: synergistic cytotoxic interaction with human interferon. Proc Natl Acad Sci USA 1983;80:5397–401.
26. Balkwill FR, Lee A, Aldam G, Moodie E, Thomas JA, Tavernier J, Fiers W. Human tumor xenografts treated with recombinant human tumor necrosis factor alone or in combination with interferons. Cancer Res 1986;46:3990–3.
27. Ruegg C, Yilmaz A, Bieler G, Bamat J, Chaubert P, Lejeune FJ. Evidence for the involvement of endothelial cell integrin alphaVbeta3 in the disruption of the tumor vasculature induced by TNF and IFN- gamma. Nat Med 1998;4:408–14.
28. Sherman ML, Spriggs DR, Arthur KA, Imamura K, Frei E, III, Kufe DW. Recombinant human tumor necrosis factor administered as a five-day continuous infusion in cancer patients: phase I toxicity and effects on lipid metabolism. J Clin Oncol 1988;6:344–50.
29. Nawroth PP, Stern DM. Modulation of endothelial cell hemostatic properties by tumor necrosis factor. J Exp Med 1986;163:740–5.
30. Kilbourn RG, Gross SS, Jubran A, Adams J, Griffith OW, Levi R, Lodato RF. NG-methyl-L-arginine inhibits tumor necrosis factor-induced hypotension: implications for the involvement of nitric oxide. Proc Natl Acad Sci USA 1990;87:3629–32.
31. Eggermont AM, ten Hagen TL. Isolated limb perfusion for extremity soft-tissue sarcomas, in-transit metastases, and other unresectable tumors: credits, debits, and future perspectives. Curr Oncol Rep 2001;3:359–67.
32. Lejeune FJ, Kroon BB, Di Filippo F, Hoekstra HJ, Santinami M, Lienard D, Eggermont AM. Isolated limb perfusion: the European experience. Surg Oncol Clin N Am 2001;10:821–32, ix.
33. Bauer S, Adrian N, Fischer E, Kleber S, Stenner F, Wadle A, Fadle N, Zoellner A, Bernhardt R, Knuth A, Old LJ, Renner C. Structure-activity profiles of Ab-derived TNF fusion proteins. J Immunol 2006; 177:2423–30.
34. Espevik T, Nissen-Meyer J. A highly sensitive cell line. WEHI 164 clone 13, for measuring cytotoxic factor/tumor necrosis factor from human monocytes. J Immunol Methods 1986;95:99–105.
35. Suk K, Chang I, Kim YH, Kim S, Kim JY, Kim H, Lee MS. Interferon gamma (IFNgamma) and tumor necrosis factor alpha synergism in ME-180 cervical cancer cell apoptosis and necrosis. IFNgamma inhibits cytoprotective. NF-kappa. B through. STAT1/IRF-1 pathways. J Biol Chem 2001;276:13153–9.
36. Steffens MG, Boerman OC, Oyen WJ, Kniest PH, Witjes JA, Oosterhof GO, van Leenders GJ, Debruyne FM, Corstens FH, Oosterwijk E. Intratumoral distribution of two consecutive injections of chimeric antibody G250 in primary renal cell carcinoma: implications for fractionated dose radioimmunotherapy. Cancer Res 1999;59:1615– 19.
37. Yilmaz A, Bieler G, Spertini O, Lejeune FJ, Ruegg C. Pulse treatment of human vascular endothelial cells with high doses of tumor necrosis factor and interferon-gamma results in simultaneous synergistic and reversible effects on proliferation and morphology. Int J Cancer 1998;77:592–9.
38. van Schaijk FG, Oosterwijk E, Molkenboer-Kuenen JD, Soede AC, McBride BJ, Goldenberg DM, Oyen WJ, Corstens FH, Boerman OC. Pretargeting with bispecific anti-renal cell carcinoma x anti-DTPA(In) antibody in 3 RCC models. J Nucl Med 2005;46:495–501.
39. Thiry A, Dogne JM, Masereel B, Supuran CT. Targeting tumor-associated carbonic anhydrase IX in cancer therapy. Trends Pharmacol Sci 2006;27:566–73.
40. Bakker WH, Krenning EP, Breeman WA, Koper JW, Kooij PP, Reubi JC, Klijn JG, Visser TJ, Docter R, Lamberts SW. Receptor scintigraphy with a radioiodinated somatostatin analogue: radiolabeling, purification, biologic activity, and in vivo application in animals. J Nucl Med 1990;31:1501–9.

41. Shaw SK, Perkins BN, Lim YC, Liu Y, Nusrat A, Schnell FJ, Parkos CA, Luscinskas FW. Reduced expression of junctional adhesion molecule and platelet/endothelial cell adhesion molecule-1 (CD31) at human vascular endothelial junctions by cytokines tumor necrosis factor-alpha plus interferon-gamma does not reduce leukocyte transmigration under flow. Am J Pathol 2001;159:2281–91.
42. Lienard D, Eggermont AM, Koops HS, Kroon B, Towse G, Hiemstra S, Schmitz P, Clarke J, Steinmann G, Rosenkaimer F, Lejeune FJ. Isolated limb perfusion with tumour necrosis factor-alpha and melphalan with or without interferon-gamma for the treatment of in-transit melanoma metastases: a multicentre randomized phase II study. Melanoma Res 1999;9:491–502.
43. Furrer M, Altermatt HJ, Ris HB, Althaus U, Ruegg C, Lienard D, Lejeune FJ. Lack of antitumour activity of human recombinant tumour necrosis factor-alpha, alone or in combination with melphalan in a nude mouse human melanoma xenograft system. Melanoma Res 1997;7(Suppl 2):S43–S49.
44. Sacchi A, Gasparri A, Curnis F, Bellone M, Corti A. Crucial role for interferon gamma in the synergism between tumor vasculature-targeted tumor necrosis factor alpha (NGR-TNF) and doxorubicin. Cancer Res 2004;64:7150–5.
45. Curnis F, Gasparri A, Sacchi A, Cattaneo A, Magni F, Corti A. Targeted delivery of IFNgamma to tumor vessels uncouples antitumor from counterregulatory mechanisms. Cancer Res 2005;65:2906–13.
46. Curnis F, Sacchi A, Corti A. Improving chemotherapeutic drug penetration in tumors by vascular targeting and barrier alteration. J Clin Invest 2002;110:475–82.
47. Aderka D. The potential biological and clinical significance of the soluble tumor necrosis factor receptors. Cytokine Growth Factor Rev 1996;7:231–40.
48. Lee JK, Sayers TJ, Brooks AD, Back TC, Young HA, Komschlies KL, Wigginton JM, Wiltrout RH. IFN-gamma-dependent delay of in vivo tumor progression by Fas overexpression on murine renal cancer cells. J Immunol 2000;164:231–9.
49. Red-Horse K, Ferrara N. Imaging tumor angiogenesis. J Clin Invest 2006;116:2585–7.
50. Aulitzky WE, Aulitzky WK, Frick J, Herold M, Gastl G, Tilg H, Berger M, Huber C. Treatment of cancer patients with recombinant interferon-gamma induces release of endogenous tumor necrosis factor-alpha. Immunobiology 1990;180:385–94.
51. Escudier B. Advanced renal cell carcinoma: current and emerging management strategies. Drugs 2007;67:1257–64.

Chapter 4

Effect of Tyrosine Kinase Inhibitor Treatment of Renal Cell Carcinoma on the Accumulation of Carbonic Anhydrase IX-specific chimeric Monoclonal Antibody cG250

Jeannette C. Oosterwijk-Wakka[1], Gürsah Kats-Ugurlu[2],
William P.J. Leenders[2], Lambertus A.L.M. Kiemeney[3], Lloyd J. Old[4],
Peter F.A. Mulders[1] and Egbert Oosterwijk[1]

[1] Department of Urology, [2] Pathology, [3] Health Evidence, Radboud university medical center, Nijmegen, The Netherlands, [4] Ludwig Institute for Cancer Research, New York Branch, Memorial Sloan Kettering Cancer Center, New York, United States

Abstract

Objective To investigate the effect of three different tyrosine kinase inhibitors (TKIs) on the biodistribution of chimeric monoclonal antibody (mAb) cG250, which identifies carbonic anhydrase IX (CAIX), in nude mice bearing human renal cell carcinoma (RCC) xenografts. TKIs represent the best, but still suboptimal treatment for metastatic RCC (mRCC) and combined therapy or sequential therapy might be beneficial. CAIX is abundantly over expressed in RCC and clinical trials have shown abundant and specific tumour accumulation of cG250. Combining a TKI with mAb cG250, involved in a different effector mechanism, might lead to improved tumour responses and survival in patients with mRCC.

Materials and methods Nude mice bearing human RCC xenografts were treated orally with 0.75 mg/day sunitinib, 1 mg/day vandetanib, 1 mg/day sorafenib or vehicle control for 7 or 14 days. At 7 days, mice were injected i.v. with 185 kBq/5 μg ^{125}I-cG250. Mice were killed at predetermined days and cG250 biodistribution was determined. Tumours were analysed by immunohistochemistry for the presence of endothelial cells, laminin, smooth muscle actin, CAIX expression and uptake of mAb cG250.

Results While on TKI treatment, tumour uptake of cG250 decreased dramatically, tumour growth was slightly inhibited and vascular density decreased considerably as judged by various markers. When treatment was stopped at 7 days, there was robust neovascularization, mainly at the tumour periphery. Consequently, cG250 uptake also recovered, albeit cG250 uptake appeared to be restricted to the tumour periphery where vigorous neovascularization was visible.

Conclusions Simultaneous administration of a TKI and mAb cG250 severely compromised mAb accumulation. However, shortly after discontinuation of TKI treatment mAb accumulation was restored. Combined treatment strategies with TKI and mAb should be carefully designed.

Introduction

RCC is the most common renal malignant neoplasm in adults, accounting for ~85% of renal tumours and 2% of all adult malignancies [1]. About one third of newly diagnosed patients present with metastatic disease (mRCC) and for these patients prognosis is poor with a 5-year survival of < 10%. Clinical management of patients with mRCC has changed dramatically since the introduction of the antiangiogenic receptor tyrosine kinase inhibitors (TKIs), sorafenib and sunitinib [2]. Treatment with these drugs significantly prolongs the progression-free survival of patients with mRCC. Clinical responses mainly comprise partial responses and stabilization of disease but the effects of the antiangiogenic therapy on overall survival are unclear. Most patients develop resistance to these drugs and currently no therapy is effective in this situation. Therefore, there is still an urgent need to develop additional strategies that improve antitumour effects and induce long lasting responses.

Combined therapy that consists of agents that target different pathways might act additively or synergistically. A TKI combined with chemotherapy has shown significant synergistic activity in glioma, colon-, and breast carcinoma [3–5]. Improved delivery of therapeutic molecules through vascular normalization and reduced tumour interstitial fluid pressure [6] has been suggested as a plausible explanation for this synergistic effect. However, RCC is unresponsive to chemotherapy.

Monoclonal antibody-based targeted therapies are becoming important treatment methods. Significant antitumour efficacy has been reported in the treatment of non-Hodgkin's lymphoma, breast cancer and chronic lymphocytic leukaemia. Chimeric monoclonal antibody (mAb) G250 (cG250) targets carbonic anhydrase IX (CAIX), which is specifically up-regulated in clear cell RCC (ccRCC). Various clinical studies have reported excellent accumulation in ccRCC [7,8]. In different phase II efficacy studies in patients with mRCC an increase in median survival and overall survival rates has been reported [9,10]. However, despite the excellent targeting capability, cG250 treatment rarely showed antitumour efficacy.

In the present study, we investigated the effect of three different TKIs on the biodistribution of cG250 in nude mice bearing human RCC xenografts.

Material and methods

Reagents

The following compounds were used: sorafenib (Bay 43–9006, Nexavar®, Bayer Pharmaceuticals, Germany), which inhibits phosphorylation of vascular endothelial growth factor receptor 2 (VEGFR-2), VEGFR-3, platelet-derived growth factor receptor β (PDGFRβ), transmembrane FMS-like tyrosine kinase 3 receptor (FLT-3), tyrosine kinase receptor c-kit, c-RAF-1 and B-RAF [2,11]; sunitinib (Su11248, Sutent®, Pfizer, USA), which inhibits phosphorylation of VEGFR-2, PDGFRβ, FLT-3 and c-kit [2,12]; and vandetanib (Zactima™, Astra Zeneca, UK) is a potent and selective inhibitor of VEGFR-2, epidermal growth factor

receptor and RET tyrosine kinases [2,13].

Sorafenib, sunitinib and vandetanib were generously provided by Bayer, the Ludwig Institute for Cancer Research, New York, USA, and Astra Zeneca, respectively.

Radiolabeling of cG250

The isolation, characteristics and the immunohistochemical reactivity of mouse mAb G250 have been described earlier [14]. The antigen (CAIX/G250/MN) is expressed on the cell surface of virtually all ccRCC and absent on most normal tissues [14–16]. The generation of cG250 has been described elsewhere [8].

The cG250 (generously provided by Wilex AG, Germany) was labelled with ^{125}I (Amersham) according to the Iodogen method [8]. The radiochemical purity of the ^{125}I-labelled cG250 (^{125}I-cG250) preparations was determined by instant thin-layer chromatography (ITLC) using ITLC silica gel strips (Gelman Sciences, USA) and 0.1 M citrate buffer (pH 6.0) as the mobile phase. The immunoreactive fraction (IRF) was determined on freshly trypsinized SKRC52 RCC cells at infinite antigen excess essentially as described by Lindmo *et al.* [17], with minor modifications [8].

Animal experiments

Female BALB/c nu/nu mice, aged 6–8 weeks, were obtained from the local central animal facility. The mice were grafted s.c. with freshly excised NU12 RCC xenograft pieces [18] of ~1 mm^3. Institutional guidelines were strictly followed for maintenance of animals and experimental procedures were approved by the Institutional Animal Care and Use Committee. NU12 tumours have a ccRCC phenotype and previous studies have shown that it is an excellent model to study mAb G250 targeting. Treatment with a TKI was started when tumours had reached a volume of ~100 mm^3.

Sorafenib and sunitinib were prepared as described [11]. Vandetanib was dissolved in 1% Tween-80 (Sigma) and prepared fresh every week.

Mice received the equivalent of 35 mg/kg (0.75 mg/200 µL) sunitinib orally per day for 7 or 14 days or 50 mg/kg (1 mg/200 µL) sorafenib orally per day for 14 days or 50 mg/kg (1 mg/100 µL) vandetanib orally per day for 14 days.

Biodistribution studies

When the NU12 tumours reached the desired volume, mice were divided into groups of four to five mice. Mice were treated with a TKI or vehicle once a day until they were killed (continuous treatment, Fig. 1A). After 7 days, all mice were injected i.v. with ^{125}I-cG250 (185 kBq/5 µg/mouse). Treatment and control groups of four to five mice were killed at 1, 2, 4 and 7 days after mAb injection; and blood, tumour, muscle, liver, lung, spleen, kidney, stomach and intestine were collected, weighed and counted in a γ-counter (Wizard; Pharmacia-LKB). The activity in the samples was expressed as percentage injected dose per gram tissue (% ID/g). In one experiment, sunitinib treatment was stopped after 7 days (7d sunitinib, Fig. 1B), mice were injected i.v. with ^{125}I-cG250 mAb and cG250 biodistribution was determined as

described above.
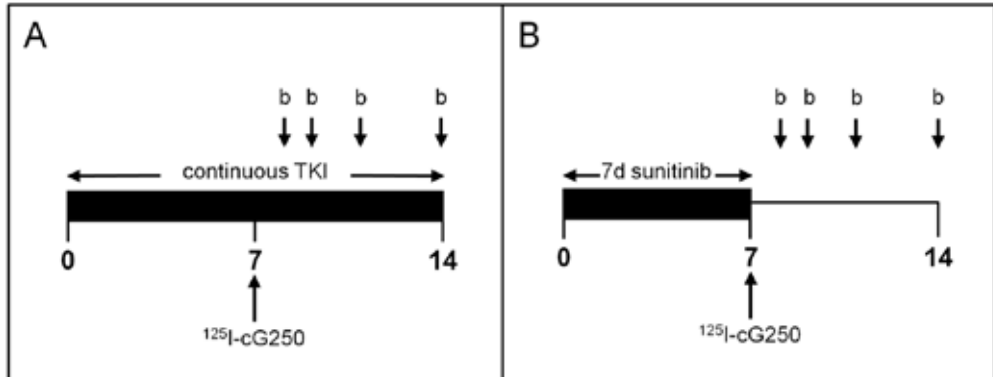
Figure 1. Treatment schedule of nude mice. **A**, continuous TKI treatment; **B**, 7 day sunitinib treatment. b, biodistribution time point.

Immunohistochemical analysis

For immunohistochemical analysis, harvested tumours were formalin fixed and embedded in paraffin, snap-frozen and stored at –80 °C. For morphological analyses, sections were stained with haematoxylin and eosin. Primary antibodies used were: cG250 to detect CAIX (Wilex, Germany, 10 µg/mL), rat-anti-mouse CD34 (Hycult Biotechnology, 5 µg/mL) or rat monoclonal 9F1 [19] (supernatant 1:50) to detect endothelial cells, mouse-anti-smooth muscle actin (SMA; α-SM1, A2547 Sigma, 1:15000) to detect perivascular cells, polyclonal rabbit-anti-laminin (Z0097,Dako, Denmark, 1:3000) to visualize basement membrane, rabbit anti-Glut-1 (A3536, Dako, Denmark, 1:200) to detect hypoxia and mouse anti-human Ki-67 (Mib-1, M7240, Dako, Denmark, 1:100) to detect proliferating cells. For visualization of CAIX expression, 4 µm cryostat sections were acetone fixed and incubated with cG250, followed by peroxidase labelled rabbit-anti-human IgG (P214, Dako) as secondary antibody.

To detect *in vivo* accumulated injected cG250, cryostat sections were incubated with rabbit-anti-human IgG–peroxidase only and 3,3'-diaminobenzidine (DAB) was used as developing agent (PowerDAB, Immunologic, Duiven, the Netherlands) .

Endothelial cells were visualized with 9F1 or anti-CD34; 9F1 staining was performed on acetone fixed 4 µm cryostat sections. After blocking with avidin, biotin and normal rabbit serum, primary antibody 9F1 was applied for 1 h at room temperature. After washing procedures, secondary antibody was applied (biotinylated anti-rat antibody, Vector) supplemented with 4% normal mouse serum. Subsequently, sections were incubated with avidin/biotinylated enzyme complex (ABC)-peroxidase with PowerDAB as developing agent.

CD34/SMA double staining was performed as described previously [20]. For laminin staining, paraffin sections were pretreated with 0.1% pronase in PBS for 10 min at 37 °C. Immunohistochemistry for Glut-1 and Ki-67 was performed on paraffin sections as described

previously [20]. After blocking with avidin and biotin, sections were blocked with either normal goat serum (for laminin and Glut-1) or normal horse serum (for Mib-1) and incubated overnight at 4 °C with the primary antibody (anti-laminin, Glut-1 or Mib-1). Subsequently, sections were incubated with the appropriate secondary antibody, ABC-peroxidase was applied and AEC (aminoethylcarbazole in dimethylformamide) reagent was used as the developing agent.

All sections with the exception of the double-stained CD34/SMA sections were counterstained with haematoxylin.

Statistical analysis

The results are given as the mean (SD). Differences in mAb cG250 uptake between treatment and control at each time-point were tested for statistical significance using the Mann–Whitney *U*-test. Statistical significance was set at a *P*-value of 0.05, without adjustments for multiple testing. All tests were two-sided.

Results

Continuous treatment of NU12 tumours with sunitinib, sorafenib, or vandetanib caused substantial inhibition of tumour growth (Table 1), regardless of the tumour volume at the initiation of the TKI treatment. After 14 days of treatment, mean tumour volumes for the sunitinib-, vandetanib- and sorafenib-treated groups were 129%, 86% and 103%, respectively, of the baseline value (100%). By contrast, the tumour volumes of the control groups were 241%, 195%, and 171%, respectively.

Table 1 Mean (SD) volume of NU12 tumours during treatment with sunitinib, sorafenib or vandetanib

Duration of treatment	Treatment	Mean (SD) volume[*], mm^3 at:		
		0 days	7 days	14 days
7 days	Sunitinib	168 (72)	208 (97)	ND
	Control	148 (73)	241 (104)	
Continuous	Sunitinib	91 (38)	126 (61)	118 (54)
	Control	96 (37)	180 (67)	232 (111)
	Vandetanib	63 (34)	69 (37)	54 (34)
	Control	64 (29)	95 (33)	125 (19)
	Sorafenib	117 (66)	91 (50)	121 (52)
	Control	112 (63)	125 (68)	192 (61)

[*]Volume (mm^3) of the tumours calculated using the formula: length x width x depth x π/6. ND, not determined.

In Fig. 2A the biodistribution of ^{125}I-cG250 (IRF 82%) in sunitinib- and untreated NU12-tumour bearing mice is shown. The amount of accumulated cG250 in the tumours of the

control mice were in the expected range, 40 (10)%, 44 (4)%, 35 (9)% and 21 (5)% at 1, 2, 4 and 7 days after injection, respectively, but these values were reduced to 11 (4)%, 12 (5)%, 9 (2)%, 8 (1)% in the treated mice, respectively. This translates into a relative decrease of 73%, 73%, 74% and 62% of cG250 accumulation, respectively (Table 2).

When sunitinib treatment was discontinued at the time of ^{125}I-cG250 injection (IRF 92%) there was a different distribution pattern (Fig. 2B). In tumours of control mice %ID/g cG250 were 34 (5)%, 31 (6)%, 30 (3)%, and 12 (3)% at 1, 2, 4 and 7 days after injection, respectively. By contrast, cG250 accumulation values for the tumours harvested from the sunitinib-treated mice were 21 (3)%, 25 (7)%, 29 (8)%, 27 (11)% at 1, 2, 4 and 7 days after injection, respectively, i.e. this translates to a relative decrease of 38%, 19%, 3% and an increase of 125%, respectively (Table 2). Sunitinib treatment did not alter cG250 distribution in other organs.
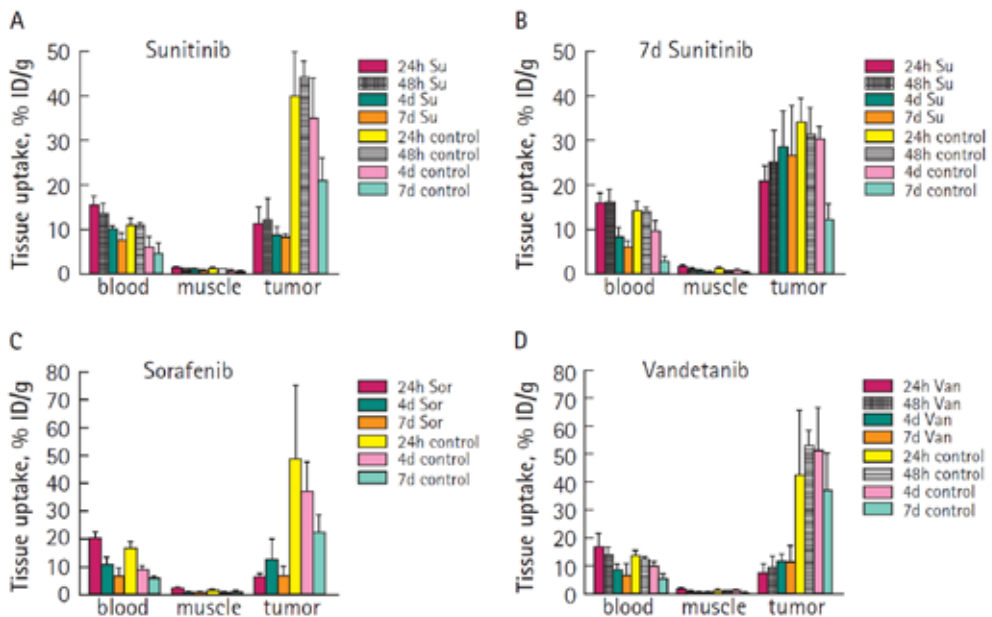
Figure 2. Biodistribution of ^{125}I-cG250 in Balb/c nu/nu mice xenografted with NU-12 (G250+) tumours. **A,** continuous sunitinib treatment; **B**, 7 day sunitinib treatment; **C**, continuous sorafenib treatment; **D**, continuous vandetanib treatment. Data from groups of four to five mice are expressed as the mean (SD). Statistical analysis was based on the Mann–Whitney test comparing treatment with control at each timepoint.

To investigate whether the effects of sunitinib on cG250 tumour accumulation could be reproduced with other TKIs, NU12-tumour bearing nude mice were treated with sorafenib or vandetanib and the biodistribution of ^{125}I-cG250 (IRF ^{125}I-cG250 91% and 87%, respectively) was determined (Fig. 2C,D). Indeed, the same inhibitory effect on tumour uptake was seen at all time points in the sorafenib- and vandetanib-treated mice. Sorafenib reduced cG250

uptake by 88%, 64%, and 68% at 1, 4 and 7 days, respectively. Finally, vandetanib treatment resulted in reduction of cG250 uptake of 83%, 81%, 68%, and 71% at 1, 2, 4 and 7 days respectively (Table 2). There was normal blood clearance in all experiments. As expected, there was no uptake of cG250 in muscle (Fig. 2) or any other tissues (results not shown).

Table 2 Relative decrease in mAb cG250 uptake after treatment with sunitinib, sorafenib or vandetanib

	Time after injection, days			
Treatment	1	2	4	7
Mean (SD) % ID/g:				
sunitinib, continous	11 (4)	12 (5)	9 (2)	8 (1)
control	40 (10)	44 (4)	35 (9)	21 (5)
Relative decrease, %[*]	**73**	**73**	**74**	**62**
P	*0.008*	*0.008*	*0.016*	*0.008*
Mean (SD) % ID/g:				
sunitinib, 7 days	21 (3)	25 (7)	29 (8)	27 (11)
control	34 (5)	31 (6)	30 (3)	12 (3)
Relative decrease, %[*]	**38**	**19**	**3**	**– 125**
P	*0.016*	*0.310*	*0.905*	*0.056*
Mean (SD) % ID/g:				
sorafenib, continous	6 (1)	ND	13 (7)	7 (3)
control	49 (26)	ND	37 (11)	22 (6)
Relative decrease, %[*]	**88**	**–**	**64**	**68**
P	*0.016*	*–*	*0.008*	*0.008*
Mean (SD) % ID/g				
vandetanib, continous	7 (3)	10 (3)	12 (3)	11 (6)
control	42 (23)	53 (6)	51 (15)	37 (13)
Relative decrease, %[*]	**83**	**81**	**68**	**71**
P	*0.016*	*0.095*	*0.016*	*0.063*

[*]**Relative decrease**, (% ID/g control – % ID/g treatment)/% ID/g control x 100 %; ND, not determined.

Immunohistochemistry

Because the studied TKIs are known antiangiogenic molecules, we analysed the tumours for the distribution of vascular markers. Additionally, tumours were analysed for CAIX expression, cG250-uptake, laminin, Ki-67 and Glut-1. Comparison of tumours harvested from TKI-treated mice with control tumours showed a dramatic decrease in vasculature as judged by CD34 or 9F1 analysis (Fig. 3G-I). There was vigorous outgrowth of endothelium in the tumour periphery, but not in the tumour centre in mice in which sunitinib treatment was stopped at 7 days (compare with Fig. 3H, I). Vascular density was considerably decreased in tumours from continuously treated mice (Fig. 3H, blue staining) as compared with control mice (Fig. 3G). TKI treatment of 7 or 14 days resulted in a slight decrease of SMA-positive cells (presumably pericytes, characteristic for mature vessels), but this decrease was less pronounced than the decrease seen with CD34 (Fig. 3G,H; red colour).

CAIX expression was homogeneous in tumours of treated and control mice (Fig. 3A–C),

i.e. expression of the cG250 target was not altered due to the TKI treatment. *In vivo* accumulated cG250 was clearly detectable in untreated mice throughout the tumours (Fig. 3D). However, accumulation of the injected cG250 could not be visualized in the tumours of mice under continuous sunitinib treatment (Fig. 3E). In contrast, when sunitinib treatment was discontinued, accumulation of the injected cG250 could readily be seen in the tumours(Fig. 3F), predominantly in the tumour periphery in areas with vigorous vascular outgrowth.

In Fig. 3J–L the expression pattern of laminin is shown. The nicely organized structure of laminin in the tumours of the control mice (Fig. 3J) was lost in the tumours of the mice treated with sunitinib for 14 days (Fig. 3K). This network was restored 7 days after treatment was stopped (Fig. 3L).

Microscopic analysis of the NU12 tumours of untreated mice showed a typical micronodular phenotype (Fig. 4A). Sunitinib treatment resulted in loss of this phenotype and in the appearance of more dispersed necrotic areas (Fig. 4D). Tumours of the vandetanib-(Fig. 4G) and the sorafenib-treated mice (Fig. 4J) showed widespread necrosis.

TKI treatment with sunitinib, sorafenib or vandetanib did not lead to differences in cell proliferation in viable tumour tissue as judged by Mib-1 (Ki-67) staining (Fig. 4C, F, I, L).

Glut-1 expression was not visible in the control tumours but clearly visible in the mice treated with sunitinib for 14 days (Fig. 4B, E), most prominently adjacent to necrotic areas. With the exception of more extensive expression of Glut-1 (Fig. 4H, K), analysis of the tumours of the sorafenib- and of the vandetanib-treated mice showed similar results as tumours from sunitinib-treated mice (not shown).

Discussion

Treatment of patients with metastasized ccRCC has changed dramatically since the introduction of TKIs. Of the two frequently used drugs, sunitinib treatment can result in significant tumour responses. Although this is a major advancement in the clinical management of these patients, unfortunately, durable responses are rare and it is currently unclear whether TKI treatment improves overall survival. Advanced RCC remains an incurable disease and therefore new (combined) therapies are still needed. It might be more effective to combine therapies that differ in their working mechanism, e.g. bevacizumab combined with erlotinib [21] or interferon α combined with bevacizumab [22] or sorafenib [23,24]. These treatment regimens lead to improved response rates, but toxicity was also augmented.

In the present study, we combined TKIs with the tumour-specific cG250, which targets CAIX, ubiquitously expressed in ccRCC. With this combination two different pathways are 'hit', which might prove beneficial. Before embarking on combined therapy studies, we studied the influence of TKI treatment on the pharmacokinetic behaviour of cG250. In general, all three TKIs tested had very similar effects. There was already a significant

decrease in cG250 tumour accumulation after 7 days of treatment with TKI, regardless of which TKI was used. *In vitro* analysis showed that antibody accretion was dramatically diminished in tumours of the TKI-treated mice. Most probably, the decreased cG250 tumour accumulation is caused by the loss of vascular integrity as shown by the marked decreased
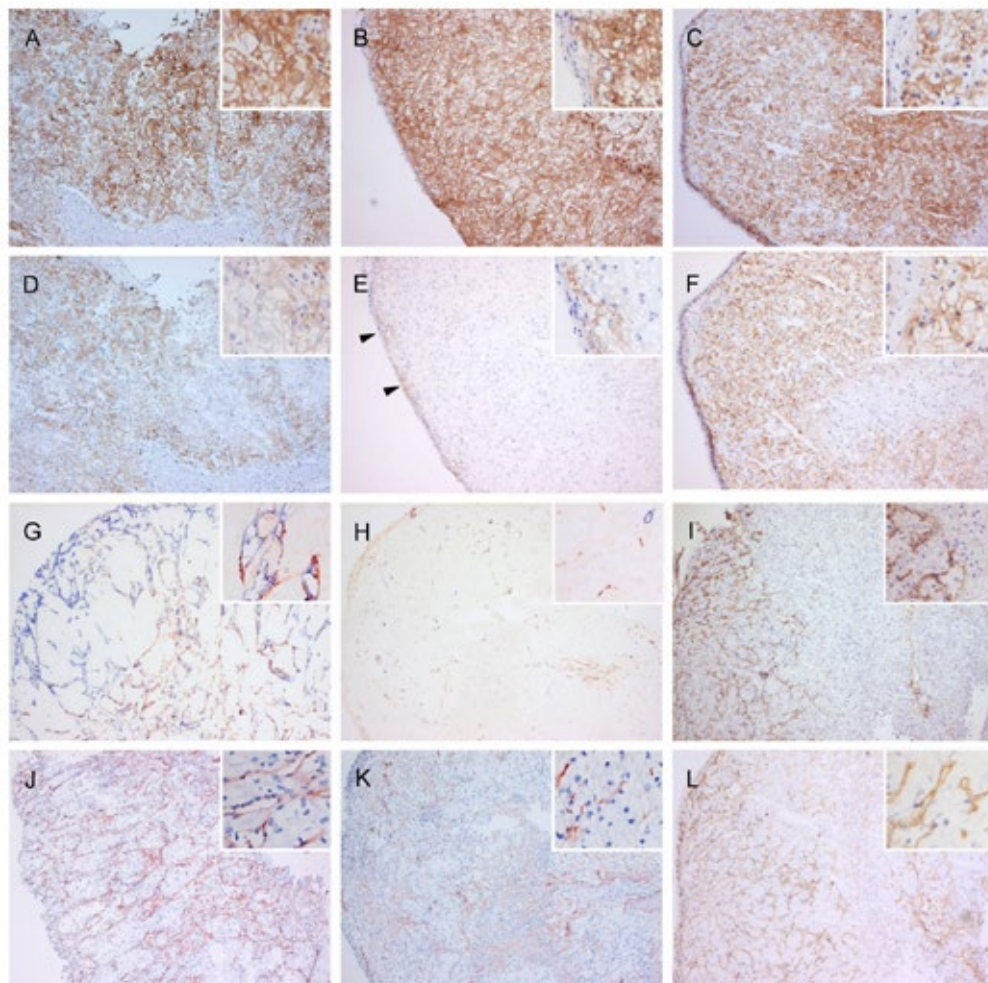
Figure 3. Immunohistochemical analysis of NU-12 tumours treated with sunitinib. Tumours were harvested 14 days after the start of treatment. **A**, **D**, **G**, **J**, untreated mice; **B**, **E**, **H**, **K**, continuously treated (14 days) mice; **C**, **F**, **I** and **L**, 7 day treated mice. **A**, **B**, **C**, CAIX expression. **D**, **E**, **F**, In vivo accumulated cG250. **G**, **H**, Staining of endothelium (CD34) in blue and staining of SMA (pericytes, characteristic for mature vessels) in red. **I**, staining of endothelium (9F1). **J**, **K**, **L**, Expression of laminin. Inserts show higher magnifications. Please note dramatic decrease of endothelium in continuously treated mice and vigorous outgrowth of endothelium in the tumour periphery when sunitinib treatment was stopped (compare **H**, **I**). There was no outgrowth of endothelium in the central region of the tumours. cG250 accumulation could barely be visualized (black arrows) during continuous sunitinib treatment (**E**). In contrast, cG250 accumulation was clearly visible in tumours of 7-day treated mice, predominantly in areas with endothelial outgrowth (**I**). A–F, x50; G–L, x25; A–L inserts, x100.
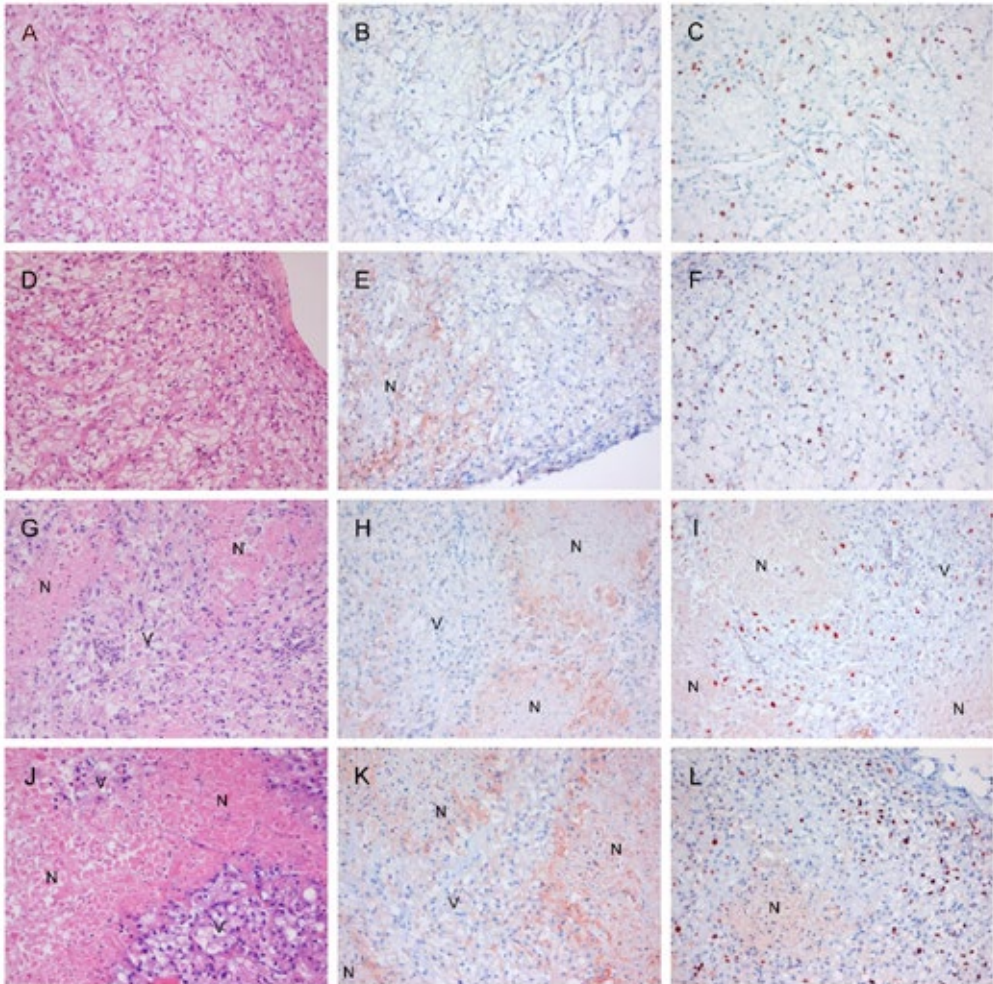
Figure 4. Immunohistochemical analysis of control NU-12 tumours (day 14, **A–C**) tumours treated with sunitinib (day 14, continuous treatment, **D–F**), vandetanib (day 14, **G–I**) and sorafenib (day 14, **J–L**). **A**, **D**, **G**, **J**, haematoxylin and eosin staining; **B**, **E**, **H**, **K**, Glut-1 expression; **C**, **F**, **I**, **L**, Ki-67 expression; original magnifications x100. N, necrotic tumour; V, viable tumour. There was no difference in Ki-67 expression when comparing the different agents. Glut-1 expression was higher in tumours when mice were treated with sorafenib or vandetanib, mainly near necrotic areas.

expression of components of more mature vessels. In addition, most tumours of TKI-treated mice had necrotic areas, which is concordant with inhibited neovascularization. It is unlikely that the decreased accumulation was the consequence of the higher necrotic content of TKI-treated tumours: CAIX expression in the viable tumour remained high and we have previously reported that CAIX expression is necessary for cG250 accumulation [25]. The present observations are in agreement with those of Chang *et al*. [26] who reported that TKI treatment resulted in enhanced hypoxia due to destruction of tumour vasculature, thereby

compromising the access of antibody to the tumour.

Strikingly, there was a rapid outgrowth of endothelium (neovascularization) when sunitinib treatment was discontinued. Thus, the nutrient supply to the tumour cells rapidly recovered. This same phenomenon may occur in patients treated with sunitinib: the current treatment schedule for patients with RCC involves 4 weeks 'on' and 2 weeks 'off' sunitinib. During the 'drug-holiday' period rapid neovascularization may also occur, which may explain why patients eventually progress on sunitinib treatment. Additionally, the schedule may lead to an antiangiogenic resistant RCC phenotype.

Discontinuation of sunitinib treatment lead to enhanced uptake of antibody 7 days after TKI treatment (Fig. 2B). This is similar to studies in a colorectal cancer model showing enhanced antibody tumour accumulation in mice treated with STI571 (imatinib) 3 days after treatment was stopped [27]. Although in the present study this effect occurred later, this might be explained by the specificity of the TKI used and the slightly different dosing schedule.

It has been suggested that antiangiogenic therapy might result in normalization of tumour vasculature [6] and to increased uptake of therapeutic modalities. Preclinical studies indicated that beneficial effects of TKI on the tumour vasculature almost exclusively concern VEGFR-TKI combined with chemotherapeutics [3,4]. These studies have convincingly shown improved growth inhibition or increased tumour distribution of the (relatively small) chemotherapeutic drugs. In the present murine model, closely resembling human ccRCC, there was no normalization, but instead simultaneous administration of TKI and mAb G250 severely compromised mAb accumulation, probably the result of the destruction of the tumour vasculature. These results suggest that major differences may exist between different tumour types or, alternatively, that the window of opportunity for increased uptake is very narrow for larger molecules such as antibodies. Possibly, a narrow time window exists in which lowered interstitial fluid pressures precedes tumour vasculature destruction. During this period, increased flow might lead to increased mAb accumulation. Alternation of a TKI and mAb administration might then lead to destruction of the central tumour mass by TKI treatment and tumour cell kill at the tumour periphery. Alternatively, entrapment of the antibody by allowing antibody localization to occur before antiangiogenic therapy, a scheme used successfully in colorectal xenografts [28], might be beneficial.

Acknowledgements

References

1. Parkin DM, Bray F, Ferlay J, Pisani P. Global cancer statistics, 2002. CA Cancer J Clin 2005; 55: 74–108

2. Reuter CW, Morgan MA, Grunwald V, Herrmann TR, Burchardt M, Ganser A. Targeting vascular endothelial growth factor (VEGF)-receptor-signaling in renal cell carcinoma. World J Urol 2007; 25: 59–72

3. Zhou Q, Guo P, Gallo JM. Impact of angiogenesis inhibition by sunitinib on tumor distribution of temozolomide. Clin Cancer Res 2008; 14: 1540–9

4. Abrams TJ, Murray LJ, Pesenti E et al. Preclinical evaluation of the tyrosine kinase inhibitor SU11248 as a single agent and in combination with 'standard of care' therapeutic agents for the treatment of breast cancer. Mol Cancer Ther 2003; 2: 1011–21

5. Hurwitz H, Fehrenbacher L, Novotny W et al. Bevacizumab plus irinotecan, fluorouracil, and leucovorin for metastatic colorectal cancer. N Engl J Med 2004; 350: 2335–42

6. Jain RK. Normalization of tumor vasculature: an emerging concept in antiangiogenic therapy. Science 2005; 307: 58–62

7. Oosterwijk E, Bander NH, Divgi CR et al. Antibody localization in human renal cell carcinoma: a phase I study of monoclonal antibody G250. J Clin Oncol 1993; 11: 738–50

8. Steffens MG, Boerman OC, Oosterwijk-Wakka JC et al. Targeting of renal cell carcinoma with iodine-131-labeled chimeric monoclonal antibody G250. J Clin Oncol 1997; 15: 1529–37

9. Bleumer I, Oosterwijk E, Oosterwijk-Wakka JC et al. A clinical trial with chimeric monoclonal antibody WX-G250 and low dose interleukin-2 pulsing scheme for advanced renal cell carcinoma. J Urol 2006; 175: 57–62

10. Bleumer I, Knuth A, Oosterwijk E et al. A phase II trial of chimeric monoclonal antibody G250 for advanced renal cell carcinoma patients. Br J Cancer 2004; 90: 985–90

11. Wilhelm SM, Carter C, Tang L et al. BAY 43–9006 exhibits broad spectrum oral antitumor activity and targets the RAF/MEK/ERK pathway and receptor tyrosine kinases involved in tumor progression and angiogenesis. Cancer Res 2004; 64: 7099–109

12. Mendel DB, Laird AD, Xin X et al. In vivo antitumor activity of SU11248, a novel tyrosine kinase inhibitor targeting vascular endothelial growth factor and platelet-derived growth factor receptors: determination of a pharmacokinetic/pharmacodynamic relationship. Clin Cancer Res 2003; 9: 327–37

13. Ciardiello F, Caputo R, Damiano V et al. Antitumor effects of ZD6474, a small molecule vascular endothelial growth factor receptor tyrosine kinase inhibitor, with additional activity against epidermal growth factor receptor tyrosine kinase. Clin Cancer Res 2003; 9: 1546–56

14. Oosterwijk E, Ruiter DJ, Hoedemaeker PJ et al. Monoclonal antibody G250 recognizes a determinant present in renal-cell carcinoma and absent from normal kidney. Int J Cancer 1986; 38: 489–94

15. Grabmaier K, Vissers JL, De Weijert MC et al. Molecular cloning and immunogenicity of renal cell carcinoma-associated antigen G250. Int J Cancer 2000; 85: 865–70

16. Uemura H, Nakagawa Y, Yoshida K et al. MN/CA IX/G250 as a potential target for immunotherapy of renal cell carcinomas. Br J Cancer 1999; 81: 741–6

17. Lindmo T, Boven E, Cuttitta F, Fedorko J, Bunn PA Jr. Determination of the immunoreactive fraction of radiolabeled monoclonal antibodies by linear extrapolation to binding at infinite antigen excess. J Immunol Methods 1984; 72: 77–89

18. Beniers AJ, Peelen WP, Schaafsma HE et al. Establishment and characterization of five new human renal tumor xenografts. Am J Pathol 1992; 140: 483–95

19. Bussink J, Kaanders JH, Rijken PF, Martindale CA, van der Kogel AJ. Multiparameter analysis of vasculature, perfusion and proliferation in human tumour xenografts. Br J Cancer 1998; 77: 57–64

20. Kusters B, Kats G, Roodink I et al. Micronodular transformation as a novel mechanism of VEGF-A-induced metastasis. Oncogene 2007; 26: 5808–15

21. Bukowski RM, Kabbinavar FF, Figlin RA et al. Randomized phase II study of erlotinib combined with bevacizumab compared with bevacizumab alone in metastatic renal cell cancer. J Clin Oncol 2007; 25: 4536–41

22. Escudier B, Pluzanska A, Koralewski P et al. Bevacizumab plus interferon alfa-2a for treatment of metastatic renal cell carcinoma: a randomised, double-blind phase III trial. Lancet 2007; 370: 2103–11

23. Ryan CW, Goldman BH, Lara PN Jr et al. Sorafenib with interferon alfa-2b as first-line treatment of advanced renal carcinoma: a phase II study of the Southwest Oncology Group. J Clin Oncol 2007; 25: 3296–301
24. Gollob JA, Rathmell WK, Richmond TM et al. Phase II trial of sorafenib plus interferon alfa-2b as first- or second-line therapy in patients with metastatic renal cell cancer. J Clin Oncol 2007; 25: 3288–95
25. Steffens MG, Oosterwijk-Wakka JC, Zegwaart-Hagemeier NE et al. Immunohistochemical analysis of tumor antigen saturation following injection of monoclonal antibody G250. Anticancer Res 1999; 19: 1197–200
26. Chang YS, Adnane J, Trail PA et al. Sorafenib (BAY 43–9006) inhibits tumor growth and vascularization and induces tumor apoptosis and hypoxia in RCC xenograft models. Cancer Chemother Pharmacol 2007; 59: 561–74
27. Baranowska-Kortylewicz J, Abe M, Pietras K et al. Effect of platelet-derived growth factor receptor-beta inhibition with STI571 on radioimmunotherapy. Cancer Res 2005; 65: 7824–31
28. Pedley RB, Hill SA, Boxer GM et al. Eradication of colorectal xenografts by combined radioimmunotherapy and combretastatin a-4 3-O-phosphate. Cancer Res 2001; 61: 4716–22

Successful Combination of Sunitinib and Girentuximab in two Renal Cell Carcinoma Animal Models: A Rationale for Combination Treatment of Patients with advanced RCC

Jeannette C. Oosterwijk-Wakka[1], Mirjam C.A. de Weijert[1], Gerben M. Franssen[2], William P.J. Leenders[3], Jeroen A.W.M. van der Laak[3], Otto C. Boerman[2], Peter F.A. Mulders[1] and Egbert Oosterwijk[1]

[1] Department of Urology, [2] Radiology and Nuclear Medicine and [3] Pathology, Radboud university medical center, Nijmegen, The Netherlands

Abstract

Anti-angiogenic treatment with tyrosine kinase inhibitors (TKI) has lead to an impressive increase in progression-free survival for patients with metastatic RCC (mRCC), but mRCC remains largely incurable. We combined sunitinib, targeting the endothelial cells, with Girentuximab, (monoclonal antibody cG250, recognizing carbonic anhydrase IX (*CAIX*) targeting the tumor cells, to study the effect of sunitinib on the biodistribution of Girentuximab because combination of modalities targeting tumor vasculature and tumor cells might result in improved effect. Nude mice with human RCC xenografts (NU12, SK-RC-52) were treated orally with 0.8 mg/day sunitinib, or vehicle for 7-14 days. Three days before start or cessation of treatment mice were injected i.v. with 0.4 MBq/5 µg ^{111}In-Girentuximab followed by biodistribution studies. Immunohistochemical analyses were performed to study the tumor vasculature and *CAIX* expression and to confirm Girentuximab uptake.

NU12 appeared to represent a sunitinib sensitive tumor: sunitinib treatment resulted in extensive necrosis and decreased microvessel density (MVD). Accumulation of Girentuximab was significantly decreased when sunitinib treatment preceded the antibody injection but remained unchanged when sunitinib followed Girentuximab injection. Cessation of therapy led to a rapid neovascularization, reminiscent of a tumor flare. SK-RC-52 appeared to represent a sunitinib-resistant tumor: (central) tumor necrosis was minimal and MVD was not affected. Sunitinib treatment resulted in increased Girentuximab uptake, regardless of the sequence of treatment. These data indicate that sunitinib can be combined with Girentuximab. Since these two modalities have different modes of action, this combination might lead to enhanced therapeutic efficacy.

Introduction

Renal cell carcinoma accounts for approximately 3% of all cancers and was diagnosed in over 115,000 individuals in Europe in 2012 [1]. Most RCC (70%) are of the clear cell type (ccRCC) that is characterized by high expression levels of Vascular Endothelial Growth Factor (*VEGF*) and, consequently, a hypervascular phenotype. Over the last few years, anti-*VEGF* therapies have significantly changed the standard of care for patients with advanced RCC [2]. Sunitinib [3], sorafenib [4], axitinib [5], pazopanib [6] and bevacizumab + interferon [7] have all been registered for the treatment of advanced RCC. Additionally, the *mTOR* inhibitors Temsirolimus and Everolimus have been registered for poor risk RCC patients [8,9]. Implementation of these new treatment modalities has lead to an impressive increase in progression-free survival [10]. Nevertheless, because eventually treatment resistance occurs, metastatic RCC remains largely incurable. Additionally these chronic treatments may coincide with significant toxicity which increases to unacceptable levels when combination treatment is applied [11]. Sequential therapy may be more promising but the most optimal sequence therapy has not been established.

There is considerable evidence that anti-*VEGF* and anti-*VEGF* receptor (*VEGFR*) drugs cause remodeling of the aberrant tumor vessels, resulting in a "normalized vasculature" [12]. This phenomenon may improve tumor perfusion and reduce tumor interstitial fluid pressure, thereby improving uptake of other drugs. Indeed, addition of bevacizumab to first-line chemotherapy in advanced colorectal cancer resulted in an overall survival benefit [13]. However, caution is warranted regarding unanticipated effects since studies with *VEGFR*-targeting compounds in murine models provided evidence for increased metastatic propensity [14,15].

Chimeric monoclonal antibody G250 (cG250/Girentuximab) targets human carbonic anhydrase IX (*CAIX*), a transmembrane protein which which catalyzes the reaction $CO_2 + H_2O \leftrightarrow HCO_3^- + H^+$. Expression of *CAIX* is regulated by hypoxia-inducible factor 1-alpha, which in turn is regulated by the Von Hippel Lindau (VHL) protein (pVHL), a gene affected in the vast majority of ccRCC patients. The molecular link between pivotal molecular events in ccRCC explains the ubiquitous expression of *CAIX* in ccRCC. In non-RCC tumors, *CAIX* is activated following hypoxia. In view of the favorable tissue distribution, the potential of CAIX targeting of RCC for diagnosis or therapy has been studied extensively [16-19]. Clinical trials have demonstrated high, specific tumor accumulation of Girentuximab, and radioimmunotherapy (RIT) with ^{177}Lu-Girentuximab can stabilize previously progressive metastatic ccRCC [20]. Combination of sunitinib with ^{177}Lu-Girentuximab RIT may act synergistically since these compounds simultaneously target the tumor blood vessel- and tumor cell compartment in patients with mRCC. We have previously shown that simultaneous administration of sunitinib and Girentuximab severely compromised mAb accumulation in mice [21], an effect that could be reiterated in patients treated with sorafenib [22]. However, shortly after discontinuation of tyrosine kinase inhibitor (TKI) treatment, mAb accumulation was restored, mainly in the tumor periphery [21]. This suggests that sequential administration

of TKIs and Girentuximab may be better than simultaneous administration. The aim of this study was to explore how tumor targeting by Girentuximab is influenced by sunitinib treatment in sequential treatment protocols.

Material and Methods

Cell lines and reagents

The human Renal Carcinoma cell line SK-RC-52 was established from a mediastinal metastasis of a primary RCC [23]. The cell line was cultured in RPMI1640 (Gibco, Bleiswijk, The Netherlands) supplemented with 10% fetal bovine serum (Sigma, Zwijndrecht, The Netherlands) and 2 mM glutamine (Gibco). Human renal cell carcinoma xenograft model NU12 [24] was maintained by passing freshly excised tumor pieces (1-2 mm^3) subcutaneously (s.c.) in mice. Both SK-RC-52 and NU12 express high levels of *CAIX* [25].

Conjugation and radiolabeling of Girentuximab

The isolation, characteristics and the immunohistochemical reactivity of mouse mAb G250 (mG250) have been described earlier [26]; mAb G250 has a high affinity for *CAIX* (Ka = 4 x 10^9 M^{-1}) which is expressed on the cell surface of >95% of ccRCC and absent on most normal tissues. The generation of Girentuximab has been described elsewhere [27].

The conjugation of Girentuximab (generously provided by Wilex AG, München, Germany) to ITC-DTPA has been described earlier [28]. The Girentuximab-ITC-DTPA conjugate (1 mg/ml) was radiolabeled with [111]InCl$_3$ (Mallinckrodt, The Netherlands) as described previously [28].

After PD10 purification the radiochemical purity of the ^{111}In-Girentuximab preparations was determined using ITLC silica gel strips (Biodex, Shirley, NJ) and 0.1 M citrate buffer pH 6.0 as the mobile phase. The radiochemical purity was 97 ± 3 %. The immunoreactive fraction (IRF), determined on freshly trypsinized SK-RC-52 RCC cells at infinite antigen excess essentially as described by Lindmo et al. [29] with minor modifications [27], was 87 ± 7%.

Animal experiments

Institutional guidelines were strictly followed for maintenance of animals and experimental procedures were approved by the Institutional Animal Care and Use Committee (IACUC). Female BALB/c nu/nu mice, 6-8 weeks of age, were obtained from Janvier, France, and maintained at the local central animal facility. Animals were either grafted s.c. with freshly excised NU12 RCC xenograft pieces [24] of approximately 1-2 mm^3 or injected s.c. with $2*10^6$ freshly trypsinized SK-RC-52 cells. Treatment with sunitinib (SU11248, Sutent®, Pfizer, NY) was started when tumors had reached a tumor volume of 100-200 mm^3.

Sunitinib was dissolved in 0.1 M Na-citrate, pH 4.5 and freshly prepared every week.

Mice received the equivalent of 40-50 mg/kg (0.8-1 mg/200 µl) sunitinib or vehicle orally per day for 7-14 days.

Biodistribution studies and SPECT/CT analysis

Once tumors reached the desired volume, mice were divided into groups of 4-5 mice (in one experiment 8-9 mice). Mice were treated with sunitinib or vehicle control every day for 7-14 days. Mice were injected intravenously with ^{111}In-Girentuximab (0.4 MBq, 5 µg) 3 days pre-sunitinib or 3 days post-sunitinib treatment. Mice were euthanized 3, 7, 10, 14 or 17 days post Girentuximab injection. Alternatively, mice were injected intravenously with ^{111}In-Girentuximab (0.4 MBq, 5 µg) 3, 7 or 10 days post-sunitinib treatment. Mice were euthanized 3 days post-injection. Animals were dissected, tissues harvested (tumor, blood, muscle, liver, spleen, kidney, stomach, lung, colon, small intestine), weighed and counted in a gamma counter (Wizard; Pharmacia-LKB, Perkin-Elmer, Boston, MA). The activity in the samples was expressed as % injected dose per gram tissue (%ID/g).

SPECT/CT analysis was performed to visualize the biodistribution and the intra-tumoral distribution of the radiolabeled antibody; sixteen mice bearing SK-RC-52 were injected with ^{111}In-Girentuximab with a specific activity of 22,5 MBq/5 µg, 3 days before start or 3 days after stop of treatment with sunitinib or vehicle for 7 days. SPECT/CT analysis (USPECT-II/CT scanner (MILabs, Utrecht, The Netherlands) was performed 3, 7 or 14 days after injection of the radiolabeled antibody with a 1.0-mm-diameter pinhole rat collimator tube. The animals were placed in the scanner in supine position. SPECT scans were acquired for 30-120 min, followed by CT scans for anatomic reference (65 kV; 612 µA; exposure time, 240 ms). 3, 7 or 14 days after injection of the radiolabeled antibody.

Antibodies and immunohistochemical analysis

Harvested tumors were snap-frozen and stored at -80°C. 4-µm cryostat sections were cut and stored at -80°C until use. Haematoxylin-Eosin staining was performed for morphological analysis of the tumors.

Primary antibodies used were: Girentuximab (Wilex, Germany, 10 µg/ml), rat-anti-mouse mAb 9F1, hybridoma supernatant 1:50 [30] , and rabbit-anti-human mAb Ki67 (clone sp6/RM-9106-S, Thermo Scientific, Astmoor Runcorn, UK, 1:200). All antibodies were diluted in 1% BSA in 50 mM phosphate buffered saline, pH 7.4, unless mentioned otherwise.

For visualization of *CAIX* expression, sections were acetone fixed and incubated with Girentuximab, washed and incubated with peroxidase (PO) conjugated rabbit-anti-human IgG (P214, Dako, Heverlee, Belgium), 1:100 as secondary antibody. To detect in vivo accumulated injected Girentuximab, cryostat sections were incubated with rabbit-anti-human IgG–PO only. Antibody 9F1 was used to detect mouse endothelial cells. After acetone fixation, primary antibody 9F1 was applied for 1 h at RT. After washing, secondary antibody goat-anti-rat-PO (Sigma) 1:100, supplemented with 4% normal mouse serum, was applied. All sections were developed with powerDAB (Immunologic, Duiven, The Netherlands) and

counterstained with haematoxylin. Microscopic evaluation was performed on an Axioskop microscope (Zeiss, Sliedrecht, The Netherlands) and pictures were taken with the Axiocam mrc5 (Zeiss) with Axio vs40 version 4.8 2.0 software (Axiovision, Zeiss).

Triple immunofluorescence was performed to visualize cell proliferation and endothelial cells simultaneously. After acetone fixation, cells were pretreated for 30 min with 1% BSA/0.2 %Triton X100 in PBS. Subsequently sections were incubated overnight at 4°C with an antibody cocktail consisting of Ki67 and 9F1 diluted in 1% BSA/0.2 %Triton X100 in PBS. After washing, sections were incubated with the secondary antibody cocktail consisting of goat-anti-rabbit Alexa 568, 1:200 and goat-anti-rat Alexa 488, 1:200 (Molecular probes, Life technologies, Bleiswijk, The Netherlands). Finally, sections were incubated with DRAQ5 (Biostatus DR50051, Leicestershire, UK, 1:200) to visualize nuclei. Microscopic evaluation of triple immunofluorescence was performed on a high content microscope (Leica, Rijswijk, The Netherlands, DMI6000B inverted microscope extended with a motorized x-y scanning stage, Leica EL6000 illumination source), equipped with a high-resolution Leica DFC360 FX CCD camera.

Microvessel density measurements

Density of microvascular profiles was assessed automatically as described previously [31] using an AxioCam MRc connected to an AxioPhot microscope (Zeiss). Images were acquired using a 20x objective (Plan Apochromat, NA=0.32), resulting in a specimen level pixel size of 0.53 μm. Microvessel density (MVD) was defined as the percentage of microvessel area/total tumor area. All image acquisition and processing was performed using custom written macros in KS400 image analysis software (Zeiss).

RT-PCR

VEGF-A/RT-PCR was performed on NU12 and SK-RC-52 cells as well as on harvested xenografts of both sunitinib-treated as control animals. Total RNA was isolated from frozen tumor sections or cultured cells using TRIzol Reagent (Life Technologies), according to the manufacturer's protocol. RNA integrity was checked by 1.0% agarose gel electrophoresis. RNA samples (2 μg) were DNAse treated (Invitrogen, Life Technologies) and reverse-transcription was performed at 42°C for 60 min, using SuperScript^{TM} II (Invitrogen). Two μl of the reaction product was subjected to standard PCR amplification using Super Taq polymerase (Sphaero, Gorinchem, The Netherlands) and *VEGF-A*-primers 5′-GCA CCC ATG GCA GAA GGA GGA-3′ (sense) and 5′-TCA CCG CCT CGG CTT GTC AC-3′ (exon 8 specific, antisense). Reaction mixture was heated 1 min at 94°C followed by 30 cycli for 30 s at 94 °C, 1 min at 61 °C, 1 min at 72 °C and 10 minutes at 72 °C.

This primer set amplifies all *VEGF-A* isoforms simultaneously, except *VEGF165b*. Expected product lengths with this primer set are 367 bp (*VEGF-121*), 436 bp (*VEGF-145*), 496 bp (*VEGF165*) and 568 bp (*VEGF189*). cDNAs were also subjected to a PCR for GAPDH as control housekeeping gene. VEGF165b was analyzed in a separate RT-reaction with forward primer as mentioned above and a reverse primer recognizing an alternative

NU12

NU12

SK-RC-52

SK-RC-52

SK-RC-52
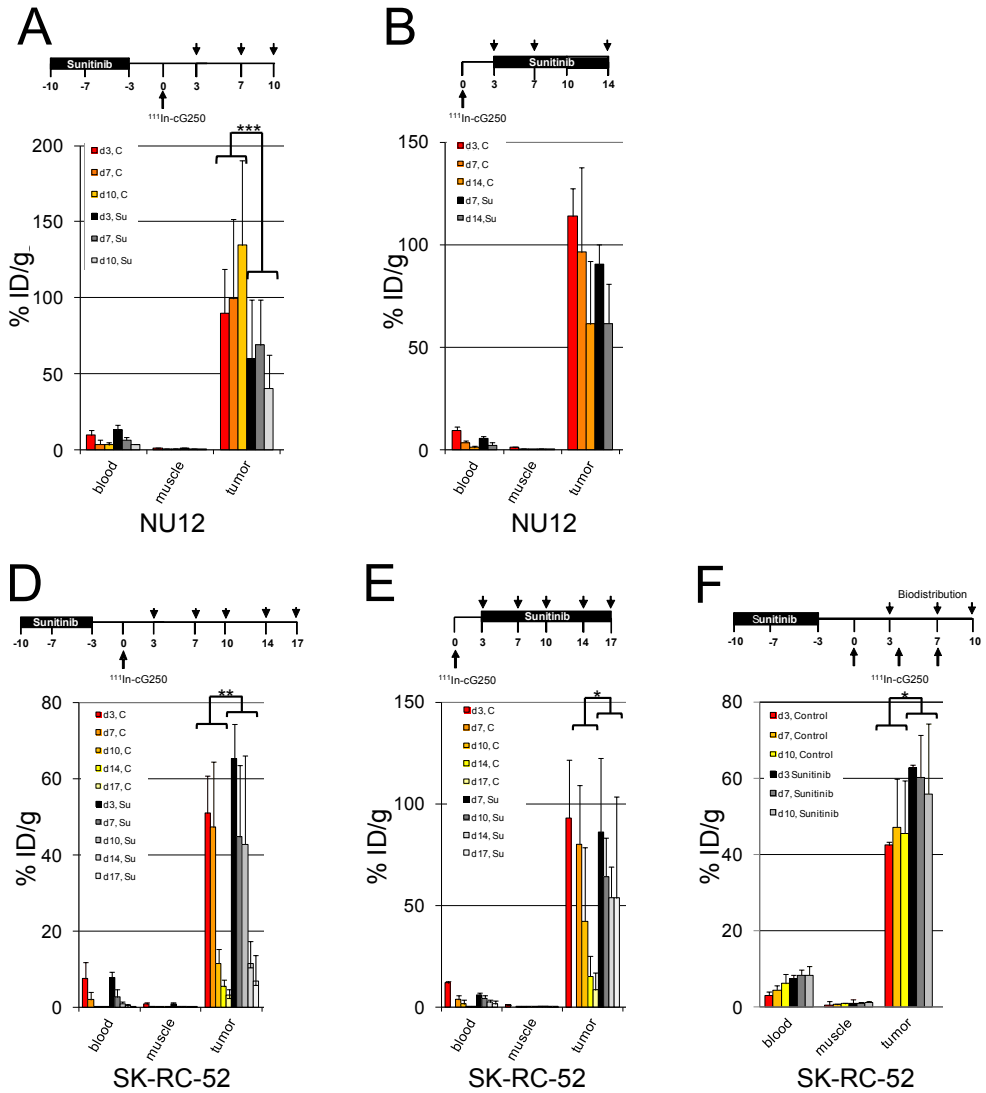
exon in *VEGF*: 5'-TCA GTC TTT CCT GGT GAG AGA TCT GCA-3'.

Statistical analysis

Results are presented as means with standard deviations (SD). For the statistical analysis, all sunitinib treated animals were clustered together to increase the number of animals. This was also done with the control animals. Differences in Girentuximab uptake and MVD between treatment and control mice at each time-point were tested for statistical significance using the two-way ANOVA with factors treatment, time and interaction. When interaction was not significant it was removed from the model and two-way ANOVA without interaction was applied. $p < 0.05$ was considered significant.
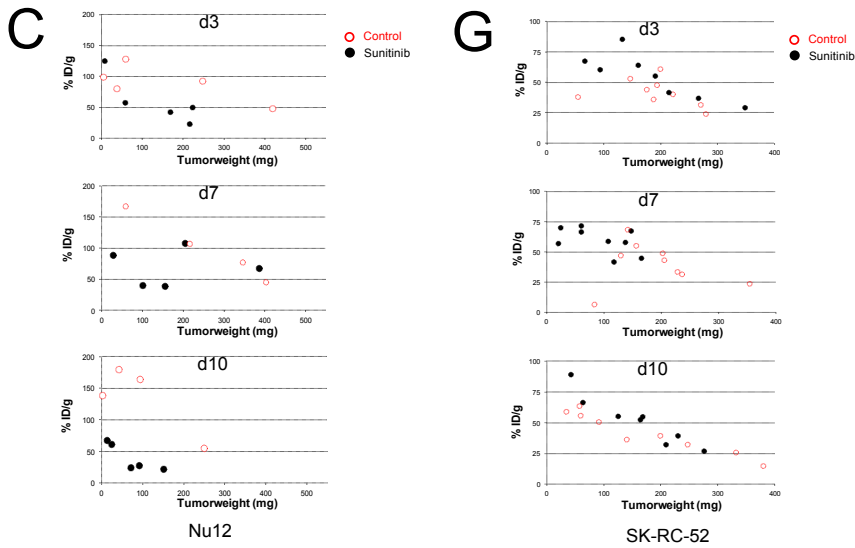
Figure 1. Biodistribution of cG250 in nude mice with NU12 and SK-RC-52 tumors. ^{111}In-Girentuximab biodistribution in BALB/c nu/nu mice shows decreased uptake with sunitinib in NU12 tumors and increased uptake with sunitinib in SK-RC-52 tumors. Treatment schedules shown on top of graphs. Groups of 4-5 mice (in F: 8-9 mice) were treated with sunitinib every day for 1 week (**A**,**D**,**F**) or until they were euthanized (**B**,**E**). Three days before start or 3d (in one experiment also 7d or 10d) after stop of treatment, mice were injected with ^{111}In-Girentuximab (0.4 MBq, 5 μg) and mice were euthanized at various timepoints. The activity in the samples was expressed as % injected dose per gram tissue (% ID/g). **A**: Biodistribution of NU12 mice with sunitinib treatment preceding ^{111}In-Girentuximab injection, **B**: Biodistribution of NU12 mice injected with ^{111}In-Girentuximab before sunitinib treatment, **C**: G250 antibody uptake was plotted for individual tumors from experiment. **A** Red open circles: control tumors; black closed circles: sunitinib treated tumors **A**, **D**: Biodistribution of SK-RC-52 mice treated with sunitinib preceding ^{111}In-Girentuximab injection, **E**: Biodistribution of SK-RC-52 mice treated with sunitinib followed by ^{111}In-Girentuximab, **F**: Biodistribution of SK-RC-52 mice with ^{111}In-Girentuximab injection 3 days, 7 days or 10 days after cessation of sunitinib, **G**: G250 antibody uptake was plotted for individual tumors from experiment F. * $p < 0.05$, ** $p < 0.01$, *** $p < 0.005$. P-values shown for the biodistribution are based on all sunitinib treated animals (N= 15, 9, 28, 18, 25 for fig 1**A**, **B**, **D**, **E** and **F** respectively) compared to all control animals (N=13, 16, 30, 18, 27 for fig 1**A**, **B**, **D**, **E** and **F** respectively).

Results

Decreased uptake of ^{111}In-Girentuximab and decreased micro vessel density when mice with NU12 tumors were treated with sunitinib

Treatment of NU12 tumors with sunitinib caused substantial decrease of tumor growth (p < 0.05; figure S1). In SK-RC-52, sunitinib treatment resulted in stabilization of tumor growth (p=0.056; figure S2). To study the influence of sunitinib treatment on the tumor uptake of Girentuximab, biodistribution studies were performed using ^{111}In-Girentuximab in BALB/c athymic mice xenografted with NU12 or SK-RC-52 (Fig. 1 and supplementary table S1-5). In
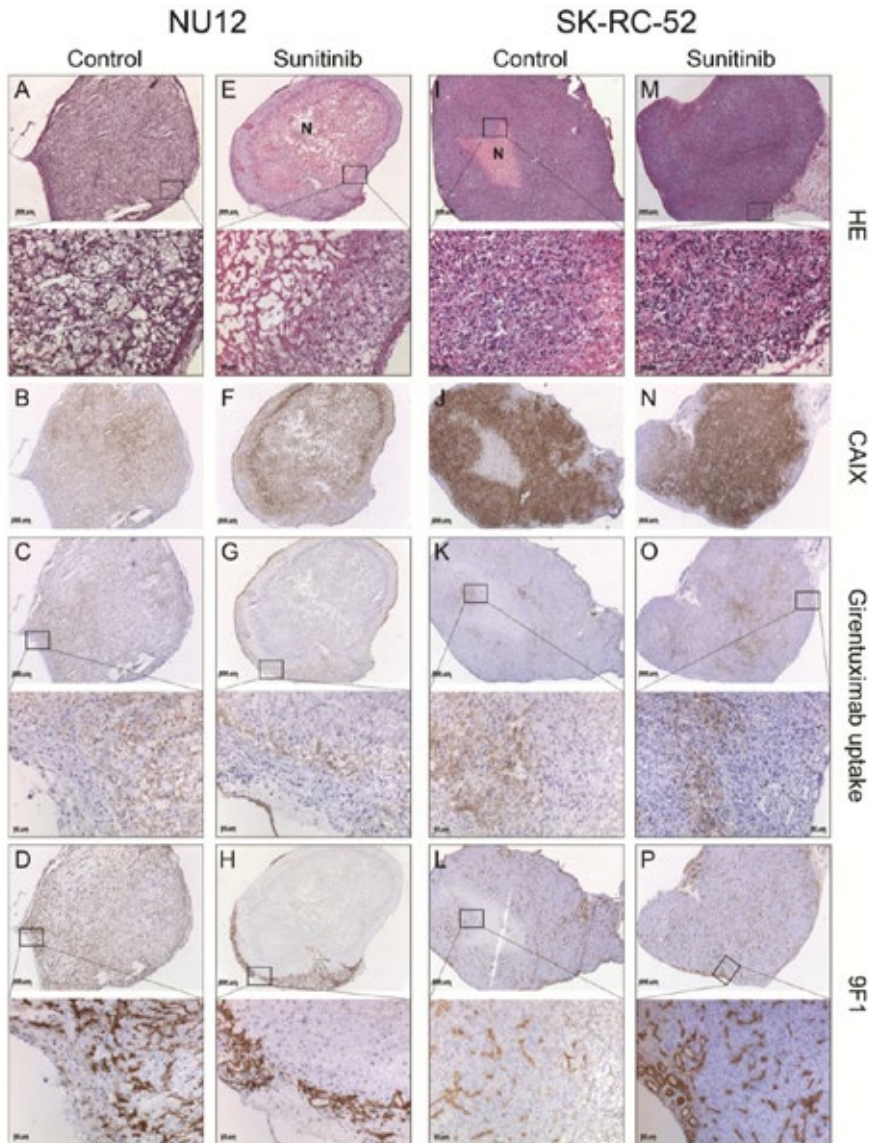
Figure 2. Phenotypic analysis of NU12 and SK-RC-52 tumors. Phenotypic analysis of NU12 and SK-RC-52 tumors of mice treated with sunitinib shows necrosis, decreased accumulated cG250 and decreased number of microvessels in NU12 tumors and very limited necrosis, increased accumulated cG250 and unchanged number of microvessels in SK-RC-52 tumors. **A-D**, NU12 control tumors; **E-H**, NU12 sunitinib treated tumors; **I-L**, SK-RC-52 control tumors; **M-P**, SK-RC-52 sunitinib treated tumors. HE staining in **A**, **E**, **I** and **M**. Sunitinib treatment did not modify CAIX expression in either NU12 or SK-RC-52 (**B,F** and **J,N**). In NU12 control tumors (**A-D**), homogeneous accumulation of cG250 (**C**) was observed. **D**: tumor vasculature visualized by staining with 9F1. In sunitinib treated NU12 tumors (**E-H**), extensive necrosis was present as judged by HE (**E**) and accumulated cG250 (**G**) and microvessels (**H**) were only observed in the tumor rim. SK-RC-52 control tumors (**I-L**), revealed focal accumulation of injected cG250 (**J**) and moderate microvessel density (MVD) as visualized by staining with 9F1 (**L**). Accumulation of cG250 was increased in sunitinib treated SK-RC-52 tumors (**O** vs. **K**) and MVD appeared to be increased (**P** vs. **L**). Necrosis was limited regardless of treatment (**I**, **M**). N: necrosis. Original magnification X25 and X200.

the NU12 model, tumor uptake of ^{111}In-Girentuximab decreased when sunitinib treatment preceded the antibody injection (Fig. 1A; p < 0.005 and supplementary table S1). Because previous experiments have shown that Girentuximab uptake inversely correlates with tumor volume [32], and sunitinib stabilizes tumor growth, Girentuximab uptake was plotted for individual tumors. This analysis demonstrated that at similar tumor volumes antibody uptake in the tumors of sunitinib-treated mice was lower than that in the control mice, most notably at day 10 (Fig. 1C).

Sunitinib treatment following ^{111}In-Girentuximab injection did not influence antibody uptake in the NU12 model (Fig. 1B, p=0.7959 and supplementary table S2, Fig. S3). Tumors were analyzed by immunohistochemistry (IHC) for the presence of vasculature, *CAIX* expression and intratumoral distribution of Girentuximab (Fig. 2, 3). Extensive necrosis was observed in the majority of sunitinib treated NU12 tumors, as judged by HE staining (Fig. 2E). Necrosis was minimal in untreated tumors (Fig. 2A). *CAIX*, the Girentuximab target, was expressed in all viable NU12 tumor cells, regardless of sunitinib treatment (Fig. 2B, F). Interestingly, *CAIX* could still be detected in necrotic tumor areas. In accordance with earlier studies, homogeneous accumulation of Girentuximab was observed in non-treated NU12 tumors (Fig. 2C). NU12 tumors harvested from non-treated animals were well vascularized (Fig. 2D). In contrast, NU12 tumors of sunitinib-treated mice displayed extensive central necrosis and Girentuximab accumulation was limited to the rim of the tumors (Fig. 2G). Quantitative microscopic analysis confirmed that the viable tumor area was markedly reduced in tumors from sunitinib-treated animals. Microvessel density in the centre of these tumors was very low as compared to control tumors (Fig. 3A, p < 0.001), whereas in the viable tumor rim a rebound effect was seen (Fig. 2H). Triple immunofluorescence staining for cell proliferation, endothelial cells and nuclei revealed low proliferation index of NU12 tumor cells, both in control as well as in tumors of sunitinib-treated mice (Fig. 3C and D respectively).

Increased uptake of ^{111}In-Girentuximab and unchanged micro vessel density when mice with SK-RC-52 tumors were treated with sunitinib

Sunitinib treatment of mice bearing SK-RC-52 tumors affected Girentuximab accumulation regardless of the sequence: Antibody uptake in the tumors of the sunitinib-treated animals was higher than in untreated animals (Fig. 1D, 1E, p = 0.0059 and p = 0.026 respectively, supplementary tables S3, S4). Plotting of antibody accumulation against the tumor volume demonstrated that at similar tumor volumes Girentuximab uptake in tumors of sunitinib-treated mice was higher than or at least equal to tumor uptake in control mice (Fig. 1G). To establish whether extension of the time interval between sunitinib treatment and antibody injection would improve Girentuximab tumor accumulation, mice were injected with Girentuximab 3, 7 and 10 days post-sunitinib, and were euthanized 3 days later (6, 10 and 13 days, respectively). In all cases Girentuximab accumulation in the SK-RC-52 tumor was higher in sunitinib-treated animals (Fig. 1F, p = 0.0114, supplementary table S5). Extension of the time interval beyond 3 days did not further improve antibody accumulation.
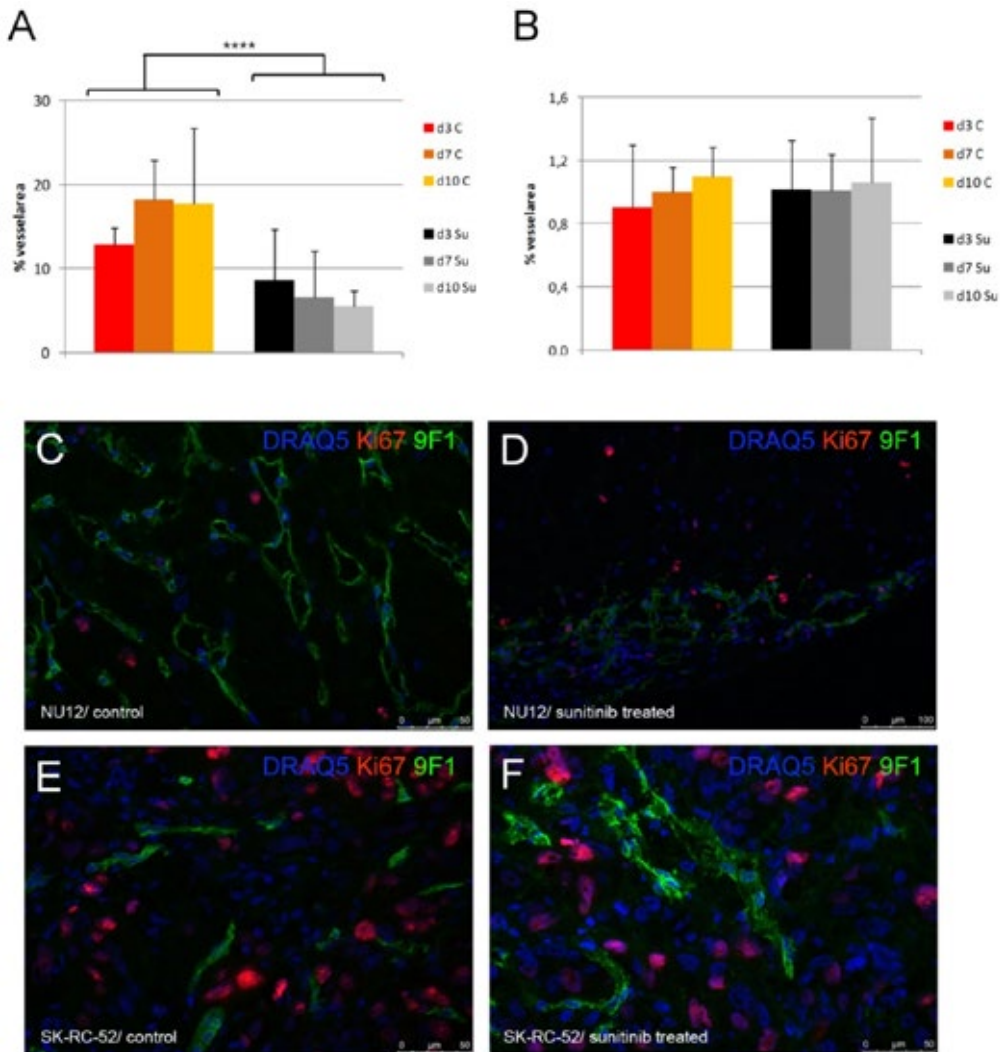
Figure 3. Microvessel density analysis. Density of microvascular profiles was assessed automatically as described previously [31] using an AxioCam MRc connected to an AxioPhot microscope (Zeiss). Microvessel density (MVD) was defined as the percentage of microvessel area/total tumor area. All image acquisition and processing was performed using custom written macros in KS400 image analysis software (Zeiss). Sunitinib treatment resulted in significant decrease in % of microvessels in NU12 tumors (**A**) but no change in % of microvessels in SK-RC-52 tumors (**B**). Triple immunofluorescence staining of NU12 control (**C**) and sunitinib treated tumor (**D**) and SK-RC-52 control (**E**) and sunitinib treated tumor (**F**). Low proliferation of NU12 tumor cells (nuclei in blue as visualized by DRAQ5) as visualized by Ki67 staining (red) is observed, both in controls (**C**) as well as in sunitinib treated tumors (**D**). Please note decrease of endothelium (9F1 staining) in sunitinib treated NU12 tumor (green). In SK-RC-52, triple immunofluorescence staining revealed high proliferation of SK-RC-52 tumor cells, both in controls (**E**) as well as in sunitinib treated tumors (**F**). Necrosis was minimal. **** $p < 0.001$.

Occasionally necrosis was observed in SK-RC-52 tumors in untreated and in sunitinib treated animals (Fig. 2I, M). Immunohistochemical analysis of SK-RC-52 tumors revealed

homogeneous *CAIX* expression regardless of sunitinib treatment (Fig. 2J, N). Control tumors showed focal elevated accumulation of Girentuximab (Fig. 2K) and moderate MVD, as visualized by staining with 9F1 (Fig. 2L). Accumulation of Girentuximab was higher in sunitinib-treated SK-RC-52 tumors (Fig. 2O) but MVD was comparable to that in control tumors (Fig. 2P, 3F). Triple immunofluorescence staining revealed high proliferation index of SK-RC-52 tumor cells, both in controls as well as in sunitinib-treated tumors (Fig. 3E and F respectively).

In previous studies we have shown that Girentuximab is internalized relatively rapidly by SK-RC-52 cells [33] precluding detection of Girentuximab beyond day 3 by immunohistochemistry. To investigate the distribution of the radiolabeled antibody in the animals, SPECT/CT analysis was performed. In agreement with the biodistribution results, more radiolabel was observed in the sunitinib treated SK-RC-52 than in control tumors (Fig. 4A). The localization of the radiolabeled antibody was not restricted to a specific compartment in the tumor, but rather distributed homogenously throughout the tumor. No differences between the various treatment groups were observed (Fig. 4B).
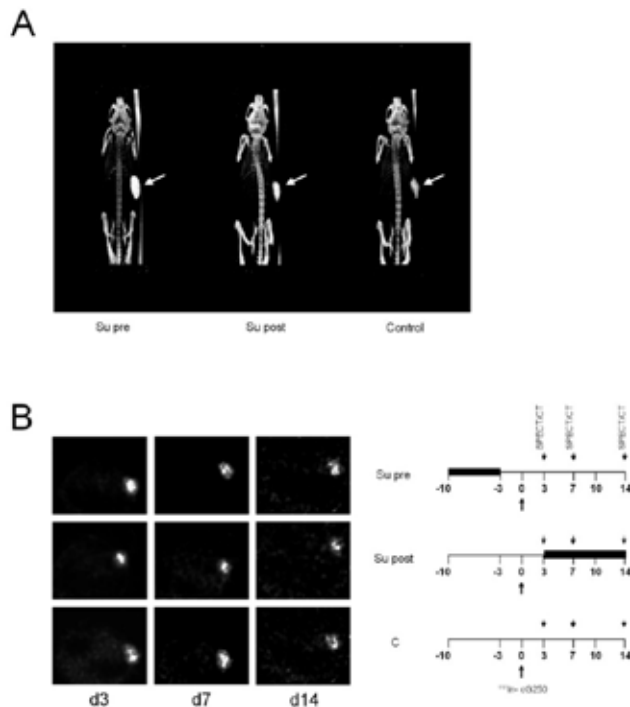
Figure 4. SPECT/CT imaging of mice with SK-RC-52 tumors. SPECT/CT analysis was performed to visualize the biodistribution and the intra-tumoral distribution of the radiolabeled antibody. Sixteen mice bearing SK-RC-52 were treated with sunitinib for 7 days and injected with ^{111}In-Girentuximab with a specific activity of 22,5 MBq/5 µg, 3 days before start or 3 days after stop of treatment. Micro-SPECT images of mouse bearing SK-RC-52 tumor on right flank (arrow) at 7 d after injection of ^{111}In-girentuximab show that in addition to tumor uptake, minimal uptake in other organs was observed. More radiolabel was observed in the sunitinib treated tumors than in vehicle (**A**).This is in concordance with the biodistribution data. In all groups radiolabel was distributed throughout the tumor and no difference in radiolabel distribution was observed in the various treatment groups (**B**).

VEGF expression of NU12 and SK-RC-52 tumors

In view of the observed differences between the two RCC xenograft models, we investigated *VEGF-A* expression as different *VEGF-A* expression levels might explain the observed differences. Non-quantitative RT-PCR did not show differences in *VEGF-A* expression in both tumor models, regardless of sunitinib treatment (Fig. 5).
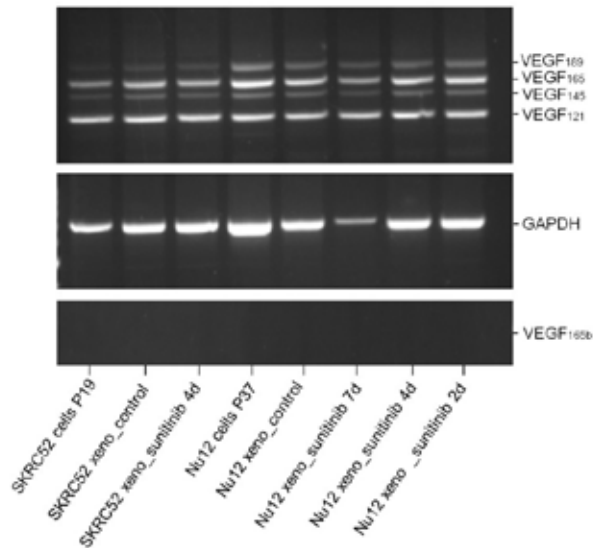
Figure 5. Expression of VEGF-A isoforms in NU12 and SK-RC-52 tumors. VEGF-A/RT-PCR was performed on NU12 and SK-RC-52 cells as well as on harvested xenografts of both sunitinib-treated (from 2 days up to 7 days) as untreated animals. After correction for loading differences (as judged by GAPDH), no differences in VEGF-A expression were observed between tumor models, regardless of sunitinib treatment.

Discussion

Sunitinib treatment can result in significant tumor control in approximately 40% of patients with mRCC [34]. This is a major improvement in the clinical management of these patients as overall survival (OS) of responding patients is significantly improved [34]. However, the prognosis of non-responding patients remains poor with a mean OS of 14.5 months [34]. Therapy with other TKI, mTOR inhibitors and Bevacizumab + Interferon show similar results [35]. Unfortunately, TKI combination therapies are not feasible due to unacceptable toxicity and therefore current efforts are aimed at sequential therapy regimens and/or the combination of surgery and TKI treatment [11]. Moreover, therapy resistance occurs almost inevitably in all patients, highlighting the need for other therapies. Combination therapy aiming at different tumor components such as tumor vasculature and the tumor cells might improve therapy outcome.

CAIX has been recognized as a potential useful target for ccRCC [36]. Diagnostic images with Girentuximab, an antibody which targets *CAIX*, were superior to CT [37], and radioimunotherapy with ^{177}Lu-labeled Girentuximab resulted in disease stabilization [20]. The failure to significantly influence disease progression and lack of partial/ complete responses might be due to the tumor bulk present. Additionally, central regions of larger tumor masses might be less accessible for Girentuximab, as central regions are poorly perfused. Unfortunately adjuvant treatment of nephrectomized RCC patients with unlabeled Girentuximab who have a high risk of relapse (ARISER trial) did not meet its primary endpoint: improvement in median DFS. However, with increasing CAIX expression in tumor tissue, as quantified by a CAIX score, the treatment was more effective [38]. Possibly only high density CAIX RCC cells can be killed by antibody-dependent cellular cytotoxicity in this adjuvant setting.

The combination of Girentuximab, aimed at tumor cells and sunitinib, aimed at the tumor vasculature, might therefore lead to superior therapy outcome. However, simultaneous administration of sunitinib and Girentuximab severely compromised mAb accumulation [21]. Since the anti-tumor effect of Girentuximab depends on tumor cell accessibility from the vascular compartment, we studied the effect of sunitinib on the biodistribution of Girentuximab when administered with a short time delay between sunitinib and antibody administration. This short drug holiday mimics TKI treatment cycles in men and might allow re-establishment of the tumor vasculature, which would permit adequate mAb delivery and accumulation.

In the NU12 model, sunitinib treatment followed by a 3-day drug holiday resulted in a reduction in antibody uptake in the tumor. Microscopic analysis showed that the amount of viable tumor cells was considerably lower in sunitinib-treated tumors, apparently due to massive destruction of tumor microvessels. This decrease in antibody uptake was less pronounced than when the antibody was administered at the same time as the sunitinib treatment [21]. Thus, a time delay between sunitinib treatment and antibody administration did increase Girentuximab uptake, albeit that accumulation did not reach the level of untreated controls. The reduced antibody uptake is probably due to the accessibility of fewer viable cells in the NU12 tumors in sunitinib-treated animals, while tumor volume was not affected. Despite the presence of *CAIX* in necrotic areas after sunitinib treatment, Girentuximab did not accumulate in those areas, showing that the vasculature in the necrotic regions was not restored. The results suggest that despite the lower Girentuximab uptake in the tumor, all viable tumor cells present at the tumor periphery are targeted. Antibody uptake was not affected when administered before sunitinib treatment. This is not unexpected because the pharmacokinetics of the mAb in sunitinib treated animals were not affected: maximum and homogeneous accumulation can be established before treatment with sunitinib is initiated. This suggests that sunitinib after Girentuximab administration might be preferred over sunitinib before Girentuximab injection. However, in this scenario almost all tumor cells are viable and the amount of targeted Girentuximab molecules per viable tumor cell is substantially lower. This will amount to higher radiation levels per tumor cell with

Girentuximab-guided radioimmunotherapy. Thus, viable tumor cells remaining at the tumor rim after anti-angiogenic therapy can be efficiently targeted and potentially lethally damaged when Girentuximab radioimmunotherapy is applied.

Unexpectedly, antibody uptake in the SK-RC-52 tumors increased in the sunitinib treated animals, regardless of sequence of the treatment. In contrast to NU12, tumor cell viability was not affected by sunitinib treatment. The increased uptake in combination with unchanged MVD after sunitinib treatment suggests functional changes in the microvasculature in this tumor. The increased uptake was not only the consequence of the smaller tumor volume, as tumors with comparable volumes of sunitinib-treated animals showed equal or higher tumor uptake of Girentuximab. Whether the increased uptake is the consequence of tumor vessel normalization (and reduced interstitial fluid pressure) as suggested in previous studies [39,40] or the consequence of increased vascular permeability is unclear.

Also in this model sunitinib treatment before antibody injection appears preferable when combination therapy is considered: Girentuximab uptake post-sunitinib is significantly higher than Girentuximab uptake pre-sunitinib.

The two RCC models used in the present studies might be very valuable in studying resistance to TKI, a phenomenon occurring in most mRCC patients as they appear to reflect the extremes that can be observed in patients: some patients respond favorably, whereas other patients do not respond. Also, in some mRCC patients unexpected rapid progression and tumor related complaints after discontinuation of oral angiogenesis inhibitors can be observed [41]. This might be explained by an increase of vascular density, tumor blood flow rate and vascular permeability. In NU12 tumors a substantial part of the tumor endothelium is destroyed after sunitinib treatment, representative of a highly sensitive tumor, and cessation of therapy led to a rapid neovascularization, reminiscent of a tumor flare. SK-RC-52 appears to represent a sunitinib-resistant tumor, with little impact of sunitinib treatment on the microvessel density, but with physiological changes of blood vessels, in concordance with the hypothesis put forward by Jain et al. [12].

The disparity to sunitinib treatment between these models is striking. Because the vasculature of the two xenograft models has the same murine origin, this implies that the differences might be due to different angiogenic gene expression profiles in the tumors. Non-quantitative RT-PCR did not demonstrate any difference in *VEGF-A* expression levels between sunitinib-treated and non-treated NU12 cells and SK-RC-52 cells nor between NU12 xenografts and SK-RC-52 xenografts. Also gene expression profiles of SK-RC-52 and NU12 determined with the RT^2 Profiler™ PCR Array Human Angiogenesis (PAHS-24Z, Qiagen) did not show differences in *VEGF-A* expression (C^t 22.0 and 20.4, respectively). In this assay 5 genes involved in angiogenesis were differentially expressed between NU12 and SK-RC-52. *VEGF-C* levels were ~100-fold lower in NU12 cells compared to SK-RC-52. *VEGF-C* is one of the main growth factors implicated in lymphangiogenesis, signals through *VEGFR-3* and plays a secondary role in angiogenesis. Expression levels of placental growth factor (*PGF)*, a homolog to vascular endothelial growth factor and *PTGS1* (prostaglandin-

endoperoxidase synthetase 1) were higher in NU12. PGF can function as decoy receptor for VEGF which may explain the observed sunitinib sensitivity of NU12. *EFNA1* and *PLAU* were over-expressed in the non-responder cell line SK-RC-52. *EFNA1* is a member of the ephrin (*EPH*) family, comprising the largest subfamily of receptor protein-tyrosine kinases. High *EFNA1* levels may aid cells in resisting TKI challenge. Moreover, high plasminogen activator urokinase (*PLAU*) levels support fractional survival of cancer cells [42]. Also, expression levels of *PGF* and *PTGS1* were lower in SK-RC-52 as in NU12. Collectively, the high expression of *EFNA1* and *PLAU* together with low expression of *PGF* and *PTGS1* may explain the resistance of SK-RC-52 in comparison to NU12.

Anti-angiogenic therapies can reduce tumor perfusion and uptake of chemotherapeutics: bevacizumab treatment of patients with non-small cell lung cancer showed rapid and significant reduction of tumor perfusion and docetaxel uptake [43]. Moreover, preclinical (ovarian and esophageal cancer) and clinical studies (RCC) with bevacizumab [44] and sorafenib [45] demonstrated that antibody-uptake in the tumor is hampered when administered immediately after cessation of anti-angiogenic therapy. The investigators emphasize that administration schedules should be carefully designed to optimize combination treatment of anti-angiogenic therapy with other treatment modalities. Our results show that TKI and mAbs can be combined, provided a short drug holiday is introduced, regardless of TKI sensitivity: for TKI sensitive tumors TKI treatment leads to central necrosis and Girentuximab can then effectively target the remaining viable RCC cells in the tumor, whereas in TKI-resistant tumors Girentuximab tumor accumulation is increased, leading to higher antibody levels and correspondingly higher radiation dose in the tumor. Because TKI and Girentuximab are directed against different target cells, and the toxicity profile differs, combination of both drugs might prove beneficial. Stabilization of previously progressive mRCC appears possible with [177]Lutetium-Girentuximab and combination with TKI might lead to better and durable responses. In view of our results, initial treatment with TKI followed by [177]Lutetium-Girentuximab may be better than the reverse: administration of Girentuximab to patients with TKI-sensitive tumors will lead to massive cell death and the remaining viable cells in the tumor periphery will be effectively targeted by the radiolabeled antibody, whereas administration of Girentuximab to patients with TKI-insensitive tumors will lead to more effective [177]Lutetium-Girentuximab accumulation, resulting in higher radiation doses.

Acknowledgements
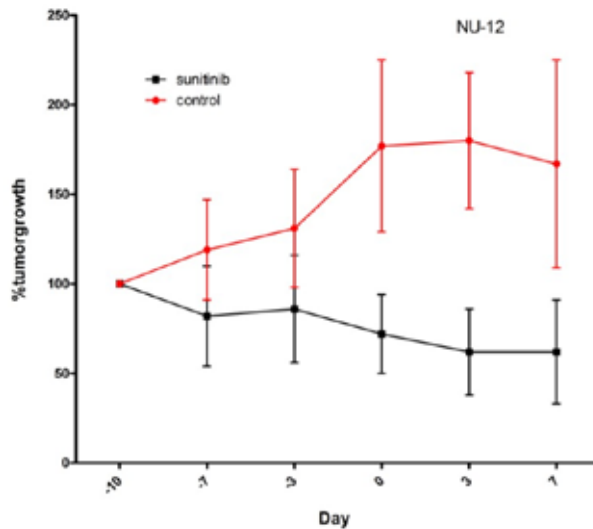
Figure S1. Mean % of growth of NU12 tumors during treatment with sunitinib. Treatment with sunitinib was started when tumors had reached a tumor volume of 100-200 mm^3 (day-10) and continued until day -3. Three days later mice were injected with ^{111}In-cG250. Percentage tumorgrowth was set at 100% at start of treatment with sunitinib. Tumorgrowth is strongly inhibited by sunitinib treatment (black line) in comparison to control (red line).
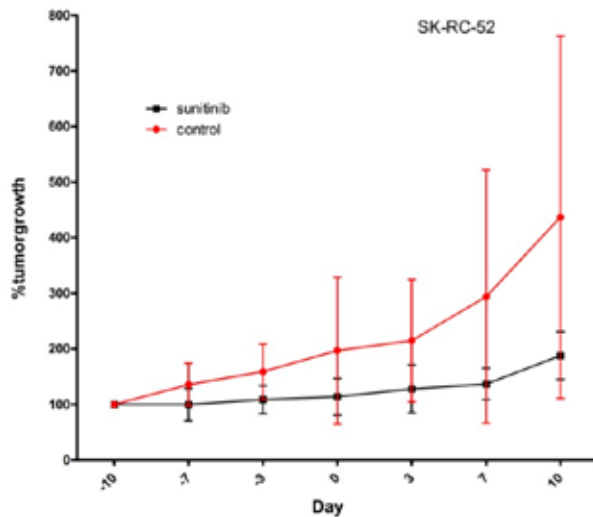
Figure S2. Mean % of growth of SK-RC-52 tumors during treatment with sunitinib. Treatment with sunitinib was started when tumors had reached a tumor volume of 100-200 mm^3 (day-10) and continued until day -3. Three days later mice were injected with ^{111}In-cG250. Percentage tumorgrowth was set at 100% at start of treatment with sunitinib.Tumorgrowth is stablized by sunitinib treatment (black line) in comparison to control (red line).
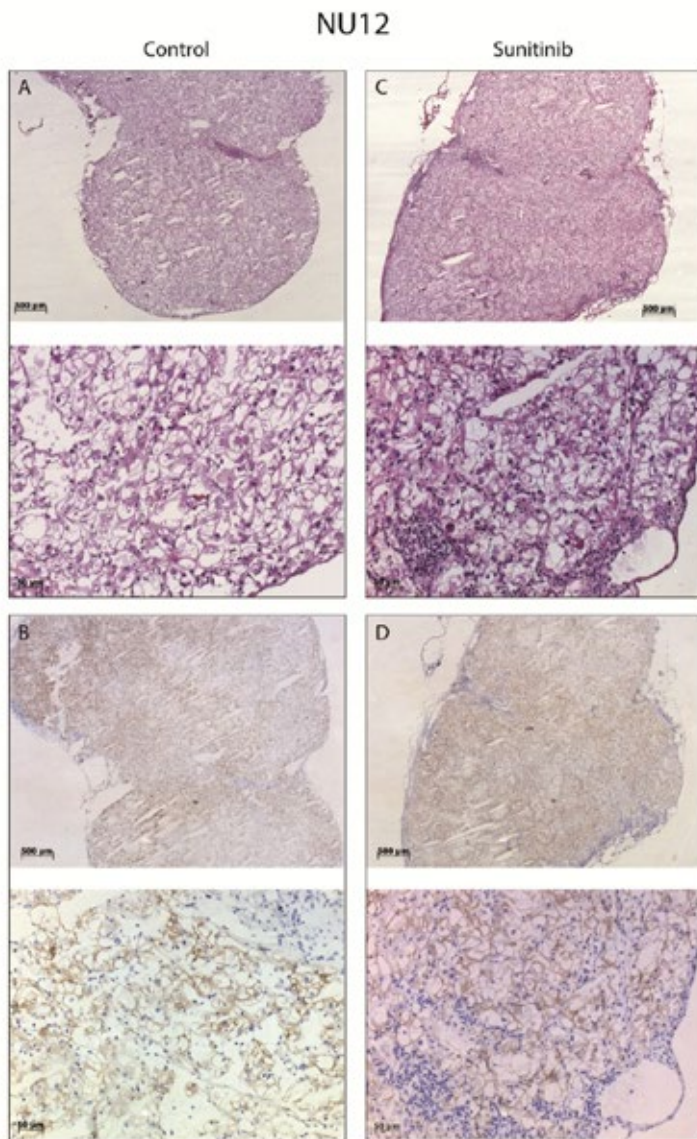
Figure S3. Phenotypic analysis of NU12 tumors. Phenotypic analysis of NU12 tumors of mice treated with sunitinib. Mice were injected intravenously with ^{111}In-Girentuximab (0.4 MBq, 5 µg) 3 days pre-sunitinib treatment. Accumulation of Girentuximab remained unchanged when sunitinib followed Girentuximab injection. Tumors shown were harvested at day 7 (4 days after start of sunitinib treatment). **A**, **C**: HE staining of untreated and sunitinib treated tumor respectively; **B**, **D**: Girentuximab accumulation. Original magnification X25 and X200.

Table S1 Biodistribution of Girentuximab in nude mice with NU12 tumors treated with sunitinib

	% ID/g[#]					
	control			sunitinib		
	3[*]	7	10	3	7	10
blood	9,7 ± 3,2	3,7 ± 2,7	3,2 ± 1,5	13,0 ± 3,3	6,6 ± 1,7	3,6 ± 0,4
muscle	1,0 ± 0,2	0,4 ± 0,3	0,4 ± 0,1	1,2 ± 0,4	0,7 ± 0,2	0,3 ± 0,1
tumor	89,8 ± 29,1	99,5 ± 51,9	134,5 ± 55,6	59,9 ± 38,8	68,8 ± 30,2	40,5 ± 22,0
liver	9,2 ± 3,2	7,8 ± 3,7	3,9 ± 0,7	7,2 ± 1,3	5,5 ± 0,3	2,2 ± 0,7
spleen	5,7 ± 4,0	3,6 ± 0,9	2,0 ± 0,4	3,9 ± 0,5	3,4 ± 0,5	1,7 ± 0,4
kidney	4,9 ± 1,0	3,8 ± 1,0	1,8 ± 0,5	5,6 ± 0,6	3,3 ± 0,3	1,4 ± 0,1
stomach	1,4 ± 0,5	0,8 ± 0,3	0,6 ± 0,1	1,6 ± 0,6	1,2 ± 0,4	0,6 ± 0,1
lung	6,7 ± 2,3	2,4 ± 1,8	2,9 ± 1,2	7,2 ± 1,5	4,6 ± 1,4	2,2 ± 0,3
small intestine	1,6 ± 0,6	0,6 ± 0,3	0,5 ± 0,2	2,1 ± 0,4	0,9 ± 0,2	0,4 ± 0,1

Biodistribution data supplementing figure 1A
[*] time post injection of ^{111}In-girentuximab in days
[#] % ID/g: mean percentage injected dose per gram tissue ± standard deviation

Table S2 Biodistribution of Girentuximab in nude mice with NU12 tumors treated with sunitinib

	% ID/g[#]				
		control		sunitinib	
	3[*]	7	14	7	14
blood	9,4 ± 1,7	3,5 ± 0,8	1,0 ± 0,7	5,3 ± 1,4	2,2 ± 1,2
muscle	1,0 ± 0,3	0,4 ± 0,1	0,1 ± 0,1	0,6 ± 0,2	0,2 ± 0,1
tumor	113,8 ± 13,7	96,4 ± 41,2	61,2 ± 30,6	90,6 ± 9,6	61,5 ± 19,5
liver	3,7 ± 0,8	5,5 ± 3,1	1,7 ± 0,3	4,3 ± 1,7	2,7 ± 0,6
spleen	3,6 ± 0,6	2,8 ± 1,8	1,3 ± 0,4	3,2 ± 0,7	1,1 ± 0,4
kidney	4,3 ± 0,8	2,9 ± 0,7	1,1 ± 0,3	2,7 ± 0,3	2,4 ± 0,7
stomach	1,4 ± 0,4	0,7 ± 0,2	0,3 ± 0,1	0,9 ± 0,2	0,4 ± 0,2
lung	4,7 ± 1,9	2,9 ± 1,2	1,0 ± 0,5	3,4 ± 0,8	1,6 ± 0,9
small intestine	1,3 ± 0,3	0,7 ± 0,2	0,2 ± 0,1	1,1 ± 0,3	0,5 ± 0,2
colon	1,0 ± 0,3	0,5 ± 0,1	0,2 ± 0,1	0,7 ± 0,5	0,3 ± 0,1

Biodistribution data supplementing figure 1B.
[*] time post injection of ^{111}In-girentuximab in days
[#] % ID/g: percentage injected dose per gram tissue ± standard deviation

Table S3   Biodistribution of Girentuximab in nude mice with SK-RC-52 tumors treated with sunitinib

	% ID/g[#]									
	control					sunitinib				
	3[*]	7	10	14	17	3	7	10	14	17
blood	7,6 ± 4,4	2,1 ± 1,9	0,1 ± 0,03	0,05 ± 0,02	0,03 ± 0,01	7,9 ± 1,5	2,7 ± 2,1	1,0 ± 0,6	0,4 ± 0,5	0,06 ± 0,04
muscle	0,9 ± 0,4	0,3 ± 0,1	0,1 ± 0,02	0,04 ± 0,03	0,04 ± 0,05	1,0 ± 0,3	0,3 ± 0,2	0,2 ± 0,2	0,1 ± 0,05	0,07 ± 0,04
tumor	51,0 ± 9,7	47,3 ± 17,2	11,64 ± 3,6	5,5 ± 1,8	3,4 ± 1,5	65,3 ± 9,0	44,8 ± 18,7	42,8 ± 23,3	11,61 ± 5,82	7,0 ± 6,6
liver	13,5 ± 4,5	12,4 ± 3,7	8,6 ± 2,7	4,8 ± 0,9	3,9 ± 0,1	10,1 ± 2,4	9,2 ± 1,8	7,0 ± 1,4	2,8 ± 0,9	3,6 ± 1,8
spleen	5,1 ± 1,3	4,8 ± 1,7	3,2 ± 1,0	2,4 ± 0,7	1,8 ± 0,5	3,5 ± 0,3	3,2 ± 1,2	3,2 ± 2,2	1,6 ± 0,5	1,9 ± 1,4
kidney	3,6 ± 1,3	1,9 ± 0,4	0,8 ± 0,1	0,7 ± 0,03	0,6 ± 0,1	3,7 ± 0,2	2,1 ± 0,4	1,4 ± 0,3	0,6 ± 0,02	0,6 ± 0,2
stomach	1,0 ± 0,4	0,4 ± 1,4	0,1 ± 0,03	0,1 ± 0,05	0,1 ± 0,03	1,1 ± 0,2	0,5 ± 0,2	0,3 ± 0,2	0,2 ± 0,1	0,1 ± 0,1
lung	4,5 ± 2,0	1,8 ± 0,4	0,3 ± 0,1	0,2 ± 0,01	0,1 ± 0,1	4,8 ± 1,1	2,0 ± 1,1	0,9 ± 0,47	0,4 ± 0,3	0,3 ± 0,3
small intestine	1,6 ± 0,5	0,6 ± 0,2	0,1 ± 0,02	0,1 ± 0,04	0,04 ± 0,01	1,4 ± 0,2	0,5 ± 0,3	0,3 ± 0,1	0,1 ± 0,1	0,08 ± 0,1
colon	0,8 ± 0,4	0,3 ± 0,3	0,1 ± 0,01	0,1 ± 0,01	0,04 ± 0,01	0,9 ± 0,1	0,4 ± 0,2	0,2 ± 0,1	0,1 ± 0,1	0,07 ± 0,05

Biodistribution data supplementing figure 1D.
[*] time post injection of ^{111}In-girentuximab in days
[#] % ID/g: percentage injected dose per gram tissue ± standard deviation

Table S4   Biodistribution of Girentuximab in nude mice with SK-RC-52 tumors treated with sunitinib

	% ID/g								
	control					sunitinib			
	3[*]	7	10	14	17	7	10	14	17
blood	12,0 ± 1,0	3,8 ± 2,2	1,7 ± 2,1	0,6 ± 1,5	0,2 ± 0,3	6,1 ± 1,2	3,1 ± 2,4	3,1 ± 1,7	1,6 ± 1,6
muscle	1,2 ± 0,1	0,4 ± 0,2	0,2 ± 0,2	0,1 ± 0,1	0,1 ± 0,01	0,6 ± 0,1	0,5 ± 0,2	0,3 ± 0,2	0,2 ± 0,1
tumor	93,1 ± 28,6	80,0 ± 29,2	42,4 ± 36,4	24,9 ± 55,6	23,4 ± 34,2	86,3 ± 36,0	47,4 ± 30,2	66,2 ± 33,0	53,7 ± 49,9
liver	8,1 ± 2,6	10,1 ± 4,8	7,9 ± 2,1	5,2 ± 0,7	4,9 ± 0,7	6,5 ± 2,1	6,5 ± 2,6	3,9 ± 1,0	4,1 ± 1,4
spleen	4,6 ± 0,3	3,5 ± 0,5	2,8 ± 0,6	2,6 ± 0,4	1,9 ± 0,9	3,8 ± 0,6	3,5 ± 0,8	3,4 ± 0,4	2,8 ± 0,7
kidney	4,5 ± 0,5	1,8 ± 0,5	1,3 ± 0,5	0,8 ± 0,5	0,6 ± 0,2	2,4 ± 0,4	1,6 ± 0,8	1,5 ± 0,4	0,9 ± 0,4
stomach	1,7 ± 0,2	0,7 ± 0,3	0,3 ± 0,3	0,2 ± 0,1	0,1 ± 0,1	1,0 ± 0,2	0,6 ± 0,4	0,6 ± 0,2	0,3 ± 0,2
lung	6,3 ± 0,6	2,8 ± 1,4	1,4 ± 1,4	0,6 ± 1,2	0,4 ± 0,3	4,0 ± 0,6	2,7 ± 2,0	2,5 ± 1,2	1,0 ± 0,9
small intestine	1,7 ± 0,3	0,6 ± 0,2	0,4 ± 0,3	0,2 ± 0,2	0,1 ± 0,1	1,2 ± 0,4	0,6 ± 0,4	0,7 ± 0,3	0,3 ± 0,2
colon	1,1 ± 0,2	0,4 ± 0,2	0,3 ± 0,2	0,1 ± 0,2	0,1 ± 0,01	0,6 ± 0,1	0,4 ± 0,2	0,3 ± 0,1	0,2 ± 0,1

Biodistribution data supplementing figure 1E.
[*] time post injection of ^{111}In-girentuximab in days
[#] % ID/g: percentage injected dose per gram tissue ± standard deviation

Table S5   Biodistribution of Girentuximab in nude mice with SK-RC-52 tumors treated with sunitinib

	% ID/g[#]					
	control			sunitinib		
	d3	d7	d10	d3	d7	d10
blood	2,9 ± 3,1	4,3 ± 1,2	6,0 ± 2,6	7,4 ± 1,4	8,2 ± 1,4	8,2 ± 2,4
muscle	0,5 ± 0,2	0,6 ± 0,1	0,7 ± 0,2	0,9 ± 0,2	0,9 ± 0,2	1,2 ± 0,1
tumor	42,3 ± 11,9	47,0 ± 12,7	45,5 ± 13,7	62,6 ± 14,5	60 ± 11,4	55,8 ± 18,5
liver	14,3 ± 2,2	13,3 ± 2,3	7,8 ± 3,2	7,4 ± 1,9	6,1 ± 1,9	8,3 ± 3,0
spleen	5,4 ± 2,2	4 ± 0,6	3,4 ± 0,7	2,9 ± 0,6	2,9 ± 0,5	3,9 ± 0,3
kidney	2,5 ± 0,4	2,7 ± 0,4	3,8 ± 0,7	3,3 ± 0,8	3,8 ± 0,4	5,0 ± 0,9
stomach	0,7 ± 0,2	0,8 ± 0,2	1,3 ± 0,4	1,2 ± 0,2	1,6 ± 0,3	1,6 ± 0,2
lung	2,4 ± 0,8	3,2 ± 0,7	4,0 ± 1,3	4,3 ± 0,9	5,2 ± 0,8	5,5 ± 1,6
small intestine	0,7 ± 0,3	0,9 ± 0,4	1,2 ± 0,6	1,0 ± 0,2	1,6 ± 0,3	1,8 ± 0,4
colon	0,4 ± 0,1	0,6 ± 0,1	1,0 ± 0,4	0,8 ± 0,1	0,9 ± 0,2	1,1 ± 0,2

Biodistribution data supplementing figure 1F.
[*] time post first injection of ^{111}In-girentuximab in days
[#] % ID/g: percentage injected dose per gram tissue ± standard deviation

References

1. Ferlay, J.; Steliarova-Foucher, E.; Lortet-Tieulent, J.; Rosso, S.; Coebergh, J.W.; Comber, H.; Forman, D.; Bray, F. Cancer incidence and mortality patterns in europe: Estimates for 40 countries in 2012. *European journal of cancer* **2013**, *49*, 1374-1403.
2. Patard, J.J.; Pignot, G.; Escudier, B.; Eisen, T.; Bex, A.; Sternberg, C.; Rini, B.; Roigas, J.; Choueiri, T.; Bukowski, R*., et al.* Icud-eau international consultation on kidney cancer 2010: Treatment of metastatic disease. *European urology* **2011**, *60*, 684-690.
3. Motzer, R.J.; Rini, B.I.; Bukowski, R.M.; Curti, B.D.; George, D.J.; Hudes, G.R.; Redman, B.G.; Margolin, K.A.; Merchan, J.R.; Wilding, G*., et al.* Sunitinib in patients with metastatic renal cell carcinoma. *JAMA : the journal of the American Medical Association* **2006**, *295*, 2516-2524.
4. Escudier, B.; Eisen, T.; Stadler, W.M.; Szczylik, C.; Oudard, S.; Siebels, M.; Negrier, S.; Chevreau, C.; Solska, E.; Desai, A.A*., et al.* Sorafenib in advanced clear-cell renal-cell carcinoma. *The New England journal of medicine* **2007**, *356*, 125-134.
5. Rixe, O.; Bukowski, R.M.; Michaelson, M.D.; Wilding, G.; Hudes, G.R.; Bolte, O.; Motzer, R.J.; Bycott, P.; Liau, K.F.; Freddo, J*., et al.* Axitinib treatment in patients with cytokine-refractory metastatic renal-cell cancer: A phase ii study. *The lancet oncology* **2007**, *8*, 975-984.
6. Sternberg, C.N.; Davis, I.D.; Mardiak, J.; Szczylik, C.; Lee, E.; Wagstaff, J.; Barrios, C.H.; Salman, P.; Gladkov, O.A.; Kavina, A*., et al.* Pazopanib in locally advanced or metastatic renal cell carcinoma: Results of a randomized phase iii trial. *Journal of clinical oncology : official journal of the American Society of Clinical Oncology* **2010**, *28*, 1061-1068.
7. Escudier, B.; Bellmunt, J.; Negrier, S.; Bajetta, E.; Melichar, B.; Bracarda, S.; Ravaud, A.; Golding, S.; Jethwa, S.; Sneller, V. Phase iii trial of bevacizumab plus interferon alfa-2a in patients with metastatic renal cell carcinoma (avoren): Final analysis of overall survival. *Journal of clinical oncology : official journal of the American Society of Clinical Oncology* **2010**, *28*, 2144-2150.
8. Hudes, G.; Carducci, M.; Tomczak, P.; Dutcher, J.; Figlin, R.; Kapoor, A.; Staroslawska, E.; Sosman, J.; McDermott, D.; Bodrogi, I*., et al.* Temsirolimus, interferon alfa, or both for advanced renal-cell carcinoma. *The New England journal of medicine* **2007**, *356*, 2271-2281.
9. Motzer, R.J.; Escudier, B.; Oudard, S.; Hutson, T.E.; Porta, C.; Bracarda, S.; Grunwald, V.; Thompson, J.A.; Figlin, R.A.; Hollaender, N*., et al.* Efficacy of everolimus in advanced renal cell carcinoma: A double-blind, randomised, placebo-controlled phase iii trial. *Lancet* **2008**, *372*, 449-456.
10. Coppin, C.; Kollmannsberger, C.; Le, L.; Porzsolt, F.; Wilt, T.J. Targeted therapy for advanced renal cell cancer (rcc): A cochrane systematic review of published randomised trials. *BJU international* **2011**, *108*, 1556-1563.
11. Sonpavde, G.; Choueiri, T.K.; Escudier, B.; Ficarra, V.; Hutson, T.E.; Mulders, P.F.; Patard, J.J.; Rini, B.I.; Staehler, M.; Sternberg, C.N*., et al.* Sequencing of agents for metastatic renal cell carcinoma: Can we customize therapy? *European urology* **2012**, *61*, 307-316.
12. Jain, R.K.; Carmeliet, P. Snapshot: Tumor angiogenesis. *Cell* **2012**, *149*, 1408-U1257.
13. Macedo, L.T.; da Costa Lima, A.B.; Sasse, A.D. Addition of bevacizumab to first-line chemotherapy in advanced colorectal cancer: A systematic review and meta-analysis, with emphasis on chemotherapy subgroups. *BMC cancer* **2012**, *12*, 89.
14. Ebos, J.M.; Lee, C.R.; Cruz-Munoz, W.; Bjarnason, G.A.; Christensen, J.G.; Kerbel, R.S. Accelerated metastasis after short-term treatment with a potent inhibitor of tumor angiogenesis. *Cancer cell* **2009**, *15*, 232-239.
15. Paez-Ribes, M.; Allen, E.; Hudock, J.; Takeda, T.; Okuyama, H.; Vinals, F.; Inoue, M.; Bergers, G.; Hanahan, D.; Casanovas, O. Antiangiogenic therapy elicits malignant progression of tumors to increased local invasion and distant metastasis. *Cancer cell* **2009**, *15*, 220-231.
16. Neri, D.; Supuran, C.T. Interfering with ph regulation in tumours as a therapeutic strategy. *Nat Rev Drug Discov* **2011**, *10*, 767-777.
17. Supuran, C.T. Carbonic anhydrases: Novel therapeutic applications for inhibitors and activators. *Nat Rev Drug Discov* **2008**, *7*, 168-181.
18. Oosterwijk, E. Carbonic anhydrase expression in kidney and renal cancer: Implications for diagnosis and treatment. *Sub-cellular biochemistry* **2014**, *75*, 181-198.
19. Pastorek, J.; Pastorekova, S. Hypoxia-induced carbonic anhydrase ix as a target for cancer therapy: From biology to clinical use. *Seminars in cancer biology* **2014**.
20. Stillebroer, A.B.; Boerman, O.C.; Desar, I.M.E.; Boers-Sonderen, M.J.; van Herpen, C.M.L.; Langenhuijsen, J.F.; Smith-Jones, P.M.; Oosterwijk, E.; Oyen, W.J.G.; Mulders, P.F.A. Phase 1 radioimmunotherapy study with lutetium 177-labeled anti-carbonic anhydrase ix monoclonal

antibody girentuximab in patients with advanced renal cell carcinoma. *Eur Urol* **2013**, *64*, 478-485.

21. Oosterwijk-Wakka, J.C.; Kats-Ugurlu, G.; Leenders, W.P.; Kiemeney, L.A.; Old, L.J.; Mulders, P.F.; Oosterwijk, E. Effect of tyrosine kinase inhibitor treatment of renal cell carcinoma on the accumulation of carbonic anhydrase ix-specific chimeric monoclonal antibody cg250. *BJU international* **2011**, *107*, 118-125.

22. Muselaers, C.H.J.; Stillebroer, A.B.; Boers-Sonderen, M.J.; Desar, I.M.E.; van Herpen, C.M.L.; Langenhuijsen, J.F.; Oosterwijk, E.; Boerman, O.C.; Mulders, P.F.A.; Oyen, W.J.G. Sorafenib reduces the tumor uptake of indium-111-girentuximab in clear cell renal cell carcinoma patients. *Eur J Nucl Med Mol I* **2012**, *39*, S188-S189.

23. Ebert, T.; Bander, N.H.; Finstad, C.L.; Ramsawak, R.D.; Old, L.J. Establishment and characterization of human renal cancer and normal kidney cell lines. *Cancer research* **1990**, *50*, 5531-5536.

24. Beniers, A.J.; Peelen, W.P.; Schaafsma, H.E.; Beck, J.L.; Ramaekers, F.C.; Debruyne, F.M.; Schalken, J.A. Establishment and characterization of five new human renal tumor xenografts. *The American journal of pathology* **1992**, *140*, 483-495.

25. van Schaijk, F.G.; Oosterwijk, E.; Molkenboer-Kuenen, J.D.; Soede, A.C.; McBride, B.J.; Goldenberg, D.M.; Oyen, W.J.; Corstens, F.H.; Boerman, O.C. Pretargeting with bispecific anti-renal cell carcinoma x anti-dtpa(in) antibody in 3 rcc models. *Journal of nuclear medicine : official publication, Society of Nuclear Medicine* **2005**, *46*, 495-501.

26. Oosterwijk, E.; Ruiter, D.J.; Hoedemaeker, P.J.; Pauwels, E.K.; Jonas, U.; Zwartendijk, J.; Warnaar, S.O. Monoclonal antibody g 250 recognizes a determinant present in renal-cell carcinoma and absent from normal kidney. *International journal of cancer. Journal international du cancer* **1986**, *38*, 489-494.

27. Steffens, M.G.; Boerman, O.C.; Oosterwijk-Wakka, J.C.; Oosterhof, G.O.; Witjes, J.A.; Koenders, E.B.; Oyen, W.J.; Buijs, W.C.; Debruyne, F.M.; Corstens, F.H*., et al.* Targeting of renal cell carcinoma with iodine-131-labeled chimeric monoclonal antibody g250. *Journal of clinical oncology : official journal of the American Society of Clinical Oncology* **1997**, *15*, 1529-1537.

28. Brouwers, A.H.; van Eerd, J.E.; Frielink, C.; Oosterwijk, E.; Oyen, W.J.; Corstens, F.H.; Boerman, O.C. Optimization of radioimmunotherapy of renal cell carcinoma: Labeling of monoclonal antibody cg250 with 131i, 90y, 177lu, or 186re. *Journal of nuclear medicine : official publication, Society of Nuclear Medicine* **2004**, *45*, 327-337.

29. Lindmo, T.; Boven, E.; Cuttitta, F.; Fedorko, J.; Bunn, P.A., Jr. Determination of the immunoreactive fraction of radiolabeled monoclonal antibodies by linear extrapolation to binding at infinite antigen excess. *Journal of immunological methods* **1984**, *72*, 77-89.

30. Bussink, J.; Kaanders, J.H.; Rijken, P.F.; Martindale, C.A.; van der Kogel, A.J. Multiparameter analysis of vasculature, perfusion and proliferation in human tumour xenografts. *British journal of cancer* **1998**, *77*, 57-64.

31. Navis, A.C.; Bourgonje, A.; Wesseling, P.; Wright, A.; Hendriks, W.; Verrijp, K.; van der Laak, J.A.W.M.; Heerschap, A.; Leenders, W.P.J. Effects of dual targeting of tumor cells and stroma in human glioblastoma xenografts with a tyrosine kinase inhibitor against c-met and vegfr2. *Plos One* **2013**, *8*.

32. Steffens, M.G.; Kranenborg, M.H.; Boerman, O.C.; Zegwaart-Hagemeier, N.E.; Debruyne, F.M.; Corstens, F.H.; Oosterwijk, E. Tumor retention of 186re-mag3, 111in-dtpa and 125i labeled monoclonal antibody g250 in nude mice with renal cell carcinoma xenografts. *Cancer biotherapy & radiopharmaceuticals* **1998**, *13*, 133-139.

33. Kranenborg, M.H.; Boerman, O.C.; de Weijert, M.C.; Oosterwijk-Wakka, J.C.; Corstens, F.H.; Oosterwijk, E. The effect of antibody protein dose of anti-renal cell carcinoma monoclonal antibodies in nude mice with renal cell carcinoma xenografts. *Cancer* **1997**, *80*, 2390-2397.

34. Molina, A.M.; Lin, X.; Korytowsky, B.; Matczak, E.; Lechuga, M.J.; Wiltshire, R.; Motzer, R.J. Sunitinib objective response in metastatic renal cell carcinoma: Analysis of 1059 patients treated on clinical trials. *European journal of cancer* **2014**, *50*, 351-358.

35. Escudier, B.; Albiges, L.; Sonpavde, G. Optimal management of metastatic renal cell carcinoma: Current status. *Drugs* **2013**, *73*, 427-438.

36. Stillebroer, A.B.; Mulders, P.F.; Boerman, O.C.; Oyen, W.J.; Oosterwijk, E. Carbonic anhydrase ix in renal cell carcinoma: Implications for prognosis, diagnosis, and therapy. *European urology* **2010**, *58*, 75-83.

37. Divgi, C.R.; Uzzo, R.G.; Gatsonis, C.; Bartz, R.; Treutner, S.; Yu, J.Q.; Chen, D.; Carrasquillo, J.A.; Larson, S.; Bevan, P*., et al.* Positron emission tomography/computed tomography

identification of clear cell renal cell carcinoma: Results from the redect trial. *Journal of clinical oncology : official journal of the American Society of Clinical Oncology* **2013**, *31*, 187-194.

38. Belldegrun, A.S.; Chamie, K.; Kloepfer, P.; Fall, B.; Bevan, P.; Storkel, S.; Wilhelm, O.; Pantuck, A.J. Ariser: A randomized double blind phase iii study to evaluate adjuvant cg250 treatment versus placebo in patients with high-risk ccrcc-results and implications for adjuvant clinical trials. *J Clin Oncol* **2013**, *31*.

39. Huang, Y.H.; Stylianopoulos, T.; Duda, D.G.; Fukumura, D.; Jain, R.K. Benefits of vascular normalization are dose and time dependent-letter. *Cancer research* **2013**, *73*, 7144-7146.

40. Jain, R.K. Normalizing tumor microenvironment to treat cancer: Bench to bedside to biomarkers. *Journal of Clinical Oncology* **2013**, *31*, 2205-U2210.

41. Buczek, M.; Escudier, B.; Bartnik, E.; Szczylik, C.; Czarnecka, A. Resistance to tyrosine kinase inhibitors in clear cell renal cell carcinoma: From the patient's bed to molecular mechanisms. *Bba-Rev Cancer* **2014**, *1845*, 31-41.

42. Pavet, V.; Shlyakhtina, Y.; He, T.; Ceschin, D.G.; Kohonen, P.; Perala, M.; Kallioniemi, O.; Gronemeyer, H. Plasminogen activator urokinase expression reveals trail responsiveness and supports fractional survival of cancer cells. *Cell death & disease* **2014**, *5*, e1043.

43. Van der Veldt, A.A.M.; Lubberink, M.; Bahce, I.; Walraven, M.; de Boer, M.P.; Greuter, H.N.J.M.; Hendrikse, N.H.; Eriksson, J.; Windhorst, A.D.; Postmus, P.E*., et al.* Rapid decrease in delivery of chemotherapy to tumors after anti-vegf therapy: Implications for scheduling of anti-angiogenic drugs. *Cancer Cell* **2012**, *21*, 82-91.

44. Arjaans, M.; Munnink, T.H.O.; Oosting, S.F.; van Scheltinga, A.G.T.T.; Gietema, J.A.; Garbacik, E.T.; Timmer-Bosscha, H.; Lub-de Hooge, M.N.; Schroder, C.P.; de Vries, E.G.E. Bevacizumab-induced normalization of blood vessels in tumors hampers antibody uptake. *Cancer research* **2013**, *73*, 3347-3355.

45. Muselaers, C.H.J.; Stillebroer, A.B.; Desar, I.M.E.; Boers-Sonderen, M.J.; van Herpen, C.M.L.; de Weijert, M.C.A.; Langenhuijsen, J.F.; Oosterwijk, E.; Leenders, W.P.J.; Boerman, O.C*., et al.* Tyrosine kinase inhibitor sorafenib decreases in-111-girentuximab uptake in patients with clear cell renal cell carcinoma. *J Nucl Med* **2014**, *55*, 242-247.

Chapter 6

Combination Therapy with 177-Lutetium labeled antibody cG250 Radioimmunotherapy and Sunitinib: A promising new therapeutic Strategy for Patients with advanced RCC

Jeannette C. Oosterwijk-Wakka[1], Gerben M. Franssen[2], Ton A.F.J. de Haan[3], Otto C. Boerman[2], Peter F.A. Mulders[1] and Egbert Oosterwijk[1]

[1] Department of Urology, [2] Radiology and Nuclear Medicine and [3] Health Evidence, Radboud university medical center, Nijmegen, The Netherlands

Abstract

Purpose: Implementation of sunitinib as treatment for patients with metastatic renal cell carcinoma (mRCC) has lead to impressive gains in efficacy. However, therapeutic progress has been primarily palliative in nature. Additionally, treatment can coincide with significant toxicity. Combination therapy with tyrosine kinase inhibitors (TKI) has not been successful due to increased toxicity. Treatment of progressive mRCC patients with ^{177}Lu-cG250 radioimmunotherapy (RIT) is well-tolerated and results in stabilization of disease in 74% of mRCC patients. The aim of this study was to enhance efficacy in mRCC by combining anti-angiogenic with anti-tumor cell therapy.

Experimental design: Nude mice with subcutaneous human RCC xenografts (NU12, SK-RC-52) were treated with sunitinib and injected i.v. with low doses of ^{177}Lu-cG250 for 1 or 2 cycles. Tumor growth was monitored and immunohistochemical analyses were performed.

Results: The best response in mice with SK-RC-52 tumors was observed with two combination treatment cycles. All animals survived the observation period with almost complete tumor ablation. Nevertheless, more treatment cycles are necessary to ablate tumors completely. In the NU12 model, 2 cycles of ^{177}Lu-cG250-RIT and 2 cycles of combination treatment were equally effective (100% survival). The ^{177}Lu-cG250-RIT was probably too effective, despite the low dose, obscuring improved survival of the combination treatment.

Conclusions: Combination of anti-angiogenic and anti-tumor cell treatment was superior over either treatment alone for SK-RC-52 tumors. Our findings provide a promising new therapeutic strategy for patients with advanced RCC.

Introduction

Sunitinib, a potent multitargeted receptor tyrosine kinase inhibitor (TKI), targeting VEGFR is standard treatment for patients with metastatic renal cell carcinoma (mRCC) [1-4]. Implementation of TKI with the tumor vascular bed as the primary target, has improved objective response rates (ORR) and median progression free survival (PFS) substantially [5,6]. However, complete responses are extraordinary rare and not all patients benefit as some patients are unresponsive and some patients experience major toxicities leading to dose reduction or treatment cessation [3]. To improve therapeutic outcome, combinations of sunitinib with cytokines [7,8], bevacizumab [9] or mTOR inhibitors [10,11] were tested, but these combinations proved to be too toxic. Additional specific inhibitors are emerging [12], but until now, no substantial improvement in efficacy has been observed. Unfortunately, almost invariably tumors become therapy-resistant in time. Current second-line therapies include treatment with axitinib, sorafenib or everolimus, but responses are usually short-term. Recently nivolumab, a programmed death 1 (PD-1) checkpoint inhibitor, was approved as second-line therapy. Among patients with previously treated advanced RCC, overall survival was longer (25.0 vs. 19.6 months) and toxicity was lower with nivolumab than with everolimus [13]. Although improvement is substantial, therapeutic progress is still palliative in nature.

Chimeric monoclonal antibody G250 (cG250) targets CAIX, a protein highly expressed in ccRCC. In radioimmunotherapy clinical trials with ^{177}Lu-labeled cG250, (^{177}Lu-cG250) stabilization of previously progressive mRCC patients was observed. Previously we have shown that the biodistribution of cG250 is influenced by sunitinib treatment [14], but regardless of TKI sensitivity, TKI and mAbs can be combined, provided a short drug holiday is introduced; in TKI 'sensitive' tumors the remaining viable RCC cells were effectively targeted by cG250, whereas in TKI-'resistant' tumors cG250 tumor accumulation was increased, leading to higher antibody levels. Since stabilization of previously progressive mRCC is possible with ^{177}Lu-cG250 [15] and sunitinib [1,4] the aim of this study was to investigate whether sunitinib combined with ^{177}Lu-cG250 RIT at low ^{177}Lu activity doses could improve therapeutic outcome.

Material and Methods

Cell lines and reagents

The human Renal Carcinoma cell line SK-RC-52 was established from a mediastinal metastasis of a primary RCC [16]. The cell line was cultured in RPMI1640 (Gibco, Bleiswijk, The Netherlands) supplemented with 10% fetal bovine serum (Sigma) and 2 mM glutamine (Gibco). Human renal cell carcinoma xenograft model NU12 [17] was maintained by passing freshly excised tumor pieces (1-2 mm^3) subcutaneously (s.c.) in mice. Both SK-RC-52 and NU12 express high levels of *CAIX* [18].

Conjugation and radiolabeling of cG250

The generation of cG250 has been described earlier [19]. Chimeric G250 has a high affinity for *CAIX* (Ka = 4 x 10^9 M^{-1}) which is expressed on the cell surface of >95% of ccRCC

The conjugation of cG250 (generously provided by Wilex AG, Munich, Germany) to isothiocyanato-benzyl-1,4,7,10-tetraazacyclododecane-1,4,7,10-tetraacetic acid (ITC-DOTA) was performed essentially as described by Lewis et al. [20]. In brief, cG250 was conjugated with ITC-DOTA (Macrocyclics, Dallas, TX) in 0.1 M $NaHCO_3$, pH 9.5 for 1 hour at room temperature, using a 15-fold molar excess of ITC-DOTA. To remove unbound ITC-DOTA, the reaction mixture was dialyzed against 0.25 M ammoniumacetate buffer, pH 5.5.

The cG250-ITC-DOTA conjugate (150-350 µg) was radiolabeled with 200-450 MBq ^{177}Lu, no-carrier-added (ITG isotope technologies, Garching GmbH, Germany) in 0.1 M MES buffer, pH 5.4 for 20 min at room temperature under strict metal-free conditions. After incubation, 50 mM EDTA was added to a final concentration of 5 mM [21,22].

Labeling efficiency of the ^{177}Lu-cG250 preparations was determined using Instant Thin Layer Chromatography (ITLC) silica gel strips (Agilent technologies, Amstelveen, The Netherlands) and 0.1 M citrate buffer, pH 6.0 as the mobile phase. When labeling efficiency was below 95%, the reaction mixture was purified on a PD-10 column (GE, Woerden, The Netherlands). The radiochemical purity exceeded 95% in all experiments. The immunoreactive fraction (IRF), determined on freshly trypsinized SK-RC-52 RCC cells at infinite antigen excess essentially as described by Lindmo et al.[23] with minor modifications [19], was 87 ± 7%.

In vivo therapy experiments

Institutional guidelines were strictly followed for maintenance of animals and experimental procedures were approved by the Institutional Animal Care and Use Committee (IACUC, RU-DEC 2012-038 and RU-DEC 2012-267). All procedures were performed using the guidelines from the Institute of Laboratory Animal Research [24]. Female BALB/c nu/nu mice, 6-8 weeks of age, were obtained from Janvier, France, and maintained at the local central animal facility. Animals were either grafted s.c. with freshly excised NU12 xenograft pieces [17] of approximately 1-2 mm^3 or injected s.c. with $2*10^6$ freshly trypsinized SK-RC-52 cells.

Once tumors reached the desired volume (50-150 mm^3) mice were divided into groups of 13-14 mice randomly and treatment was initiated. Sunitinib (SU11248, Sutent®, Pfizer) was dissolved in 0.1 M Na-citrate, pH 4.5.

In Fig. 1, the treatment schedule is depicted for both SK-RC-52 as NU12. In short, mice received the equivalent of 40 mg/kg (0.8 mg/200 µl) sunitinib orally per day for 14 days. Three days thereafter, animals received 6.5 MBq/10 µg ^{177}Lu-cG250 (1/3 of Maximum Tolerated Dose) by intravenous injection (1st cycle). Six to seven weeks (NU12 and SK-RC-52 respectively) after start of the 1st cycle another cycle of treatment was administered (Su + Lu-cG250 2x). Comparator groups were treated with 1 cycle of combined treatment (Su + Lu-cG250 1x), 1 or 2 cycles of ^{177}Lu-cG250 (Lu-cG250 1x/ 2x), 2 cycles of sunitinib (Su 2x) or

were left untreated (control). Tumor volumes were determined twice a week, using a caliper by an evaluator blinded to the treatment groups. Tumor volume was estimated using the following formula: (length x width x depth) x $\pi/6$. The last observed tumor volume was used to calculate average tumor volumes, i.e., when mice were killed, because the tumor volume exceeded 1500 mm^3 (a predetermined humane endpoint).
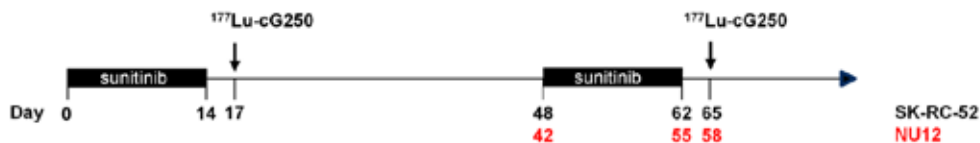

Figure 1. Treatment schedule of mice with SK-RC-52 or NU12 tumors

Mice were euthanized when either tumor burden reached 1500 mm^3 or when mice reached a predetermined humane endpoint. After the animals were euthanized, tumors were dissected and analyzed. Kaplan-Meier curves for overall survival (OS) were generated. Mice that were sacrificed because of other reasons than reaching maximal tumor burden were excluded. Included number of mice with SK-RC-52 tumors was: 13, 10, 11, 12, 13 and 10 for Su+^{177}Lu-cG250 1 cycle, Su+^{177}Lu-cG250 2 cycles, ^{177}Lu-cG250 1 cycle, ^{177}Lu-cG250 2 cycles, Su 2 cycles, and Control respectively. For NU12, included number of mice was 12, 13, 14, 14, 14 and 14 for Su+^{177}Lu-cG250 1 cycle, Su+^{177}Lu-cG250 2 cycles, ^{177}Lu-cG250 1 cycle, ^{177}Lu-cG250 2 cycles, Su 2 cycles, and control respectively.

Immunohistochemical analysis

Harvested tumors were snap-frozen and stored at -80°C and/or formalin-fixed and paraffin embedded. Four μm cryostat sections were cut and stored at -80°C until use. Haematoxylin-Eosin staining was performed for morphological analyses of the tumors.

Primary antibodies used were: mAb cG250 (Wilex, 10 μg/ml) and rabbit-anti-human mAb Ki67 (clone sp6/RM-9106-S, Thermo Scientific, 1:200,). All antibodies were diluted in 1% BSA in 50mM phosphate buffered saline, pH 7.4 unless mentioned otherwise.

For visualization of cell proliferation, paraffin sections were deparaffinized and rehydrated. Endogenous peroxidase was blocked with 3% H_2O_2 in PBS for 5 min. Slides were washed with PBS and antigen retrieval was performed in 0.1 M citrate buffer, pH 6.0 for 10 min. Subsequently sections were blocked with 20% normal swine serum and incubated for 1-2 hrs with primary antibody Ki67 diluted in 1% BSA/ PBS. After washing, sections were incubated with PO conjugated swine-anti-rabbit IgG (Dako), 1:100. Sections were developed with Bright DAB (Immunologic) and counterstained with haematoxylin. Microscopic evaluation was

performed on an Axioskop microscope (Zeiss) and images acquired on the Axiocam mrc5 (Zeiss) with Axio vs40 version 4.8 2.0 software (Axiovision, Zeiss).

Statistical analysis

A mixed model analysis was used to compare the tumor growth in the six treatment groups. For each treatment group the development in time was described with a fifth degree polynomial (fixed effects). The individual mice were allowed to follow their own curve (all six coefficients for the polynomial function in time were random). Using this model the geometric mean tumor volume at the end of sunitinib 1st cycle (Day 14), start of 2nd cycle (day 42 or 48), end of sunitinib 2nd cycle (day 55/62), evaluation of 2nd cycle (day 91/98) and end of experiment (day147/160) for NU12/SK-RC-52 respectively was compared between treatment groups for selected hypotheses. Correction for multiple comparisons was done per day using Holm's method (improved Bonferroni method) [25].

For survival analysis, p-values were calculated from the log rank or Gehan-Breslow-Wilcoxon test corrected for multiple comparisons.

Results

To study efficacy and duration of response of combination treatment, BALB/c nu/nu mice, xenografted with SK-RC-52 or NU12, were treated with 1 or 2 cycles of sunitinib and ^{177}Lu-cG250 RIT. To be able to evaluate the additive or synergistic effect of the combination the ^{177}Lu activity dose was reduced to one-third of the maximum tolerated dose that was previously described for SK-RC-52 [22].

Treatment of mice with SK-RC-52 tumors

Approximately 4 weeks after tumor cell inoculation, tumor volumes reached 80 mm^3 ± 35 mm^3 and treatment was started. In Fig. 2, the tumor growth curves of individual mice (A-F) as well as the average tumor volumes (G) of the SK-RC-52 tumors treated with different treatment regimens are shown. The median values of the tumor volumes are shown in table 1. In mice with established SK-RC-52 tumors, no significant delay of tumor growth was observed when they were treated with one cycle of sunitinib (Su) (p = 0.168; day 14 and p = 0.442; day 48) or 1 cycle of ^{177}Lu-G250 (p = 0.126; day 48). In contrast, 1 cycle of Su+[177]Lu-cG250 did result in a significant tumor growth delay (p < 0.001; day 48) which lasted even without retreatment (Fig 2A, G, Table 1, p = 0.024 at day 98).Two cycles of ^{177}Lu-cG250 resulted in a moderate, but not significant growth delay of SK-RC-52 tumors (p = 0.123; day 98). On the other hand, 2 sequential combination treatments resulted in almost complete tumor stasis (p<0.001). At day 160, when the experiment was finalized, mean tumor volume of mice treated with 1 or 2 cycles Su+[177]Lu-cG250 was substantially lower (135.7 mm^3 and 40.9 mm^3 respectively) than of mice treated with 1 or 2 cycles of Lu-cG250 (573.8 mm^3 and
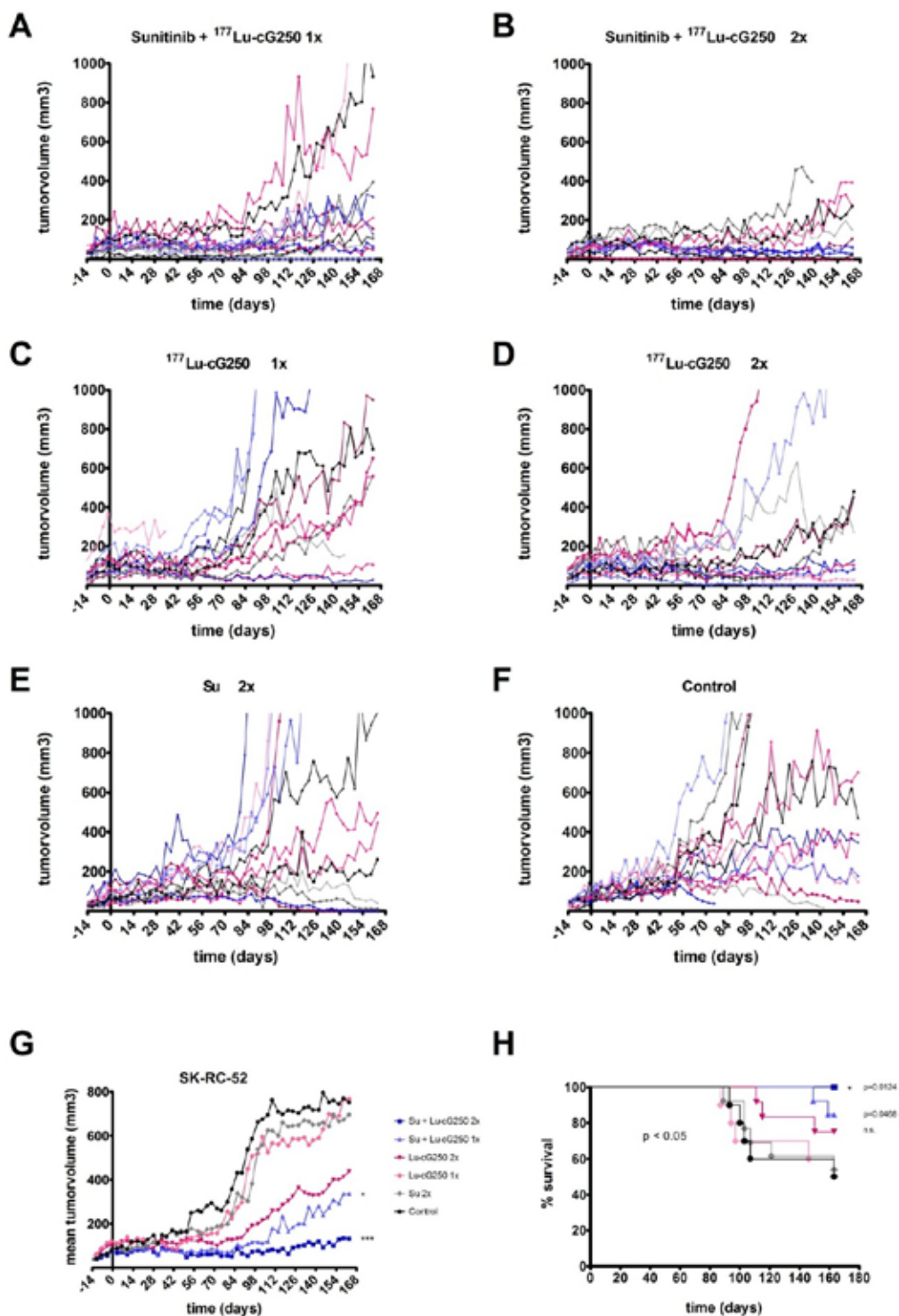
Figure 2. Tumor growth and survival of SK-RC-52 tumors during treatment with sunitinib and/or ^{177}Lu-cG250 RIT. Treatment with sunitinib was started when tumors reached a volume of 80 mm^3 ± 35 mm^3 (day 0) and continued until day 14. Three days later mice were injected with 6,5 MBq/10 µg ^{177}Lu-cG250 by intravenous injection (1st cycle, Su+Lu-cG250). Seven weeks (day 48) after start of the 1st cycle a 2nd cycle of treatment was administered (Su+Lu-cG250 2x). **A-F**: Growth curves of individual mice. **A**: Su+Lu-cG250 1 cycle, **B**: Su+Lu-cG250 2 cycles, **C**: Lu-cG250 1 cycle, **D**: Lu-cG250 2 cycles, **E**: Su 2 cycles, **F**: Control. **G**: Mean tumor volume of all treatment groups, * p < 0.05, *** p < 0.001. P-values shown are Holm's adjusted for the comparison of mean tumor volumes for comparisons of all treatment groups vs control group on day 98 (end of 2nd cycle) **H**: overall survival of treatment groups. Mice that were sacrificed because of other reasons than reaching maximal tumor burden, were excluded. Included number of mice was: 13, 10, 11, 12, 13 and 10 for Su+Lu-cG250 1 cycle, Su+Lu-cG250 2 cycles, Lu-cG250 1 cycle, Lu-cG250 2 cycles, Su 2 cycles, and Control respectively. Overall comparison of survival curves was significant with p<0.05. P-values shown for the Su+Lu-cG250 1x and 2x, and Lu-cG250 2x all vs Control were calculated from the log rank or Gehan-Breslow-Wilcoxon test corrected for multiple comparisons (p = 0.0124 for Su+Lu-cG250 2x vs Control, p = 0.0468 for Su+Lu-cG250 1x vs Control and p = 0.129 for Lu-cG250 2x vs Control).

Table 1

| | Day | | | | | | | | | | | | | | |
| | 14 | | | 48 | | | 62 | | | 98 | | | 160 | | |
	median	95% confidence interval		median	95% confidence interval		median	95% confidence interval		median	95% confidence interval		median	95% confidence interval	
Control	**101.6**	72.6	142.1	**163.5**	103.5	258.2	**200.8**	119.8	336.5	**323.2**	145.0	720.3	**310.8**	68.1	1417.7
Su 2x	**88.0**	62.9	123.2	**127.2**	80.5	200.9	**151.5**	90.4	253.8	**261.0**	117.4	580.3	**279.3**	63.4	1230.3
Lu-cG250 1x	**109.6**	78.3	153.4	**101.1**	63.9	159.9	**122.2**	72.6	205.8	**314.5**	138.4	714.4	**573.8**	123.2	2672.4
Lu-cG250 2x	**103.0**	73.6	144.2	**91.6**	58.0	144.6	**86.8**	51.8	145.4	**92.6**	41.6	205.8	**207.0**	48.7	880.1
Su + Lu-cG250 1x	**72.7**	52.0	101.8	**57.5**	36.4	90.8	**51.7**	30.9	86.6	**57.7**	26.0	128.3	**135.7**	33.2	554.5
Su + Lu-cG250 2x	**58.8**	42.0	82.2	**42.6**	27.0	67.3	**35.3**	21.0	59.1	**26.6**	11.9	59.6	**40.8**	9.4	178.1

SK-RC-52 tumor volumes by treatment group and follow up day with 95% confidence limits (uncorrected) A mixed model analysis was used for comparing the tumor growth between the six treatment groups. For each treatment group the development in time was described with a fifth degree polynomial (fixed effects). The individual mice were allowed to follow their own curve (all six coefficients for the polynomial function in time were random). Using this model the median tumor volume at days 14 (end 1st cycle of Su), 48 (start 2nd cycle), 62 (end 2nd cycle of Su), 98 (evaluation 2nd cycle) and 160 was compared between treatment groups for selected hypotheses. Correction for multiple comparisons was done per day using Holm's method (improved Bonferroni method).

207 mm^3 respectively). Moreover, 85% and 100% of the mice were alive when treated with 1 or 2 cycles of combination treatment, (Fig. 2H). When mice received 2 cycles of ^{177}Lu-G250 75% of mice survived. Treatment with either 1 cycle of Lu-cG250, 2 cycles of Su or no treatment resulted in 54-60% survival of mice. No vital tumor could be detected at the end of treatment as revealed by Haematoxylin/Eosin and KI67 staining in 7 animals: 2 mice treated with 2 cycles of Su+Lu-cG250, one mouse each treated with one cycle of Su+Lu-cG250 or 1 cycle of Lu-cG250 and 3 mice which were treated with 2 cycles of sunitinib. In all other mice, vital tumors were present.
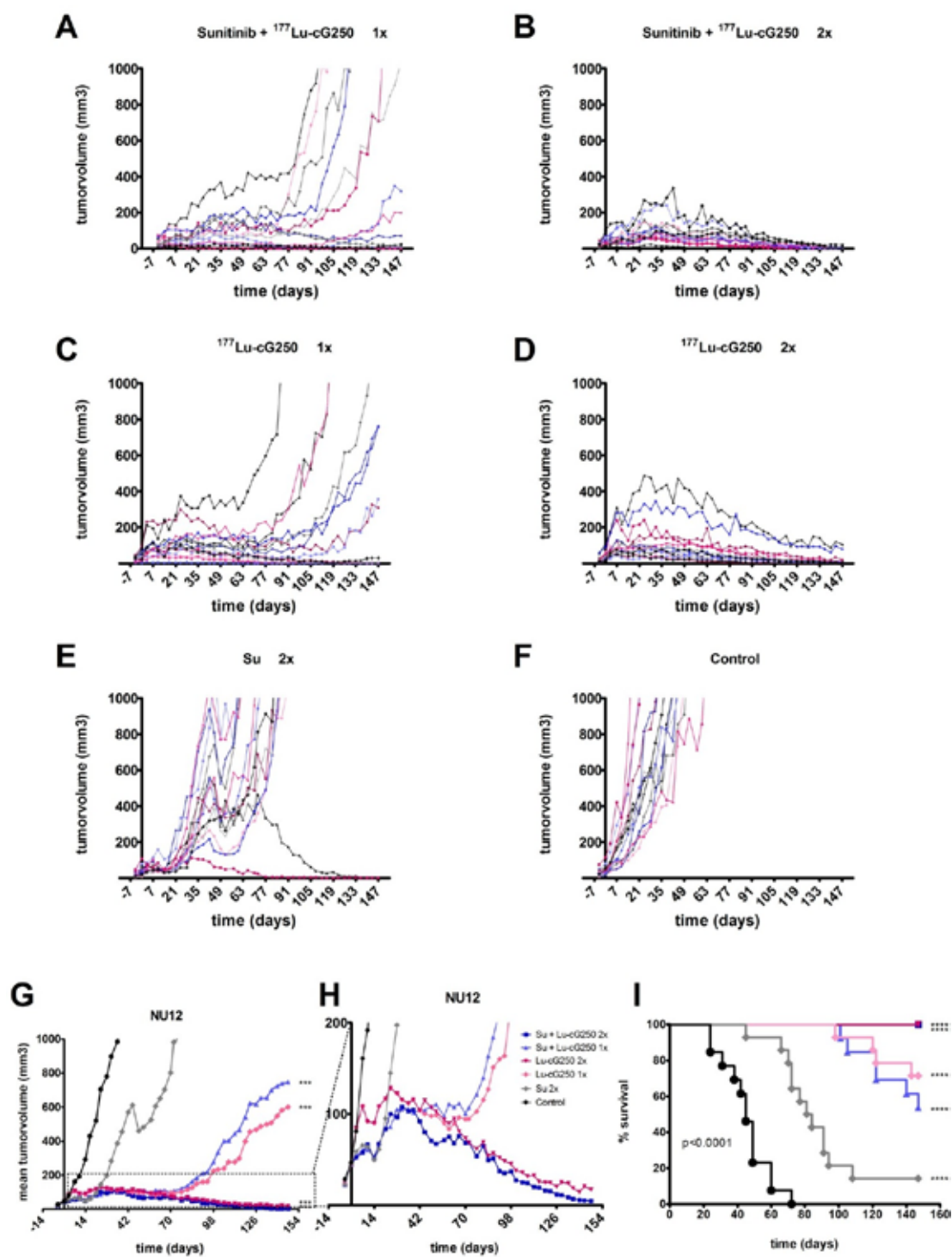
Combination therapy with ^{177}Lu-cG250 RIT and sunitinib in RCC

Figure 3. Tumor growth and survival of NU12 tumors during treatment with sunitinib and/or ^{177}Lu-cG250 RIT. Treatment with sunitinib was started when tumors reached a volume of 44 mm^3 ± 27 mm^3 (day 0) and continued until day 14. Three days later mice were injected with 6.5 MBq/10 μg ^{177}Lu-cG250 by intravenous injection (1st cycle, Su+Lu-cG250). Seven weeks (day 42) after start of the 1st cycle a 2nd cycle of treatment was started (Su+Lu-cG250 2x). **A-F**: Growth curves of individual mice. **A**: Su+Lu-cG250 1 cycle, **B**: Su+Lu-cG250 2 cycles, **C**: Lu-cG250 1 cycle, **D**: Lu-cG250 2 cycles, **E**: Su 2 cycles, **F**: Control. **G,H**: Mean tumor volume of all treatment groups. *** P< 0.001. P-values shown are Holm's adjusted for the comparison of mean tumor volumes for comparisons of all treatment groups vs control group on day 91 (end of 2nd cycle) **I**: overall survival of treatment groups. Mice that were sacrificed because of other reasons than reaching maximal tumor burden, were excluded. Included number of mice was: 13, 12, 14, 14, 14 and 14 for Su+Lu-cG250 1 cycle, Su+Lu-cG250 2 cycles, Lu-cG250 1 cycle, Lu-cG250 2 cycles, Su 2 cycles and Control respectively. Overall comparison of survival curves was significant with p<0.0001. P-values shown for all treatment groups vs Control were calculated from the log rank or Gehan-Breslow-Wilcoxon test corrected for multiple comparisons (**** p<0.0001).

Treatment of mice with NU12 tumors

Approximately 17 days after mice were grafted with fresh NU12 tumor pieces, tumor volumes reached 44 mm^3 ± 27 mm^3 and treatment was started. In Fig. 3, the tumor growth curves of individual mice (A-F) and the average tumor volumes (G, H) of the treatment groups with NU12 tumors treated with various treatment regimens are shown. In table 2, the median values of the tumor volumes are depicted.

Table 2

| | Day | | | | | | | | | | | | | | |
| | 14 | | | 42 | | | 55 | | | 91 | | | 147 | | |
	median	95% confidence interval		median	95% confidence interval		median	95% confidence interval		median	95% confidence interval		median	95% confidence interval	
Control	**261.3**	172.3	396.3	**1455.6**	800.8	2645.7	**2856.6**	1419.9	5746.8						
Su 2x	**63.6**	42.6	95.0	**351.9**	199.9	619.6	**489.4**	259.3	923.7	**1253.3**	463.6	3388.2	**4371.1**	323.3	59090.0
Lu-cG250 1x	**72.1**	48.4	107.6	**63.2**	35.9	111.2	**49.0**	26.0	92.5	**33.6**	13.0	87.2	**56.3**	9.9	319.1
Lu-cG250 2x	**88.5**	59.3	131.9	**79.8**	45.3	140.4	**61.9**	32.8	116.7	**24.9**	9.6	64.4	**3.1**	0.6	17.2
Su + Lu-cG250 1x	**46.0**	30.7	68.8	**55.1**	31.0	98.1	**51.0**	26.7	97.4	**47.9**	18.0	127.5	**233.5**	38.0	1436.9
Su + Lu-cG250 2x	**59.3**	39.8	88.5	**70.1**	39.8	123.3	**60.3**	32.0	113.8	**27.7**	10.6	72.7	**1.9**	0.3	11.2

NU12 tumor volumes by treatment group and follow up day with 95% confidence limits (uncorrected). A mixed model analysis was used for comparing the tumor growth between the six treatment groups. For each treatment group the development in time was described with a fifth degree polynomial (fixed effects). The individual mice were allowed to follow their own curve (all six coefficients for the polynomial function in time were random). Using this model the median tumor volume at days 14 (end 1st cycle of Su), 42 (start 2nd cycle), 55 (end 2nd cycle of Su), 91 (evaluation 2nd cycle) and 147 was compared between treatment groups for selected hypotheses. Correction for multiple comparisons was done per day using Holm's method (improved Bonferroni method).

A significant tumor growth delay was observed in mice treated with 1 or 2 cycles of either Su, ^{177}Lu-cG250 or Su+[177]Lu-cG250 (P<0.001; d14, and d48). Mean tumor volumes ranged from 44 to 88 mm^3 for the various treatment groups and were 261 mm^3 for the control group. Treatment with a 2nd cycle of sunitinib resulted in an additional tumor response (Fig. 3E, G), but tumor growth resumed immediately after cessation of sunitinib treatment. Growth of the

NU12 tumors in mice treated with one cycle of ^{177}Lu-cG250 or 1 cycle of Su+[177]Lu-cG250, resumed 9 to 10 weeks after cessation of therapy and tumors grew steadily thereafter (Fig. 3A, C, G, H). In contrast, when animals were treated with 2 cycles of ^{177}Lu-cG250 or 2 cycles of Su+[177]Lu-cG250 complete tumor regression was observed, which continued until the experiment was finalized, without additional treatment (p < 0.001; day 91).

At the end of the experiment (day 147), treatment with 2 cycles of Su+[177]Lu-cG250 or 2 cycles of ^{177}Lu-cG250 resulted in 100% survival (Fig. 3I). Seventy one percent of mice survived when treated with one cycle of ^{177}Lu-cG250. Treatment with one cycle of Su+[177]Lu-cG250 resulted in 54% survival. Only 14% of mice treated with 2 cycles of Su and none of the untreated mice survived.

To determine whether mice were cured or remnants of viable tumor cells were still present, harvested tumor areas were analyzed. Based on morphology by HE and cell proliferation evaluation, 83% and 86% of the mice treated with 2 cycles of Su+[177]Lu-cG250 or 2 cycles of ^{177}Lu-cG250 were cured: no viable tumor cells were detected. Although 71% of mice survived during the experimental period when treated with one cycle of ^{177}Lu-cG250, only 29% were cured with no evidence of disease. Fourteen percent and 8% of mice were cured when treated with 2 cycles of Su or one cycle of Su+[177]Lu-cG250 respectively. None of the control mice survived.

Discussion

To improve the treatment of patients with mRCC new approaches are urgently needed. We studied the combination of sunitinib with ^{177}Lu-cG250 RIT in nude mice with RCC to determine whether a combined attack on tumor vasculature and tumor cells might be beneficial. We show in two RCC models that when sunitinib is combined with ^{177}Lu-G250 RIT tumors can be ablated.

When ^{177}Lu-cG250 RIT was combined with sunitinib a pronounced effect on SK-RC-52 tumor growth was observed. One cycle of sunitinib combined with Lu-cG250 was sufficient to induce significant tumor growth inhibition, emphasizing that targeting blood vessels and tumor cells is more effective than targeting either compartment alone. This effect was superior compared to 2 cycles of sunitinib and to ^{177}Lu-cG250 RIT alone. Implementation of a second combination treatment cycle induced a long-lasting tumor response: PFS increased to ~150 days and OS increased to 100%. SK-RC-52 is considered sunitinib resistant and treatment with sunitinib leads to increased antibody accumulation in the tumors [14]. Consequently, tumor radiation doses are increased when sunitinib and ^{177}Lu-cG250 RIT are combined, explaining the superiority of the combination treatment in this model. Nevertheless, most animals were not tumor free, indicating that more treatment cycles are necessary to achieve complete cure.

In the fast growing NU12 tumor, a pronounced effect on tumor growth was observed when animals were treated with sunitinib leading to NU12 tumor regression, whereas SK-RC-52

tumors stabilized. NU12 is considered as a sunitinib sensitive tumor, with extensive necrosis after sunitinib treatment [14]. Although in vitro experiments showed a 5-fold higher sunitinib sensitivity for NU12 compared to SK-RC-52 (IC$_{50}$ 0.6 μM vs. 3 μM, data not shown), continued sunitinib treatment was necessary to induce a long-lasting response: drug withdrawal lead to rapid induction of tumor growth. One cycle of low dose ^{177}Lu-cG250 RIT was sufficient to increase PFS to ~65 days and OS increased to 71% compared to 14% for sunitinib treated animals. Remarkably, 2 cycles of low dose ^{177}Lu-G250 resulted in 100% survival and complete cures in 86% of mice: no viable tumor cells could be detected by microscopic analysis. Sunitinib combined with low dose ^{177}Lu-cG250 RIT and low dose ^{177}Lu-cG250 RIT alone were equally effective, indicating that the addition of sunitinib did not enhance the anti-tumor effect of the low-dose ^{177}Lu-cG250 RIT. Two cycles of Su+^{177}Lu-cG250 were equally effective (100% survival and 83% cures), suggesting that most probably the anti-tumor effect of the combination treatment was accountable to ^{177}Lu-cG250. Apparently, NU12 is both sunitinib and ^{177}Lu sensitive. In this "sensitive" model, the 6.5 MBq dose of ^{177}Lu most likely was too high to observe improved survival of the combination treatment.

Animals with a small tumor load responded better to ^{177}Lu-cG250 RIT than animals with higher tumor burden. It is well established that RIT performs better in small volume disease [26-28]. In previous studies three fold higher doses of ^{177}Lu (18.5 MBq (=MTD) vs. 6.5 MBq) were required to induce a tumor response in SK-RC-52 [22]. Since high dose RIT leads to bone marrow toxicity and can deplete the bone marrow reserve in (a subset of) patients, repeated high dose RIT is not feasible [29]. In the current study two cycles of low activity ^{177}Lu-cG250 RIT were insufficient to control tumor outgrowth although progression free survival increased to approximately 80 days and OS to 69%. However in combination with sunitinib tumors regressed. The recommended treatment for patients with mRCC currently exists of 50 mg of sunitinib per day for 4 weeks followed by 2 weeks off-treatment (Schedule 4/2). Combination with low dose ^{177}Lu-cG250 RIT may be relatively easy as bone marrow toxicity will be substantially reduced compared to high dose ^{177}Lu-cG250 RIT.

Several studies have confirmed the feasibility and enhanced efficacy of combination of antibody and TKI. Kelly et al. [30] observed that combination of ^{177}Lu-hu3S193 RIT with EGFR inhibitor AG1478 significantly improved efficacy in mice with prostate carcinoma. The enhanced effect with the EGFR inhibitor was attributed to the simultaneous targeting of tumor cells by two different drugs. In a recently performed meta analysis for the treatment of non-small cell lung cancer, the authors showed that chemotherapy or EGFR-TKIs with bevacizumab significantly prolonged PFS and OS as first-line treatment for NSCLC compared with chemotherapy or TKIs alone, indicating that combinations can be more efficacious [31]. In our study, combining antibody with TKI also lead to a substantial improvement of efficacy, but in our case two different cell types were targeted (tumor and endothelium). Whether this combination is superior to simultaneous targeting of tumor cells with different drugs remains to be established.

Although sunitinib alone showed little SK-RC-52 tumor growth inhibition, an additive effect was observed when combined with ^{177}Lu-cG250 RIT, possibly due to the enhanced uptake of G250 antibody [14]. Recently, Jedeszko et al. [32] investigated the combination of pazopanib and chemotherapy in an orthotopic RCC mouse model and claimed that pazopanib enhanced the intracellular uptake of a chemotherapeutic drug by a direct sensitization effect on tumor cells. It is possible that a similar effect applies to our studies and that sunitinib has a direct sensitization effect on SK-RC-52 tumor cells, leading to increased uptake of mAb G250. The enhanced uptake was not observed in NU-12 tumors, but this can be explained by different internalization rates of the two tumor cell types [18]. In SK-RC-52, cG250 internalization and subsequent metabolization plays a role whereas internalization is almost absent in NU-12.

There are several limitations to our study results. Whether this combination is superior in NU-12-like tumors is uncertain, because the activity dose we used was too effective to begin with. Additional therapeutic experiments with even lower doses of ^{177}Lu should be performed to confirm our hypothesis. We are currently investigating the optimal dose schedule for treatment of mRCC patients. Furthermore, future experiments are needed to elucidate the mechanism leading to enhanced uptake of antibody by treatment with sunitinib. Once we know the mechanism of action, it will be easier to design efficacious therapy strategies.

In conclusion, since for patients with mRCC the efficacy of targeted agents such as TKI is limited by both intrinsic and acquired resistance improvement is needed. Enhanced therapeutic efficacy can be reached when two agents that on their own do not induce satisfactory response levels in preclinical models resembling sunitinib and RIT sensitive tumors are combined. Our findings provide a promising new therapeutic strategy for patients with advanced RCC.

References

1. Motzer, R.J.; Hutson, T.E.; Tomczak, P.; Michaelson, M.D.; Bukowski, R.M.; Rixe, O.; Oudard, S.; Negrier, S.; Szczylik, C.; Kim, S.T*., et al.* Sunitinib versus interferon alfa in metastatic renal-cell carcinoma. *New Engl J Med* **2007**, *356*, 115-124.
2. Motzer, R.J.; Rini, B.I.; Bukowski, R.M.; Curti, B.D.; George, D.J.; Hudes, G.R.; Redman, B.G.; Margolin, K.A.; Merchan, J.R.; Wilding, G*., et al.* Sunitinib in patients with metastatic renal cell carcinoma. *Jama-J Am Med Assoc* **2006**, *295*, 2516-2524.
3. Ljungberg, B.; Bensalah, K.; Canfield, S.; Dabestani, S.; Hofmann, F.; Hora, M.; Kuczyk, M.A.; Lam, T.; Marconi, L.; Merseburger, A.S*., et al.* Eau guidelines on renal cell carcinoma: 2014 update. *Eur Urol* **2015**, *67*, 913-924.
4. Motzer, R.J.; Hutson, T.E.; Tomczak, P.; Michaelson, M.D.; Bukowski, R.M.; Oudard, S.; Negrier, S.; Szczylik, C.; Pili, R.; Bjarnason, G.A*., et al.* Overall survival and updated results for sunitinib compared with interferon alfa in patients with metastatic renal cell carcinoma. *J Clin Oncol* **2009**, *27*, 3584-3590.
5. Sternberg, C.N.; Davis, I.D.; Mardiak, J.; Szczylik, C.; Lee, E.; Wagstaff, J.; Barrios, C.H.; Salman, P.; Gladkov, O.A.; Kavina, A*., et al.* Pazopanib in locally advanced or metastatic renal cell carcinoma: Results of a randomized phase iii trial. *J Clin Oncol* **2010**, *28*, 1061-1068.
6. Bracarda, S.; Bellmunt, J.; Melichar, B.; Negrier, S.; Bajetta, E.; Ravaud, A.; Sneller, V.; Escudier, B. Overall survival in patients with metastatic renal cell carcinoma initially treated with bevacizumab plus interferon-alpha 2a and subsequent therapy with tyrosine kinase inhibitors: A retrospective analysis of the phase iii avoren trial. *Bju Int* **2011**, *107*, 214-219.
7. Motzer, R.J.; Hudes, G.; Wilding, G.; Schwartz, L.H.; Hariharan, S.; Kempin, S.; Fayyad, R.; Figlin, R.A. Phase i trial of sunitinib malate plus interferon-alpha for patients with metastatic renal cell carcinoma. *Clin Genitourin Canc* **2009**, *7*, 28-33.
8. Grunwald, V.; Desar, I.M.E.; Haanen, J.; Fiedler, W.; Mouritzen, U.; Olsen, M.W.B.; van Herpen, C.M.L. A phase i study of recombinant human interleukin-21 (ril-21) in combination with sunitinib in patients with metastatic renal cell carcinoma (rcc). *Acta Oncol* **2011**, *50*, 121-126.
9. Feldman, D.R.; Baum, M.S.; Ginsberg, M.S.; Hassoun, H.; Flombaum, C.D.; Velasco, S.; Fischer, P.; Ronnen, E.; Ishill, N.; Patil, S*., et al.* Phase i trial of bevacizumab plus escalated doses of sunitinib in patients with metastatic renal cell carcinoma. *J Clin Oncol* **2009**, *27*, 1432-1439.
10. Patel, P.H.; Senico, P.L.; Curiel, R.E.; Motzer, R.J. Phase i study combining treatment with temsirolimus and sunitinib malate in patients with advanced renal cell carcinoma. *Clin Genitourin Canc* **2009**, *7*, 24-27.
11. Molina, A.M.; Feldman, D.R.; Voss, M.H.; Ginsberg, M.S.; Baum, M.S.; Brocks, D.R.; Fischer, P.M.; Trinos, M.J.; Patil, S.; Motzer, R.J. Phase 1 trial of everolimus plus sunitinib in patients with metastatic renal cell carcinoma. *Cancer-Am Cancer Soc* **2012**, *118*, 1868-1876.
12. Sonpavde, G.; Choueiri, T.K.; Escudier, B.; Ficarra, V.; Hutson, T.E.; Mulders, P.F.; Patard, J.J.; Rini, B.I.; Staehler, M.; Sternberg, C.N*., et al.* Sequencing of agents for metastatic renal cell carcinoma: Can we customize therapy? *Eur Urol* **2012**, *61*, 307-316.
13. Motzer, R.J.; Escudier, B.; McDermott, D.F.; George, S.; Hammers, H.J.; Srinivas, S.; Tykodi, S.S.; Sosman, J.A.; Procopio, G.; Plimack, E.R*., et al.* Nivolumab versus everolimus in advanced renal-cell carcinoma. *New Engl J Med* **2015**, *373*, 1803-1813.
14. Oosterwijk-Wakka, J.C.; de Weijert, M.C.; Franssen, G.M.; Leenders, W.P.; van der Laak, J.A.; Boerman, O.C.; Mulders, P.F.; Oosterwijk, E. Successful combination of sunitinib and girentuximab in two renal cell carcinoma animal models: A rationale for combination treatment of patients with advanced rcc. *Neoplasia* **2015**, *17*, 215-224.
15. Stillebroer, A.B.; Boerman, O.C.; Desar, I.M.; Boers-Sonderen, M.J.; van Herpen, C.M.; Langenhuijsen, J.F.; Smith-Jones, P.M.; Oosterwijk, E.; Oyen, W.J.; Mulders, P.F. Phase 1 radioimmunotherapy study with lutetium 177-labeled anti-carbonic anhydrase ix monoclonal antibody girentuximab in patients with advanced renal cell carcinoma. *Eur Urol* **2013**, *64*, 478-485.
16. Ebert, T.; Bander, N.H.; Finstad, C.L.; Ramsawak, R.D.; Old, L.J. Establishment and characterization of human renal cancer and normal kidney cell lines. *Cancer research* **1990**, *50*, 5531-5536.
17. Beniers, A.J.; Peelen, W.P.; Schaafsma, H.E.; Beck, J.L.; Ramaekers, F.C.; Debruyne, F.M.; Schalken, J.A. Establishment and characterization of five new human renal tumor xenografts. *The American journal of pathology* **1992**, *140*, 483-495.

18. van Schaijk, F.G.; Oosterwijk, E.; Molkenboer-Kuenen, J.D.; Soede, A.C.; McBride, B.J.; Goldenberg, D.M.; Oyen, W.J.; Corstens, F.H.; Boerman, O.C. Pretargeting with bispecific anti-renal cell carcinoma x anti-dtpa(in) antibody in 3 rcc models. *J Nucl Med* **2005**, *46*, 495-501.

19. Steffens, M.G.; Boerman, O.C.; Oosterwijk-Wakka, J.C.; Oosterhof, G.O.; Witjes, J.A.; Koenders, E.B.; Oyen, W.J.; Buijs, W.C.; Debruyne, F.M.; Corstens, F.H*., et al.* Targeting of renal cell carcinoma with iodine-131-labeled chimeric monoclonal antibody g250. *Journal of clinical oncology : official journal of the American Society of Clinical Oncology* **1997**, *15*, 1529-1537.

20. Lewis, M.R.; Raubitschek, A.; Shively, J.E. A facile, water-soluble method for modification of proteins with dota. Use of elevated temperature and optimized ph to achieve high specific activity and high chelate stability in radiolabeled immunoconjugates. *Bioconjug Chem* **1994**, *5*, 565-576.

21. Muselaers, C.H.; Oosterwijk, E.; Bos, D.L.; Oyen, W.J.; Mulders, P.F.; Boerman, O.C. Optimizing lutetium 177-anti-carbonic anhydrase ix radioimmunotherapy in an intraperitoneal clear cell renal cell carcinoma xenograft model. *Mol Imaging* **2014**, *13*, 1-7.

22. Brouwers, A.H.; van Eerd, J.E.M.; Frielink, C.; Oosterwijk, E.; Oyen, W.J.G.; Corstens, F.H.M.; Boerman, O.C. Optimization of radioimmunotherapy of renal cell carcinoma: Labeling of monoclonal antibody cg250 with i-131, y-90, lu-177, or re-186. *J Nucl Med* **2004**, *45*, 327-337.

23. Lindmo, T.; Boven, E.; Cuttitta, F.; Fedorko, J.; Bunn, P.A., Jr. Determination of the immunoreactive fraction of radiolabeled monoclonal antibodies by linear extrapolation to binding at infinite antigen excess. *Journal of immunological methods* **1984**, *72*, 77-89.

24. *Guide for the care and use of laboratory animals: Eighth edition*. The National Academies Press: 2011.

25. Goeman, J.J.; Solari, A. Multiple hypothesis testing in genomics. *Statistics in medicine* **2014**, *33*, 1946-1978.

26. Brouwers, A.H.; Mulders, P.F.A.; de Mulder, P.H.M.; van den Broek, W.J.M.; Buijs, W.C.A.M.; Mala, C.; Joosten, F.B.M.; Oosterwijk, E.; Boerman, O.C.; Corstens, F.H.M*., et al.* Lack of efficacy of two consecutive treatments of radioimmunotherapy with i-131-cg250 in patients with metastasized clear cell renal cell carcinoma. *J Clin Oncol* **2005**, *23*, 6540-6548.

27. Bouchelouche, K.; Tagawa, S.T.; Goldsmith, S.J.; Turkbey, B.; Capala, J.; Choyke, P. Pet/ct imaging and radioimmunotherapy of prostate cancer. *Semin Nucl Med* **2011**, *41*, 29-44.

28. David, K.A.; Milowsky, M.I.; Kostakoglu, L.; Vallabhajosula, S.; Goldsmith, S.J.; Nanus, D.M.; Bander, N.H. Clinical utility of radiolabeled monoclonal antibodies in prostate cancer. *Clin Genitourin Canc* **2006**, *4*, 249-256.

29. Muselaers, C.H.J.; Boers-Sonderen, M.J.; van Oostenbrugge, T.J.; Boerman, O.C.; Desar, I.M.E.; Stillebroer, A.B.; Mulder, S.F.; van Herpen, C.M.L.; Langenhuijsen, J.F.; Oosterwijk, E*., et al.* Phase ii study of lutetium-177-labeled anti carbonic anhydrase ix monoclonal antibody girentuximab in patients with advanced renal cell carcinoma. *Eur J Nucl Med Mol I* **2015**, *42*, S170-S170.

30. Kelly, M.P.; Lee, S.T.; Lee, F.T.; Smyth, F.E.; Davis, I.D.; Brechbiel, M.W.; Scott, A.M. Therapeutic efficacy of lu-177-chx-a "-dtpa-hu3s193 radioimmunotherapy in prostate cancer is enhanced by egfr inhibition or docetaxel chemotherapy. *Prostate* **2009**, *69*, 92-104.

31. Sun, L.; Ma, J.T.; Zhang, S.L.; Zou, H.W.; Han, C.B. Efficacy and safety of chemotherapy or tyrosine kinase inhibitors combined with bevacizumab versus chemotherapy or tyrosine kinase inhibitors alone in the treatment of non-small cell lung cancer: A systematic review and meta-analysis. *Med Oncol* **2015**, *32*, 473.

32. Jedeszko, C.; Paez-Ribes, M.; Di Desidero, T.; Man, S.; Lee, C.R.; Xu, P.; Bjarnason, G.A.; Bocci, G.; Kerbel, R.S. Postsurgical adjuvant or metastatic renal cell carcinoma therapy models reveal potent antitumor activity of metronomic oral topotecan with pazopanib. *Science translational medicine* **2015**, *7*, 282ra250.

Summary

Summary

The aim of this thesis was to investigate new therapeutic strategies with chimeric monoclonal antibody G250 (cG250/Girentuximab) in preclinical models for patients with advanced RCC.

Chimeric G250 recognizes a conformational epitope on carbonic anhydrase IX (CAIX), a transmembrane protein which is expressed at high levels in clear cell renal cell carcinoma (ccRCC).

Chapter 2 reviews preclinical and clinical studies with mAb G250 since the original description in 1986. Preclinical studies indicated excellent targeting in RCC xenografts and clinical studies confirmed the outstanding targeting ability of mAb G250. cG250-based immunoPET imaging holds great promise for the future as diagnostic modality in detecting localized and advanced disease and possibly in monitoring therapy response.

Despite the outstanding accumulation levels of cG250, radioimmunotherapy (RIT) trials have been somewhat disappointing. Responses in progressive mRCC patients were limited to stabilization of disease and cures were not observed. 177-Lutetium labeled cG250 RIT might be of use for treatment of patients with small-volume disease.

Clinical therapy studies showed that multiple doses of unmodified cG250 were well tolerated and combination with low dose IL-2 resulted in disease stabilization, indicating that the antibody could lyse tumor cells by antibody-dependent cellular cytotoxicity (ADCC). The results of a large adjuvant trial indicate that cG250 alone may be of value to reduce recurrence of disease in high risk patients with high CAIX expression. Confirmatory studies are needed to substantiate the value of the antibody.

Prior studies showed that the therapeutic efficacy of tumor specific antibodies could be enhanced by gene fusion to tumor necrosis factor (TNF). In **Chapter 3**, the construction, expression and purification of a cG250-TNF fusion protein is described. In this way cG250 is used as a carrier for site specific delivery of TNF to human RCC xenografts. Genetically engineered TNF constructs were designed as CH2/CH3 truncated cG250-TNF fusion proteins and eukaryotic expression was optimized. The cG250-TNF construct was characterized in-vitro by biochemical analysis and bioactivity assays. Specific accumulation and retention of cG250-TNF in the tumor was observed, resulting in growth control of established human RCC xenografts in vivo. In addition, combined administration of cG250-TNF and IFNγ significantly increased the antitumor response resulting in improved progression free survival and overall survival. Moreover, since TNF subunits were forced to form a dimer, toxicity was significantly lower than observed with wild type TNF or trimeric TNF antibody constructs. Considering the poor outcome of patients with advanced RCC, cG250-TNF-based immunotherapeutic approaches justify clinical investigation.

With the development and approval of targeted agents such as sunitinib, sorafenib, bevacizumab and pazopanib, the therapeutic landscape has changed dramatically for patients with mRCC. These agents are aimed at inhibition of the tumor vasculature. Although an impressive increase in progression-free survival is observed for patients with mRCC, patients remain largely incurable, due to the development of treatment resistance. Additionally, these chronic treatments may coincide with significant toxicity which increases to unacceptable levels when combination treatment is applied. Sequential therapy may be more promising but the most optimal sequence therapy has not been established.

The combination of a tyrosine kinase inhibitor (TKI) with mAb cG250, involved in a distinct effector mechanism, might lead to improved tumor responses and survival in patients with mRCC. In **Chapter 4** the combination of TKI with mAb cG250 was investigated. The effect of sunitinib, sorafenib and vandetanib treatment on the accumulation of cG250 was studied in nude mice with human RCC xenografts . Mice were treated with TKI for 1-2 weeks followed by injection with radiolabeled cG250. While on TKI treatment, tumor uptake of cG250 decreased dramatically, tumor growth was slightly inhibited and vascular density decreased considerably as judged by various markers. When treatment was stopped there was robust neovascularization, mainly at the tumor periphery. Consequently, cG250 uptake recovered, albeit that cG250 uptake appeared to be restricted to the tumor periphery where vigorous neovascularization was visible. These results indicate that simultaneous administration of a TKI and cG250-RIT is unfavorable. Thus, a time-delay between the two modalities is required when designing combined treatment strategies with TKI and mAb G250.

In **Chapter 5** the effect of sunitinib on the biodistribution of cG250 when administered with a short time delay after sunitinib treatment was studied. Mice were injected with ^{111}In-cG250 either 3 days before initiation or 3 days after cessation of sunitinib treatment to assess the optimal sequence in RCC xenografts. Differences in response to sunitinib were observed in the two xenograft models used. One model represented a sunitinib-sensitive tumor; sunitinib treatment resulted in extensive necrosis and decreased microvessel density (MVD). Accumulation of cG250 was significantly decreased when sunitinib treatment preceded the antibody injection but remained unchanged when sunitinib followed cG250 injection. Cessation of therapy led to a rapid neovascularization, reminiscent of a tumor flare. The other RCC xenograft model studied represented a sunitinib-resistant tumor: (central) tumor necrosis was minimal and MVD was not affected. Sunitinib treatment resulted in increased cG250 uptake, regardless of the sequence of treatment. Thus, regardless of TKI sensitivity, TKI and mAbs can be combined, provided a short drug holiday is introduced. Since these two treatment modalities have different modes of action, the combination of sunitinib and cG250-RIT could lead to enhanced therapeutic efficacy.

In **chapter 6** the combination of sunitinib treatment with [177]Lutetium-cG250 RIT (at 1/3 of previously used doses) was studied in mice with established human RCC xenografts. In the

fast growing sunitinib-sensitive RCC xenograft, the effect of 2 cycles of ^{177}Lu-cG250 was comparable to 2 cycles of sunitinib + ^{177}Lu-cG250, indicating that the anti-tumor effect was achieved by the radiolabel. Apparently this tumor is both sunitinib and 177-Lutetium sensitive. In this sunitinib-sensitive model the 177-Lutetium dose was probably too high to observe a difference between these two therapy regimens, indicating that in patients with small tumorload and/or in patients with sunitinib-sensitive tumors, the addition of ^{177}Lu-cG250 to sunitinib might not improve response. In contrast, in the sunitinib-resistant model, superior tumorgrowth inhibition was achieved when sunitinib and ^{177}Lu-cG250 were combined, substantiating the hypothesis that targeting both bloodvessels and tumorcells is more effective than either treatment alone. Collectively this indicates that the combination of these two therapeutic entities can be beneficial in a patient setting. However, whether cG250-based RIT can be combined with TKI in patients, which constitutes the current standard treatment for mRCC, needs to be established in large randomized clinical trials.

Chapter 7

Samenvatting

Samenvatting

Het doel van dit proefschrift was het testen van nieuwe therapeutische strategieën met monoklonaal antilichaam chimeer G250 (cG250/Girentuximab) in preklinische modellen voor patiënten met uitgezaaid niercelcarcinoom. Chimeer G250 herkent een epitoop op carbonic anhydrase IX (CAIX), een transmembraan eiwit dat hoog tot expressie komt in heldercellige niercelcarcinomen (ccRCC).

Hoofdstuk 2 geeft een overzicht van preklinische en klinische studies uitgevoerd met monoklonaal antilichaam G250 (mAbG250) vanaf de isolatie van het antilichaam in 1986 tot heden. Preklinische studies hebben aangetoond dat mAbG250 zeer goed accumuleert in humane niercelcarcinomen en met klinische studies is de uitzonderlijk goede accumulatie van mAbG250 in ccRCC bewezen. Klinische studies hebben laten zien dat positon emissie tomografie met cG250 (cG250-immunoPET) veelbelovend is voor de detectie van gelokaliseerde en gemetastaseerde ziekte en voor het meten van het therapie effect. Ondanks de superieure accumulatie van cG250 vallen de uitkomsten van de radioimmuuntherapie (RIT) studies enigszins tegen. In patiënten met progressieve ziekte werd vooral stabilisatie van ziekte maar geen genezing waargenomen. RIT met ^{177}Lu-cG250 is waarschijnlijk het meest effectief in patiënten met minimale ziekte.

Klinische therapie studies hebben aangetoond dat meerdere doses van ongemodificeerd cG250 goed verdragen worden. In combinatie met lage doses Interleukine-2 kan dit leiden tot stabilisatie van ziekte; wat doet vermoeden dat het antilichaam de tumorcellen kan vernietigen d.m.v. "antilichaam-afhankelijke cellulaire cytotoxicity" (ADCC). De adjuvante studies met ongemodificeerde cG250 suggereren dat monotherapie met cG250 van waarde kan zijn om terugkeer van ziekte in patiënten met hoge CAIX expressie te verminderen. Klinische studies met grote patiëntencohorten moeten deze resultaten bevestigen.

Eerdere studies hebben aangetoond dat de therapeutische werkzaamheid van tumor specifieke antilichamen vergroot kan worden door genfusie met tumor necrose factor (TNF). In **Hoofdstuk 3** wordt de constructie, expressie en zuivering van het cG250-TNF fusie eiwit beschreven. Hiermee wordt de specificiteit van cG250 gebruikt om TNF specifiek naar humane niertumoren te leiden. Het cG250-TNF fusie eiwit werd geconstrueerd door de CH2-CH3 staart van het parentale cG250 antilichaam te vervangen door twee humane TNF moleculen. Vervolgens werd de eukaryotische expressie geoptimaliseerd, zijn biochemische analyses uitgevoerd en is de bioactiviteit van het fusie eiwit gemeten. In *vivo* werd specifieke accumulatie van cG250-TNF in de tumor en groeiremming van humane niercelcarcinomen waargenomen. Toediening van cG250-TNF met Interferon-γ leidde tot een verhoogde antitumor response met een verbetering van zowel progressievrije overleving als algehele overleving. Bovendien was de toxiciteit van het cG250-TNF significant verlaagd t.o.v. het wild type TNF of trimeer TNF antilichaam constructen, waarschijnlijk omdat de TNF subeenheden

geforceerd worden tot dimerisatie. Gezien de slechte vooruitzichten voor patiënten met mRCC lijkt het zinvol om nader klinisch onderzoek te doen naar immunotherapeutische toepassingen die op cG250-TNF gebaseerd zijn.

Voor patiënten met mRCC is het therapeutisch landschap aanzienlijk gewijzigd door de ontwikkeling en goedkeuring van doelgerichte middelen zoals sunitinib, sorafenib, bevacizumab and pazopanib. Deze middelen remmen het ontstaan van nieuwe bloedvaten in de tumoren. Hoewel er een grote toename van de progressievrije overleving van patiënten met mRCC is waargenomen, treedt geen genezing op doordat tumoren op den duur ongevoelig worden voor deze middelen. Deze chronische behandelingen gaan bovendien vaak gepaard met bijwerkingen die zeer ernstig kunnen zijn wanneer deze behandelingen gecombineerd worden. Sequentiële therapie zou beter kunnen werken maar tot op heden is de meest optimale therapie niet vastgesteld.

De combinatie van een doelgericht middel, zoals een tyrosine kinase remmer (TKI), met antilichaam cG250, zou in patiënten met mRCC tot verbeterde tumor responses en overleving kunnen leiden omdat ze gericht zijn tegen verschillende tumorcomponenten. In **Hoofdstuk 4** is de combinatie van TKIs met cG250 onderzocht. Het effect van sunitinib, sorafenib en vandetanib behandeling op de accumulatie van cG250 werd bestudeerd in immuundeficiënte muizen met humane niercelcarcinomen. Muizen werden 1-2 weken behandeld met TKI waarna ze geïnjecteerd werden met radioactief gelabeld cG250. Analyse toonde aan dat door behandeling met TKI de accumulatie van cG250 in de tumor drastisch afnam, de tumorgroei enigszins verminderde en de bloedvat dichtheid substantieel verminderde. Op het moment dat behandeling gestopt werd werden veel nieuwe bloedvaten gevormd, voornamelijk aan de rand van de tumor. Als gevolg daarvan nam de cG250 opname vooral in de tumor rand toe, daar waar vorming van nieuwe bloedvaten zichtbaar was. Uit deze resultaten blijkt dat gelijktijdige toediening van een TKI en cG250-RIT ongunstig is. Wanneer behandeld wordt met een combinatie van TKI en cG250, dan is een tijdsinterval tussen toediening van de twee modaliteiten noodzakelijk.

In **Hoofdstuk 5 is** het effect van sunitinib op de biodistributie van cG250 bestudeerd. Na behandeling met sunitinib werd een korte pauze ingelast waarna cG250 toegediend werd. Muizen werden 3 dagen voor het begin of 3 dagen na het einde van de sunitinib behandeling met ^{111}In-cG250 geïnjecteerd om de optimale volgorde te bepalen in twee humane niercelcarcinomen. In de twee gebruikte tumor modellen werden verschillen gevonden in de response op sunitinib behandeling. Eén tumor was sunitinib-gevoelig: Sunitinib behandeling leidde tot uitgebreide necrose en verminderde microvasculaire dichtheid (MVD). Accumulatie van cG250 was significant verlaagd wanneer sunitinib behandeling vóór de antilichaam injectie plaatsvond maar bleef ongewijzigd wanneer sunitinib na de cG250 injectie gegeven werd. Het beëindigen van de therapie leidde tot snelle bloedvatvorming, waardoor een explosieve tumorgroei plaatsvond. De andere tumor was sunitinib-resistent; (centrale) tumor necrose was minimaal en MVD veranderde niet. Sunitinib behandeling resulteerde in

verhoogde opname van cG250, ongeacht de volgorde van behandeling. Dit betekent dat ongeacht gevoeligheid voor TKI, antilichamen en TKI gecombineerd kunnen worden als een korte pauze wordt ingevoerd. Omdat deze twee middelen verschillende werkingsmechanismen hebben, kan de combinatie van sunitinib met cG250-RIT potentieel tot verbeterde therapeutische effecten leiden.

In **hoofdstuk 6** is de combinatie van sunitinib behandeling met [177]Lutetium-cG250 RIT (op 1/3 van de vroegere effectieve dosis) onderzocht in muizen met humane niercelcarcinomen. In de snel groeiende sunitinib-gevoelige tumor was het effect van 2 cycli ^{177}Lu-cG250 vergelijkbaar met die van 2 cycli sunitinib + ^{177}Lu-cG250; d.w.z. het anti-tumor effect was waarschijnlijk het gevolg van het radioactieve label (^{177}Lu-cG250). Klaarblijkelijk is deze tumor zowel sunitinib als 177-Lutetium gevoelig. In dit model was de 177-Lutetium dosis waarschijnlijk te hoog om een verschil tussen deze twee behandelingsmethoden te zien. Dat betekent dat in patiënten met een kleine tumormassa en/of in patiënten met sunitinib-gevoelige tumoren de toevoeging van ^{177}Lu-cG250 misschien niet tot een verbeterde response zal leiden. Daarentegen werd in de sunitinib-resistente tumor superieure tumorgroei inhibitie bereikt wanneer sunitinib met ^{177}Lu-cG250 gecombineerd werd. Hiermee wordt aangetoond dat behandeling met middelen die zowel de bloedvaten als de tumorcellen aanvallen effectiever is dan behandeling met elk middel afzonderlijk. Gezamenlijk betekent dit dat de combinatie van deze twee therapeutische middelen gunstig kan zijn voor patiënten met mRCC. Echter, of op cG250-gebaseerde RIT gecombineerd kan worden met de huidige standaard TKI behandeling van patiënten zal moeten worden onderzocht in grote gerandomiseerde klinische studies.

Chapter 8

Future prospects

Future prospects

Although significant progress has been made in the management of patients with advanced RCC, the treatment remains problematic: TKI treatment is mainly palliative and whether treatment with checkpoint inhibitors will lead to durable responses in the majority of patients is unclear. Whereas TKIs act predominantly on the tumor vasculature, checkpoint inhibitors unleash the immune system in a generalized fashion. While the inhibition of tumor-specific immune cells is released, auto-reactive T cells are also activated, leading to graft-versus-host like toxicities. Up to now, clinical investigations combining various targeted agents are disappointing because of enhanced toxicity and lack of improved efficacy. New therapeutic strategies specifically targeting the tumor cells might be highly beneficial for the treatment of advanced RCC. As described in this thesis, mAb cG250 and its target CAIX appear to be ideally suited to reach this goal. Earlier studies showed that advanced RCC patients could benefit from cG250 treatment in various regimens. Nevertheless, further improvements are needed to truly impact on the disease course of mRCC patients.

G250-TNF

Treatment of mice with CAIX$^+$ human renal cell carcinoma xenografts with the fusion protein cG250-TNF, combining the targeting ability of cG250 with the cytolytic capacity of TNF, demonstrated impressive therapeutic efficacy. Therapy with cG250-TNF resulted in significant remission of established xenografts which was further improved by addition of low doses of IFNγ without significant increase in side effects. The encouraging targeting and strong anti-tumor properties of cG250-TNF (in combination with IFNγ) and the strong and stable expression pattern of CAIX/G250 in sporadic and inherited forms of RCC warrant further evaluation of this construct in a clinical setting.

Combination of targeted therapy with checkpoint inhibitors

The understanding of the mechanisms of T-cell activation and inhibition has led to the development of therapeutic antibodies targeting immune checkpoint pathways causing reduction of tumor growth and proliferation [1-3]. Clinical trials with CTLA-4 (ipilimumab), and PD-1/PD-L1 inhibitors (i.e. nivolumab and pembrolizumab) have shown clinical benefit in a subset of cancer patients with less toxicity than observed in previous immunotherapy with IL-2 and/or IFNα [4,5]. The clinical activity of these drugs in melanoma, RCC and NSCLC has been confirmed [6-8]. Nivolumab is now approved as second-line therapy for patients with mRCC on the basis of a better overall survival (OS) and lower toxicity compared to everolimus [9]. New immune checkpoint inhibitors are in the developmental phase.

This field is rapidly expanding with several clinical trials ongoing, in different stages. With checkpoint inhibitors durable clinical responses can be elicited. However, the majority of patients treated with anti-PD-1/PD-L1 monotherapies do not achieve objective responses, and most tumor regressions are partial rather than complete. Moreover toxicities can be

severe and managing of these toxicities is challenging. Especially with anti-CTLA-4 blockade, care should be taken since this can lead to life threatening toxicities and death.

Currently, multiple clinical studies combining checkpoint inhibition with targeted therapy are either planned or ongoing to improve response rates in patients with mRCC [1]. These include combinations of bevacizumab with nivolumab, atezolizumab or prembrolizumab, combinations of axitinib with avelumab or prembrolizumab, and combinations of cabozantinib with nivolumab or nivolumab and ipilimumab. The rationale of these combinations is that different pathways are targeted, possibly leading to improved responses. This was illustrated in the trial where nivolumab was combined with ipilimumab (N3I1 regimen) with an objective response rate of 48% [10]. The outcome of the phase III trial comparing 1st line sunitinib vs. N3I1 regimen will be of importance to demonstrate superiority of these new treatment modalities compared to current standard treatment.

In designing these combinations one should consider dose regiments (concurrent or sequential), minimize treatment related toxicities and select appropriate end points to assess efficacy. Interestingly, targeted agents can upregulate tumor antigen presentation, T-cell infiltration and PD-1/PD-L1 expression, possibly priming a response to checkpoint inhibitors. Concurrent therapy may be most beneficial. However concurrent therapy can also induce greater and unexpected toxicities compared to sequential therapy [11]. Sequential treatment of targeted therapy followed by immunotherapy before disease progression might be a viable alternative. The challenge of the upcoming clinical trials is to establish optimal timing [1]. Finally, response definitions should be considered: In a subset of patients treated with checkpoint inhibitors 'pseudoprogression', a lag in response and initial increase in lesion size, was observed. Current response criteria such as Response Evaluation Criteria in Solid Tumors (RECIST) may not reflect efficacy of checkpoint inhibition therapy and response criteria may have to be modified to evaluate efficacy of checkpoint inhibitors [12,13].

Combination of cG250 based RIT with sunitinib

The results described in this thesis suggest that combination of tyrosine kinase inhibitors with cG250 based RIT holds great promise for the future of patients with advanced RCC. Our animal studies indicate that by targeting both endothelial cells and tumor cells improved responses are achievable. Theoretically, the addition of cG250-RIT to the current sunitinib treatment schedule (4 weeks on/2 weeks off drug) appears to be feasible. Patients could receive the ^{177}Lu-cG250 RIT during the second week off sunitinib .The observation that lower ^{177}Lu activity doses were effective suggests that bone marrow toxicity, the main toxicity of RIT, i.e. thrombocytopenia, can be largely prevented while keeping the efficacy at satisfying levels. However, even at low ^{177}Lu-cG250 RIT doses (1/3 of MTD), low grade hematological toxicity was observed with a nadir at 6 weeks post injection [14]. Full recovery was observed 12 weeks p.i. suggesting that when sunitinib is combined with ^{177}Lu-cG250 RIT, the sunitinib-free period should be prolonged. Whether patients with a sunitinib sensitive tumor will benefit from this combination needs to be established. Moreover, sunitinib-sensitive and sunitinib-resistant patients may need to be stratified.

Combination of cG250 based RIT with checkpoint inhibitors

As mentioned above, although encouraging results have been reported from clinical trials exploring combinations of PD-1 and PD-L1 inhibitors with radiation therapy, sunitinib or pazopanib, toxicity can be severe [15]. Combination of ^{177}Lu-cG250 with checkpoint inhibitors may be another possibility: the initiation of specific tumor cell kill followed by T cell influx in combination with a checkpoint inhibitor may license the activation and expansion of tumor-specific T cells in a more specific fashion that the combination TKI-checkpoint inhibitors. Since the MTD of ^{177}Lu-cG250 has been well established, clinical investigations along these lines may be attractive.

The severe toxicities observed with checkpoint immunotherapy combined with targeted therapy or other checkpoint immunotherapies may be reduced when checkpoint inhibition is combined with ^{177}Lu-cG250 RIT. Although ^{177}Lu-cG250 treatment can lead to grade 3-4 myelotoxicity, in general the myelotoxicity has been transient. Also toxicity can be tailored to individual patients based on dosimetric analysis of the data acquired during the pretreatment imaging. This is likely to improve ^{177}Lu-cG250 RIT [16,17]. Since ^{177}Lu-cG250 RIT has a different mechanism of action than mAbs targeting immune checkpoints the combination might increase efficacy in patients with mRCC. Animal studies are needed to demonstrate if these treatment combinations show synergistic or additive effects. Careful development and rational design is necessary to determine the timing and sequencing of these agents.

Combination of cG250 based RIT with clinical grade active NK-cells

Clinical studies with unmodified cG250 with or without low dose IL-2 suggested that Natural killer (NK) cell-mediated cG250-dependent cellular-cytotoxicity (ADCC) was the mechanism that influenced the clinical course of mRCC patients. In progressive RCC patients stabilization of disease (SD) was observed when cG250 was administered. Similarly, when cG250 was combined with low-dose IL-2 a clinical benefit was noted. Collectively, results of the clinical trials with unmodified cG250, either as monotherapy or in combination with low dose IL-2, suggest that cG250 treatment can alter disease progression.

NK cells are major effector cells of the innate immune system and play a key role in control against virus infection and tumor immunosurveillance. Recent advances in the isolation and expansion of pure, clinically applicable NK cells derived from umbilical cord blood-derived hematopoietic progenitor cells (HPC-NK) have paved the way to combine antibodies with these cells [18,19]. Indeed, functional analysis demonstrated that these active NK cells generate natural cytolysis and ADCC-dependent killing of cancer cells [20,21]. Preliminary experiments showed that HPC-NK cells generated from several donors showed high and dose dependent cytolytic activity for all RCC cell lines tested with >90% cell kill at Effector to Target ratio of 3:1. Addition of mAb cG250 enhanced cytotoxicity in CAIX^{+} cells but not in CAIX^{-} cells. Reactivity toward target cells was confirmed by elevated levels of granzyme B (~30%) and IFNγ secretion produced by NK cells (unpublished results). Combining the specific targeting of cG250 with adoptive transfer of highly activated NK cells

may become an effective therapy approach for patients with metastasized RCC or at high risk of recurrence.

Thus, several options are available to improve therapy for patients with advanced RCC. The main challenge will be to select patients for a particular treatment: Personalized medicine. Currently, mRCC patients are stratified into different risk groups based on clinical parameters. This stratification has a clear prognostic value but is still far from optimal. Comparison of several risk models showed a concordance level of 0.66, indicating that a ceiling has been reached for clinical risk models to predict prognosis based solely on clinical factors [22,23]. Other and better prognostic and predictive biomarkers are needed to improve patient stratification and to abandon the current trial and error type of patient management. Current research is focusing on molecular biomarkers with better predictive ability. In a large FP7 funded program (EuroTARGET) data from several high throughput platforms are going to be integrated in an effort to identify and characterize biomarkers to predict responders from non-responders to targeted therapy with the ultimate goal to personalize medicine. Such biomarkers are pivotal because not all patients show clinical benefit from targeted therapy and since an increasing number of compounds and therapeutic options is becoming available, the choice of therapy and sequencing or combination is becoming extraordinary challenging. Continued effort is needed at the level of new therapies and biomarkers to personalize medicine for patients with mRCC to improve responses substantially in still a devastating disease.

In the last decade major steps have been taken in the management of patients with mRCC. A large number of agents have been developed based on the improved molecular insight in this disease and several are now used as first or second line treatment. Clinical responses have improved dramatically in a subset of patients. However, up to now, monotherapy has not resulted in durable clinical responses in the majority of patients. Combination of agents targeting different pathways of the tumor is expected to ultimately lead to durable responses. The most challenging will be to select the right patient for the right combination to achieve personalized treatment.

References

1. Hughes, P.E.; Caenepeel, S.; Wu, L.C. Targeted therapy and checkpoint immunotherapy combinations for the treatment of cancer. *Trends in immunology* **2016**, *37*, 462-476.
2. Callahan, M.K.; Postow, M.A.; Wolchok, J.D. Targeting t cell co-receptors for cancer therapy. *Immunity* **2016**, *44*, 1069-1078.
3. Nurieva, R.I.; Liu, X.K.; Dong, C. Yin-yang of costimulation: Crucial controls of immune tolerance and function. *Immunol Rev* **2009**, *229*, 88-100.
4. Topalian, S.L.; Hodi, F.S.; Brahmer, J.R.; Gettinger, S.N.; Smith, D.C.; McDermott, D.F.; Powderly, J.D.; Carvajal, R.D.; Sosman, J.A.; Atkins, M.B., *et al.* Safety, activity, and immune correlates of anti-pd-1 antibody in cancer. *New Engl J Med* **2012**, *366*, 2443-2454.
5. Topalian, S.L.; Drake, C.G.; Pardoll, D.M. Immune checkpoint blockade: A common denominator approach to cancer therapy. *Cancer Cell* **2015**, *27*, 450-461.
6. Brahmer, J.R.; Tykodi, S.S.; Chow, L.Q.M.; Hwu, W.J.; Topalian, S.L.; Hwu, P.; Drake, C.G.; Camacho, L.H.; Kauh, J.; Odunsi, K., *et al.* Safety and activity of anti-pd-l1 antibody in patients with advanced cancer. *New Engl J Med* **2012**, *366*, 2455-2465.
7. Herbst, R.S.; Soria, J.C.; Kowanetz, M.; Fine, G.D.; Hamid, O.; Gordon, M.S.; Sosman, J.A.; McDermott, D.F.; Powderly, J.D.; Gettinger, S.N., *et al.* Predictive correlates of response to the anti-pd-l1 antibody mpdl3280a in cancer patients. *Nature* **2014**, *515*, 563-565.
8. Motzer, R.J.; Rini, B.I.; McDermott, D.F.; Redman, B.G.; Kuzel, T.M.; Harrison, M.R.; Vaishampayan, U.N.; Drabkin, H.A.; George, S.; Logan, T.F., *et al.* Nivolumab for metastatic renal cell carcinoma: Results of a randomized phase ii trial. *J Clin Oncol* **2015**, *33*, 1430-1437.
9. Motzer, R.J.; Escudier, B.; McDermott, D.F.; George, S.; Hammers, H.J.; Srinivas, S.; Tykodi, S.S.; Sosman, J.A.; Procopio, G.; Plimack, E.R., *et al.* Nivolumab versus everolimus in advanced renal-cell carcinoma. *New Engl J Med* **2015**, *373*, 1803-1813.
10. Hammers, H.; Plimack, E.R.; Infante, J.R.; Ernstoff, M.S.; Rini, B.; Mcdermott, D.F.; Razak, A.; Pal, S.K.; Voss, M.H.; Sharma, P., *et al.* Phase i study of nivolumab in combination with ipilimumab (ipi) in metastatic renal cell carcinoma (mrcc). *Bju Int* **2014**, *114*, 8-8.
11. Ribas, A.; Hodi, F.S.; Callahan, M.; Konto, C.; Wolchok, J. Hepatotoxicity with combination of vemurafenib and ipilimumab. *New Engl J Med* **2013**, *368*, 1365-1366.
12. Wolchok, J.D.; Hoos, A.; O'Day, S.; Weber, J.S.; Hamid, O.; Lebbe, C.; Maio, M.; Binder, M.; Bohnsack, O.; Nichol, G., *et al.* Guidelines for the evaluation of immune therapy activity in solid tumors: Immune-related response criteria. *Clin Cancer Res* **2009**, *15*, 7412-7420.
13. Schreiber, R.D.; Old, L.J.; Smyth, M.J. Cancer immunoediting: Integrating immunity's roles in cancer suppression and promotion. *Science* **2011**, *331*, 1565-1570.
14. Stillebroer, A.B.; Boerman, O.C.; Desar, I.M.E.; Boers-Sonderen, M.J.; van Herpen, C.M.L.; Langenhuijsen, J.F.; Smith-Jones, P.M.; Oosterwijk, E.; Oyen, W.J.G.; Mulders, P.F.A. Phase 1 radioimmunotherapy study with lutetium 177-labeled anti-carbonic anhydrase ix monoclonal antibody girentuximab in patients with advanced renal cell carcinoma. *Eur Urol* **2013**, *64*, 478-485.
15. Mahoney, K.M.; Rennert, P.D.; Freeman, G.J. Combination cancer immunotherapy and new immunomodulatory targets. *Nat Rev Drug Discov* **2015**, *14*, 561-584.
16. Schwartz, J.; Humm, J.L.; Divgi, C.R.; Larson, S.M.; O' Donoghue, J.A. Bone marrow dosimetry using i-124-pet. *J Nucl Med* **2012**, *53*, 615-621.
17. Stillebroer, A.B.; Zegers, C.M.L.; Boerman, O.C.; Oosterwijk, E.; Mulders, P.F.A.; O'Donoghue, J.A.; Visser, E.P.; Oyen, W.J.G. Dosimetric analysis of lu-177-cg250 radioimmunotherapy in renal cell carcinoma patients: Correlation with myelotoxicity and pretherapeutic absorbed dose predictions based on in-111-cg250 imaging. *J Nucl Med* **2012**, *53*, 82-89.
18. Spanholtz, J.; Tordoir, M.; Eissens, D.; Preijers, F.; van der Meer, A.; Joosten, I.; Schaap, N.; de Witte, T.M.; Dolstra, H. High log-scale expansion of functional human natural killer cells from umbilical cord blood cd34-positive cells for adoptive cancer immunotherapy. *Plos One* **2010**, *5, e9221*.
19. Spanholtz, J.; Preijers, F.; Tordoir, M.; Trilsbeek, C.; Paardekooper, J.; de Witte, T.; Schaap, N.; Dolstra, H. Clinical-grade generation of active nk cells from cord blood hematopoietic progenitor cells for immunotherapy using a closed-system culture process. *Plos One* **2011**, *6, e20740*.
20. Cany, J.; van der Waart, A.B.; Tordoir, M.; Franssen, G.M.; Hangalapura, B.N.; de Vries, J.; Boerman, O.; Schaap, N.; van der Voort, R.; Spanholtz, J., *et al.* Natural killer cells generated from cord blood hematopoietic progenitor cells efficiently target bone marrow-residing human leukemia cells in nod/scid/il2rg(null) mice. *Plos One* **2013**, *8,e64384*.

21. Cany, J.; van der Waart, A.B.; Spanholtz, J.; Tordoir, M.; Jansen, J.H.; van der Voort, R.; Schaap, N.M.; Dolstra, H. Combined il-15 and il-12 drives the generation of cd34(+)-derived natural killer cells with superior maturation and alloreactivity potential following adoptive transfer. *Oncoimmunology* **2015**, *4, e1017701*.

22. Grepin, R.; Ambrosetti, D.; Marsaud, A.; Gastaud, L.; Amiel, J.; Pedeutour, F.; Pages, G. The relevance of testing the efficacy of anti-angiogenesis treatments on cells derived from primary tumors: A new method for the personalized treatment of renal cell carcinoma. *Plos One* **2014**, *9*, e89449.

23. Ko, J.J.; Choueiri, T.K.; Rini, B.I.; Lee, J.L.; Kroeger, N.; Srinivas, S.; Harshman, L.C.; Knox, J.J.; Bjarnason, G.A.; MacKenzie, M.J.*, et al.* First-, second-, third-line therapy for mrcc: Benchmarks for trial design from the imdc. *Brit J Cancer* **2014**, *110*, 1917-1922.

List of Publications

List of Publications

1. Oosterwijk E, Ruiter DJ, **Wakka JC**, Huiskens-van der Meij JW, Jonas U, Fleuren GJ, Zwartendijk J, Hoedemaeker P, Warnaar SO: Immunohistochemical analysis of monoclonal antibodies to renal antigens. Application in the diagnosis of renal cell carcinoma. Am J Pathol 1986;123(2):301-9

2. Oosterwijk E, Van Muijen GN, **Oosterwijk-Wakka JC**, Warnaar SO: Expression of intermediate-sized filaments in developing and adult human kidney and in renal cell carcinoma. J Histochem Cytochem 1990;38(3):385-92

3. Oosterwijk E, Kalisiak A, **Wakka JC**, Scheinberg DA, Old LJ.: Monoclonal antibodies against Gal alpha 1-4Gal beta 1-4Glc (Pk, CD77) produced with a synthetic glycoconjugate as immunogen: reactivity with carbohydrates, with fresh frozen human tissues and hematopoietic tumors. Int J Cancer 1991;48(6):848-54

4. Oosterwijk E, Bander NH, Divgi CR, Welt S, **Wakka JC**, Finn RD, Carswell EA, Larson SM, Warnaar SO, Fleuren GJ, et al.: Antibody localization in human renal cell carcinoma: a phase I study of monoclonal antibody G250. J Clin Oncol 1993; 11(4):738-50

5. Kranenborg MH, Boerman OC, **Oosterwijk-Wakka JC**, de Weijert MC, Corstens FH, Oosterwijk E. Development and characterization of anti-renal cell carcinoma x antichelate bispecific monoclonal antibodies for two-phase targeting of renal cell carcinoma. Cancer Res 1995;55:5864s-5867s

6. Steffens MG, Boerman OC, **Oosterwijk-Wakka JC**, Oosterhof GO, Witjes JA, Koenders EB, Oyen WJ, Buijs WC, Debruyne FM, Corstens FH, Oosterwijk E: Targeting of renal cell carcinoma with iodine-131-labeled chimeric monoclonal antibody G250. J Clin Oncol 1997;15(4):1529-37

7. Kranenborg MH, Boerman OC, de Weijert MC, **Oosterwijk-Wakka JC**, Corstens FH, Oosterwijk E. The effect of antibody protein dose of anti-renal cell carcinoma monoclonal antibodies in nude mice with renal cell carcinoma xenografts. Cancer 1997;80(12 Suppl):2390-7

8. Kranenborg MH, Boerman OC, **Oosterwijk-Wakka JC**, de Weijert MC, Corstens FH, Oosterwijk E: Two-step radio-immunotargeting of renal-cell carcinoma xenografts in nude mice with anti-renal-cell-carcinoma X anti-DTPA bispecific monoclonal antibodies. Int J Cancer 1998;75(1):74-80

9. Shimazui T, Oosterwijk E, Akaza H, Bringuier P, Ruijter E, van Berkel H, **Wakka JO**, van Bokhoven A, Debruyne FM, Schalken JA: Expression of cadherin-6 as a novel diagnostic tool to predict prognosis of patients with E-cadherin-absent renal cell carcinoma. Clin Cancer Res 1998;4(10):2419-24

10. Steffens MG, **Oosterwijk-Wakka JC**, Zegwaart-Hagemeier NE, Boerman OC, Debruyne FM, Corstens FH, Oosterwijk E: Immunohistochemical analysis of tumor antigen saturation following injection of monoclonal antibody G250. Anticancer Res 1999;19(2A):1197-200

11. Boerman OC, Kranenborg MH, Oosterwijk E, Griffiths GL, McBride WJ, Oyen WJ, de Weijert M, **Oosterwijk-Wakka J**, Hansen HJ, Corstens FH: Pretargeting of renal cell carcinoma: improved tumor targeting with a bivalent chelate. Cancer Res 1999;59(17):4400-5

12. Steffens MG, Boerman OC, de Mulder PH, Oyen WJ, Buijs WC, Witjes JA, van den Broek WJ, **Oosterwijk-Wakka JC**, Debruyne FM, Corstens FH, Oosterwijk E: Phase I radioimmunotherapy of metastatic renal cell carcinoma with 131I-labeled chimeric monoclonal antibody G250. Clin Cancer Res 1999;5(10 Suppl):3268s-3274s

13. Grabmaier K, Vissers JL, De Weijert MC, **Oosterwijk-Wakka JC**, Van Bokhoven A, Brakenhoff RH, Noessner E, Mulders PA, Merkx G, Figdor CG, Adema GJ, Oosterwijk E: Molecular cloning and immunogenicity of renal cell carcinoma-associated antigen G250. Int J Cancer 2000;85(6):865-70

14. Shimazui T, **Oosterwijk-Wakka J**, Akaza H, Bringuier PP, Ruijter E, Debruyne FM, Schalken JA, Oosterwijk E.: Alterations in expression of cadherin-6 and E-cadherin during kidney development and in renal cell carcinoma. Eur Urol 2000;38(3):331-8

15. **Oosterwijk-Wakka JC**, Tiemessen DM, Bleumer I, de Vries IJ, Jongmans W, Adema GJ, Debruyne FM, de Mulder PH, Oosterwijk E, Mulders PF: Vaccination of patients with metastatic renal cell carcinoma with autologous dendritic cells pulsed with autologous tumor antigens in combination with interleukin-2: a phase 1 study. J Immunother 2002 ;25(6):500-8

16. Nuininga JE, van Moerkerk H, Hanssen A, Hulsbergen CA, **Oosterwijk-Wakka J**, Oosterwijk E, de Gier RP, Schalken JA, van Kuppevelt T, Feitz WF: Rabbit urethra replacement with a defined biomatrix or small intestinal submucosa. Eur Urol 2003;44(2):266-71

17. Nuininga JE, van Moerkerk H, Hanssen A, Hulsbergen CA, **Oosterwijk-Wakka J**, Oosterwijk E, de Gier RP, Schalken JA, van Kuppevelt TH, Feitz WF: A rabbit model to tissue engineer the bladder. Biomaterials 2004;25(9):1657-61

18. Bleumer I, Oosterwijk E, **Oosterwijk-Wakka JC**, Voller MC, Melchior S, Warnaar SO, Mala C, Beck J, Mulders PF: A clinical trial with chimeric monoclonal antibody WX-G250 and low dose interleukin-2 pulsing scheme for advanced renal cell carcinoma. J Urol 2006;175(1):57-62

19. Bleumer I, Tiemessen DM, **Oosterwijk-Wakka JC,** Voller MCW, de Weijer K, Mulders, PFA, Oosterwijk E: Preliminary Analysis of Patients With Progressive Renal Cell Carcinoma Vaccinated With CA9-peptide-Pulsed Mature Dendritic Cells**.** J. of Immunother 2007;30(1):116-122

20. Johanna Sandlund, Egbert Oosterwijk, Kjell Grankvist, **Jeannette Oosterwijk-Wakka**, Börje Ljungberg and Torgny Rasmuson Prognostic impact of carbonic anhydrase IX expression in human renal cell carcinoma. BJU Int 2007; 100: 556-560

21. Bauer S, **Oosterwijk-Wakka JC**, Adrian N, Oosterwijk E, Fischer E, Wüest T, Stenner F, Perani A, Cohen L, Knuth A, Divgi C, Jäger D, Scott AM, Ritter G, Old LJ, Renner C: Targeted therapy of renal cell carcinoma: Synergistic activity of cG250-TNF and IFNg**.** Int. J. Cancer 2009;125:115-123

22. **Oosterwijk-Wakka JC**, Boerman OC, Mulders PFA, Oosterwijk E. Monoclonal antibody G250 recognizing Carbonic Anhydrase IX in Renal Cell Carcinoma: Biological and clinical studies. Bukowski RM, Figlin RA, Motzer RJ, editors. Renal Cell Carcinoma, molecular targets and clinical applications. New York: Humana Press; 2009: P231-47

23. **Oosterwijk-Wakka JC**, Kats-Ugurlu G, Leenders WP, Kiemeney LA, Old LJ, Mulders PF, Oosterwijk E: Effect of tyrosine kinase inhibitor treatment of renal cell carcinoma on the accumulation of carbonic anhydrase IX-specific chimeric monoclonal antibody cG250. BJU Int 2011;107: 118-125

24. Cor HJ Lamers, Ralph A Willemsen, Pascal Elzakker, Sabine Steenbergen-Langeveld, Marieke Broertjes, **Jeannette Oosterwijk-Wakka**, Egbert Oosterwijk, Stefan Sleijfer, Reno Debets, and Jan Willem Gratama: Immune responses to transgene and retroviral vector in patients treated with ex vivo engineered T cells. Blood 2011;117(1): 72-82

25. **Oosterwijk-Wakka JC**, Boerman OC, Mulders PFA, Oosterwijk E. Application of Monoclonal Antibody G250 Recognizing Carbonic Anhydrase IX in Renal Cell Carcinoma. International Journal of Molecular Sciences 2013; 14(6):11402-11423.

26. Kats-Ugurlu G, Oosterwijk E, Muselaers S, **Oosterwijk-Wakka J**, Hulsbergen-van de Kaa C, de Weijert M , van Krieken H, Desar I, van Herpen C, Maass C, Mulders P, Leenders W: Neoadjuvant Sorafenib Treatment of Clear Cell Renal Cell Carcinoma and Release of Circulating Tumor Fragments Neoplasia 2014;16(3): P221-8

27. **Jeannette C. Oosterwijk-Wakka**, Mirjam C.A. de Weijert, Gerben M. Franssen, William P.J. Leenders, Jeroen A.W.M. van der Laak, Otto C. Boerman, Peter F.A. Mulders and Egbert Oosterwijk: Successful combination of Sunitinib and Girentuximab in two renal cell carcinoma animal models: a rationale for combination treatment of patients with advanced RCC. Neoplasia 2015;17: 215–224

28. Oosterwijk E**,** Boerman OC**,** Oyen WJ**, Oosterwijk-Wakka JC**, Mulders PFA,. Carbonic anhydrase IX and monoclonal antibody G250: Relevance as a clinical and biologic target in renal cell carcinoma. Bukowski RM, Figlin RA, Motzer RJ, editors. Renal Cell Carcinoma, molecular targets and clinical applications. New York: Humana Press; 2015: P263-84

Curriculum Vitae

Curriculum Vitae

Jeannette Catharine Wakka is geboren op 16 augustus 1961 te Leiden. In 1979 behaalde zij haar VWO diploma aan de Vlietschans te Leiden. Daarna volgde zij de studie analytische chemie aan de Laboratorium school Rijnland te Leiderdorp, die ze in mei 1983 afsloot met een diploma. Aansluitend volgde zij de studie HTS-chemie aan het van 't Hoff instituut te Rotterdam. Deze werd in mei 1985 cum laude afgesloten. Van september 1984 tot maart 1987 heeft ze als research analist gewerkt op de afdeling pathologie van het Leids Universitair Medisch Centrum aan de ontwikkeling van monoklonale antilichamen voor de behandeling van nierkanker. Vervolgens heeft ze van maart 1987 tot september 1991 als research analist gewerkt in het Memorial Sloan Kettering Cancer Center te New York in het laboratorium Human Immunology van Dr. L.J. Old gevolgd door een aanstelling bij het Ludwig Institute for Cancer Research, New York branch. Daar heeft zij o.a. gewerkt aan de eerste klinische studie van monoklonaal antilichaam G250. Van februari 1993 tot heden werkt zij als senior research analist op het laboratorium Experimentele Urologie, afdeling Urologie aan het Radboudumc te Nijmegen aan onderzoek naar nieuwe therapeutische behandelingen van patiënten met nierkanker. In 2014 ontving ze de derde prijs voor "best abstract in Oncology" voor "Combination therapy with sunitinib and ^{177}Lu-Girentuximab in RCC" op het congres van de European Association of Urology te Stockholm.

Jeannette woont in Beuningen, is getrouwd met Egbert Oosterwijk en heeft 3 kinderen: Roos (1992), Roderick (1994) en Jesse (1997).

Dankwoord

Dankwoord

Eindelijk ligt het er dan, mijn proefschrift! Wat ben ik blij dat het af is. Mede dankzij de hulp van velen is dit boekje tot stand gekomen. Een aantal mensen wil ik persoonlijk bedanken.

Prof. Dr. Peter Mulders. Beste Peter, super dat je me de kans hebt gegeven om het promotieonderzoek te doen wat tot dit boekje heeft geleid. De werkbesprekingen van de 'nierkanker groep' op dinsdag om 11.00 uur waarin jij altijd zeer geïnteresseerd en kritisch was op de resultaten van experimenten waren zeer waardevol en hielden me scherp. Wat knap dat jij naast je taken als afdelingshoofd en je klinische taken ook nog tijd vindt om onderzoek te doen. Bedankt dat jij mijn promotor wil zijn.

Dear Prof Dr. CR Divgi, dear Chetan, we both have a great interest in cG250 and you have been one of the driving forces to move clinical implementation forward. I feel honored that you are part of my defense committee.

Beste Jack, nadat ik had aangegeven aan een nieuwe uitdaging toe te zijn en wilde promoveren heb jij me gestimuleerd om dat ook daadwerkelijk te doen. Dat zetje had ik nodig om er ook echt voor te gaan. Ik hou van jouw laagdrempelige manier van leidinggeven. Heerlijk ook de discussies aan de koffietafel op maandagochtend waarin de vorderingen van Ajax ruim aan bod kwamen. Bedankt voor je steun.

Lieve Egbert, naast mijn lief ben je ook mijn copromotor. Samen hebben we G250 "ontdekt" en in New York naar de kliniek gebracht. Nu ben jij copromotor op mijn promotie waarin G250 opnieuw centraal staat. Hoe bijzonder! Ik bewonder je enorme kennis, relativeringsvermogen en je veerkracht. Zonder jouw kritische blik op mijn manuscripten en jouw schrijftalent was dit boekje er niet gekomen. Ik ben enorm trots dat jij copromotor bij mijn promotie bent.

Mirjam en Dorien, wat leuk dat jullie op 9 december aan mijn zijde staan als paranimf.
Beste Mirjam, wij zijn bijna tegelijkertijd op het lab experimentele urologie gestart (toen nog URL). Samen hebben we vanaf 1993 aan diverse promotieonderzoeken meegewerkt. Ik bewonder jouw expertise, betrokkenheid en je enorme creativiteit. Je bent een gezellige collega die ik zelden hoor zeuren. Ik hoop nog lang met je samen te werken.
Beste Dorien, hoewel de laatste jaren niet direct betrokken bij mijn onderzoek door jouw overstap naar tissue-engineering hebben wij een aantal jaar geleden veel samengewerkt o.a. aan de klinische studie met DC-vaccin waarin we uren hebben doorgebracht in de cleanroom of op de OK om vaccins te bereiden en patiënten materiaal te verzamelen. Met jou is het altijd lachen geblazen, je vrolijkheid werkt heel aanstekelijk. Jouw inzet en betrokkenheid maken jou tot een zeer gewaardeerde collega.
Bedankt voor jullie gezelligheid, hulp bij de experimenten en steun bij de laatste loodjes van het manuscript.

Analisten van het van het lab experimentele urologie: Tilly, Kees, Onno, Cindy, Marion en Elze. Jullie zijn eigenlijk mijn labfamilie. Het feit dat jullie al heel lang op dit lab werken zegt wel iets over de goede werksfeer op het "URL". Bedankt voor de samenwerking en de gezelligheid, door jullie voelt werk meer als een hobby. Dank ook voor jullie interesse in de voortgang van mijn promotie. Beste Kees, jou wil ik in het bijzonder bedanken voor je hulp bij de dierexperimenten. Jij bent nooit te beroerd om bij te springen.

Alle promovendi, postdocs en studenten van het lab experimentele urologie, bedankt voor de goede samenwerking, gezellige koffiemomenten, de congressen, borrels en leuke etentjes. Op het lab is het nooit saai. Super dat we zo'n internationaal gezelschap zijn, dat maakt het werken op het lab nog leuker.

Maureen, jij was mijn "U-genootje" tot je vertrek van het lab. Bedankt voor de goede gesprekken en gezellige bioscoopavondjes. Ik hoop snel weer af te spreken om te kunnen bijkletsen. Heel veel succes in je nieuwe baan!

Medewerkers van PRIME, in het bijzonder, Bianca, Kitty, Henk en Iris. Jullie vaardigheid, kennis en inzet was ontzettend belangrijk voor de uitvoering van de dierexperimenten die een essentieel onderdeel vormen van dit boekje. Hartelijk dank voor al jullie hulp.

Ik wil ook een aantal mensen bedanken van de afdeling Radiologie en Nucleaire geneeskunde en afdeling Pathologie waar ik een deel van het werk heb uitgevoerd. Prof. Dr. Boerman, beste Otto, je kritisch commentaar op mijn manuscripten en je hulp bij het ontwerpen van de dierexperimenten waren heel waardevol en verhoogden de kwaliteit. Gerben, bedankt voor je hulp met de In-111 en Lu-177 labelingen. Ondanks de lastige logistiek zag je altijd kans op de afgesproken tijd materiaal klaar te hebben. Janneke, bedankt voor je hulp met het zetten van de NU12 tumoren. Jij was degene die hierin het meeste geïnvesteerd heeft en deze tumor jaren voor ons in stand hebt gehouden. We zien elkaar nog regelmatig na je overstap van Urologie naar Nucleaire geneeskunde. Dit model blijft belangrijk. Cathelijne en Lieke, bedankt voor de hulp die jullie mij hebben geboden bij o.a. labelingen en autoradiografie op jullie lab. William, jouw kennis en enthousiasme over angiogenese remmers zijn ongekend. Onze samenwerking is zeer vruchtbaar en ik hoop dat er nog vele artikelen zullen volgen waarin jij een aandeel hebt.

Lieve vrienden,
De "kampeerclub": Mathieu, Annelies, Klaas, Nel, Marco, Sietske, Renee en Fieke. Bedankt voor jullie jarenlange vriendschap die dateert van vóór ons New York avontuur en voor de mooie kampeerweekenden de afgelopen jaren met onze gezinnen. We doen niet veel meer dan bbq'en, wijn drinken en bijkletsen en oké af en toe een fietstochtje maar de sfeer is altijd super en relaxed. Volgend jaar nemen we de beroemde "Egbert's BBQ' weer mee!

Het pufclubje: Ina, Henk, Andy en Hank, we kennen elkaar nu al meer dan 20 jaar. De vele gezellige etentjes en avondjes met jullie hebben gezorgd voor de nodige ontspanning. Bij jullie voel ik me enorm op mijn gemak. Bedankt voor jullie vriendschap.

Marijke en Peter, ondanks onze volle agenda's blijven vinden we toch altijd weer een gaatje om elkaar te zien. Naar Sauna of restaurant of op vakantie, met jullie is het altijd goed toeven. Bedankt voor jullie vriendschap.

Gerald en Heidi, Ik hou enorm van jullie nuchtere kijk en directheid. Spelletjes avonden en etentjes, er wordt altijd veel gelachen. Met onze gezinnen hebben we mooie vakanties gemaakt naar Thailand en Marokko. Ik heb er ontzettend van genoten en hoop dat er nog leuke reisjes zullen volgen (met of zonder kids). Bedankt voor de gezelligheid en jullie vriendschap.

"Sisters" en "(Ex-)Kleidonkers", Theo, Petra, Arnold, Jeanet, Leo en Lucia, Marianne, Frank, Renée, Marloes en Jeanne, bedankt voor alle gezellige musical-, spelletjes-, 4-daagse-, dansavonden en wat al niet meer waarin ook heel veel gelachen werd. Dat er nog veel leuke momenten mogen volgen!

Dear Paco, Chetan, Martina, Nuria, Michelle and Tom, we may not see each other often but when we do it's like old times. I cherish the time we had together in New York at 81st Street, where our friendship started when we were at Memorial Sloan Kettering Cancer Center. I hope we can see each other more often in the future despite all our commitments. Thanx for your comradeship.

Lieve familie,

Ik hoop dat jullie na het lezen van de Nederlandse samenvatting enigszins begrijpen wat ik de afgelopen jaren heb gedaan.

Lieve zus Lotte, onze band is heel sterk. Je interesse en steun in de voortgang van mijn promotie waren voor mij heel belangrijk. Jij staat altijd voor mij klaar en dat is heel bijzonder. Als deze promotie achter de rug is heb ik weer tijd om samen leuke dingen te doen. Ben, Susanne, Rian, Sebastiaan, Mariko, Jasmijn en Joel. Wij zijn een hechte familie en missen doorgaans niets van elkaar. Bedankt voor jullie gezelligheid tijdens feesten, verjaardagen, en familie-uitjes.

Lieve mama, zonder papa en jou had ik hier niet gestaan. Dankzij jullie ben ik geworden wie ik ben. Jammer dat papa dit niet meer kan meemaken, ik weet dat hij enorm trots op me zou zijn geweest. Gelukkig kun jij deze bijzondere dag wel met ons allen in goede gezondheid meemaken. Mam, bedankt voor je liefde, goede zorgen en nooit aflatende steun. Bedankt voor alles.

Roos, Roderick en Jesse, wat ben ik trots op jullie. Lieve Roos, jouw lef, gedrevenheid en ambitie hebben er toe geleid dat je na afgestudeerd te zijn als bewegingswetenschapper nu als trainee bij het ministerie van VWS in dienst bent. Een prestigieuze baan, supergoed gedaan! Je bent daarnaast ook heerlijk spontaan en zeer sociaal. Heel veel succes in Den Haag en veel geluk met Tom.

Lieve Roderick, dit jaar ben je zonder vertraging aan je master Biomedical Engineering in Eindhoven begonnen, een knappe prestatie. Je bent toegewijd, gedreven, sociaal en betrokken en ik ben overtuigd dat deze eigenschappen je een goede toekomst zullen bieden. Geloof in jezelf!

Lieve Jesse, jouw studentenleven is dit jaar echt begonnen. Ik hoop dat dit voor jou een super jaar wordt, waarin alles op zijn plaats valt en dat je snel je draai in Eindhoven kunt vinden bij de studie MWT. Met jouw slimheid, sociale karakter en het snel kunnen schakelen denk ik dat het zeker gaat lukken. Gezellig dat je nog even thuis blijft wonen. Heel veel geluk met je liefde Jessica.

Lieve kinderen, bedankt voor jullie onvoorwaardelijke liefde.

Lieve Egbert, de steun die je als promovendus van je partner ondervindt is het allerbelangrijkste. Al bijna 30 jaar ben jij mijn rots in de branding. Jij hebt me geholpen om dit promotietraject door te zetten, jij wist mij te motiveren en helpen. Het schrijven van dit proefschrift was alleen mogelijk dankzij jouw onvoorwaardelijke steun en liefde en je geloof in mij. Dank voor alles.